WATER STABILIZATION USING MICROPARTICLES

Except where reference is made to the work of others, the work described in this thesis is my own or was done in collaboration with my advisory committee. This thesis does not contain proprietary information.

_____
Bryan Taylor Shiver

Certificate of Approval:

_____   _____
Dan A. Brown   David J. Elton, Chair
Gottlieb Associate Professor   Associate Professor
Civil Engineering   Civil Engineering

_____   _____
Frazier Parker, Jr.   Joe F. Pittman
Associate Professor   Interim Dean
Civil Engineering   Graduate School

WATER STABILIZATION USING MICROPARTICLES

Bryan Taylor Shiver

A Thesis

submitted to

the Graduate Faculty of

Auburn University

in Partial Fulfillment of the

requirements for the

Degree of

Master of Science

Auburn, Alabama
August 4, 2007

WATER STABILIZATION USING MICROPARTICLES

Bryan Taylor Shiver

_____

Signature of Author

_____

Date of Graduation

THESIS ABSTRACT

WATER STABILIZATION USING MICROPARTICLES

Bryan Taylor Shiver

Master of Science, August 4, 2007
(B.S.C.E., Auburn University, 2002)

245 Typed Pages

Directed by David J. Elton

Liquefaction is a phenomenon in which saturated, loose, cohesionless soil loses

its strength due to earthquake shaking or some other loading. A major occurrence of

liquefaction was observed by engineers in 1964 during earthquakes in Niigata, Japan, and

Prince William Sound, Alaska. Both earthquakes produced amazing examples of

liquefaction induced damage, including bridge and building collapse. Since these

earthquakes, research on liquefaction, its evaluation, and mitigation have been conducted

by researchers around the world. However, research in mitigation of liquefaction at post-

construction sites has been scarce and options available to engineers to remediate hazards

in this situation are lacking. Therefore, this study uses polyacrylamide hydrogel, or just

hydrogel, a water absorbing polymer, as a soil additive to mitigate liquefaction on post-

construction sites. Testing was conducted on prepared Ottawa sand samples using

increasing percentages of hydrogel. Testing included static consolidated undrained

triaxial, flex-wall permeameter, uplift pressure, and cyclic mobility. Triaxial testing

showed hydrogel had no effect on pore pressure but did reduce sample dilation and strength. Permeability testing produced a reduction in permeability with increasing percent hydrogel. A 0.20 tsf uplift pressure was produced with 0.50% hydrogel. Cyclic mobility testing showed decreased liquefaction susceptibility with increased percent hydrogel.

ACKNOWLEDGEMENTS

Style manual or journal used:

American Society of Civil Engineers Guide for Authors

Computer software used:

Microsoft Word

TABLE OF CONTENTS

LIST OF FIGURES

CHAPTER 4: LABORATORY TESTING RESULTS

147

CHAPTER 5: CONCLUSIONS FROM LABORATORY TESTING RESULTS

APPENDIX C: DETAILED LABORATORY PROCEDURES

CHAPTER 1: INTRODUCTION

1.1 Liquefaction Overview

The 1964 earthquakes in Niigata, Japan, and Prince William Sound, Alaska,

brought the damaging effects of liquefaction to the forefront of earthquake engineering

research around the world. Liquefaction is a phenomenon in which a saturated, loose,

cohesionless soil loses its strength due to earthquake shaking or some other loading.

Liquefaction produced during these earthquakes had devastating effects on structures and

lives in these areas. In the 40 years since, liquefaction has been observed and researched

extensively producing evaluation and mitigation methods. While evaluation of

liquefaction susceptibility can be conducted at most sites, mitigation of liquefaction

hazards cannot. Many proven methods exist to mitigate hazards at a preconstruction site,

but at sites where structures are already present, few mitigation options are available.

This lack of mitigation techniques at post-construction sites led to the idea of using

polyacrylamide hydrogel, or just hydrogel, a water absorbing polymer, in the soil under a

structure to alleviate liquefaction hazards.

1.2 Hydrogel

This study revolved around the use of hydrogel to prevent liquefaction in sandy

soils. Hydrogel is a water absorbing polymer and as it absorbs water, hydrogel expands.

Hydrogel is to be placed in the void spaces of the soil. Here a dry hydrogel particle will absorb any water in the void. In absorbing this water hydrogel will expand to fill the void. In this way hydrogel is used to absorb and "trap" the water in the soil. Water will be contained in a hydrogel particle thereby, not allow the absorbed water *to transfer pressure to the soil*. Therefore, as a soil containing hydrogel is stressed, pore pressure would be lowered. To test this hypothesis, sand samples containing hydrogel were tested for strength and permeability.

1.3   Scope of the Project

This project began a study of hydrogel and its effect on sand samples. Laboratory tests were run on prepared Ottawa sand samples in order to evaluate the effect hydrogel had on the strength, pore pressure, and permeability properties. To analyze the effects of hydrogel on these properties, static consolidated undrained triaxial and flex-wall permeameter tests were run on Ottawa sand samples containing varying percentages of hydrogel. This resulted in data showing how hydrogel changed the strength, pore pressure, and permeability properties of Ottawa sand.

Once triaxial and permeability tests were completed, two other laboratory tests were run to further evaluate the effect of hydrogel on Ottawa sand samples. These tests were improvised from available equipment and do not follow ASTM standards. An uplift pressure test was conducted to measure the uplift pressure hydrogel expansion creates. Also, a test termed "cyclic mobility test" was performed to observe how Ottawa sand samples containing hydrogel reacted under unconfined dynamic load.

All testing samples were prepared to simulate hydrogel having already been placed in the soil. This project does not discuss methods for inserting hydrogel into the ground.

1.4 Overview of Testing Results

Triaxial testing showed a reduction in sample dilation and strength and little effect on peak pore pressure with increasing percent hydrogel. Permeability was reduced with increasing hydrogel percentage. 0.50% hydrogel caused a 0.20 tsf uplift pressure. An increasing percent hydrogel produced a reduction in liquefaction susceptibility in cyclic mobility testing. This paper presents an in depth study of these tests, their results, and conclusions drawn from them.

CHAPTER 2: LITERATURE REVIEW

2.1 Liquefaction

2.1.1 Introduction

Liquefaction is one of the most important, interesting, complex, and controversial topics in geotechnical earthquake engineering (Kramer 1996). Liquefaction is a phenomenon in which a saturated, cohesionless soil loses its strength due to earthquake shaking or some other loading. Liquefaction has been responsible for large amounts of damage to structures in earthquakes around the world.

Its devastating effects sprang to the attention of geotechnical engineers in a three-month period in 1964 when the Good Friday earthquake in Alaska was followed by the Niigata earthquake in Japan. Both earthquakes produced spectacular examples of liquefaction-induced damage, including slope failures, bridge and foundation failures, and floatation of buried structures (Kramer 1996). In the forty years since these earthquakes, liquefaction has been studied extensively by researchers around the world. This research has produced advances in the understanding of the liquefaction phenomena and testing methods, both laboratory and field, to analyze the liquefaction potential of a soil mass. This chapter presents a literature review of the current knowledge on the subject of liquefaction and its evaluation.

2.1.2   Effects of Liquefaction

2.1.2.1   Loss of Strength

In saturated soils, the void spaces between individual soil particles are filled with water. Pressure in the water influences how tightly the soil particles are pressed together. Under everyday conditions the water pressure in the soil is low and does not cause problems, but under earthquake or other loads this pressure can become large. As the water pressure increases inter-particle soil contact decreases and at high pressures the soil particles can begin to move with respect to one another. This is what happens during liquefaction and is defined by the effective stress equation.

Effective stress is defined as the total stress minus the water pressure, and it determines the strength of the soil. When the water pressure increases to the point that it is equal to the total stress, effective stress becomes zero, the soil loses its strength, and liquefaction occurs.

It is important to note that liquefaction is not a type of ground failure; it is a physical process that takes place during some earthquakes that may lead to ground failure. As a consequence of liquefaction, clay-free soil deposits, primarily sands and silts, temporarily lose strength and behave as viscous fluids rather than as solids. Liquefaction causes three types of ground failure: lateral spreads, flow failures, and loss of bearing capacity. In addition, liquefaction enhances ground settlement and sometimes generates sand boils (fountains of water and sediment emanating from the pressurized liquefied zone). Sand boils can cause local flooding and the deposition or accumulation of silt (Hays 1981).

2.1.2.1.1 Lateral Spread (Hays 1981)

Lateral spreads involve the lateral movement of large blocks of soil as a result of liquefaction in a subsurface layer. Movement takes place in response to the ground shaking generated by an earthquake. Lateral spreads generally develop on gentle slopes, most commonly on those between 0.3 and 3 degrees. Horizontal movements on lateral spreads commonly are as much as 10 to 15 feet, but where slopes are particularly favorable and the duration of ground shaking is long, lateral movement may be as much as 100 to 150 feet. Lateral spreads usually break up internally forming numerous fissures and scarps.

2.1.2.1.2 Flow Failures (Hays 1981)

Flow failures, consisting of liquefied soil or blocks of intact material riding on a layer of liquefied soil, are the most catastrophic type of ground failure caused by liquefaction. These failures commonly move several tens of feet and if geometric conditions permit, several tens of miles. Flows travel at velocities as great as many tens of miles per hour. Flow failures usually form in loose saturated sands or silts on slopes greater than 3 degrees.

2.1.2.1.3 Loss of Bearing Capacity (Hays 1981)

When the soil supporting a building or some other structure liquefies and loses strength, large deformations can occur within the soil allowing the structure to settle and tip. Soils that typify the general subsurface geometry required for liquefaction-caused bearing failures are a layer of saturated, cohesionless soil (sand

or silt) extending from near the ground surface to a depth of about the width of the building.

2.1.2.2   Notable Events

2.1.2.2.1   Niigata, Japan 1964

The Niigata earthquake, magnitude 7.5, occurred on June 16, 1964, and caused extensive soil liquefaction in Niigata City and the surrounding areas. This earthquake led to research of the phenomenon of liquefaction in loose, saturated sand.
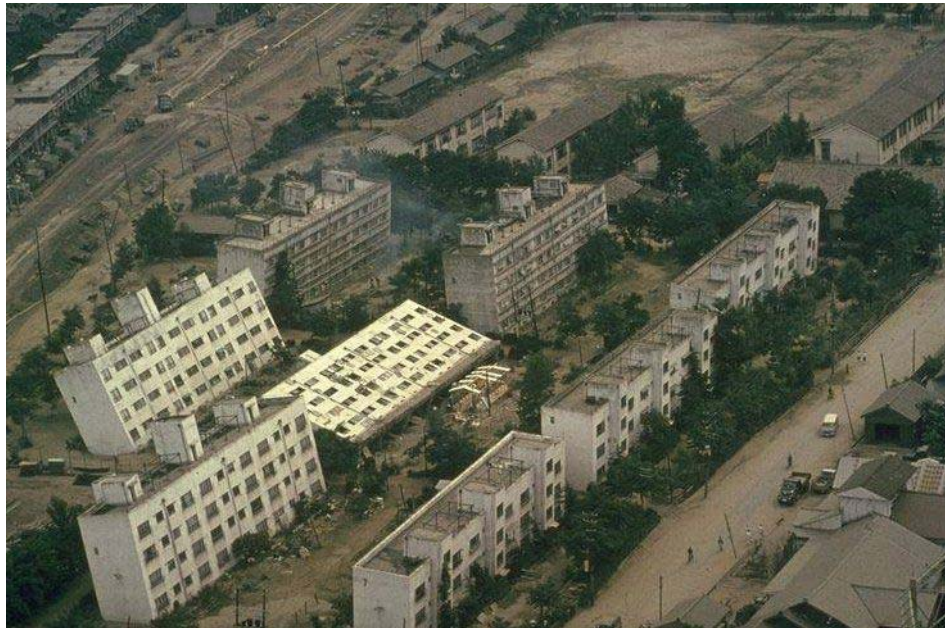
Figure 2.1: Liquefaction-induced bearing capacity failures of the Kawagishi-cho apartment buildings following the 1964 Nigata earthquake (http://www.ce.washington.edu/~liquefaction/).

Figure 2.2: Collapse of the Showa Bridge due to liquefaction-induced lateral spreading after the 1964 Niigata earthquake (http://www.ce.washington.edu/~liquefaction/).

2.1.2.2.2 "Good Friday" Earthquake, Alaska 1964

On March 27, 1964, the largest earthquake in U.S. history, magnitude 9.2, occurred in Prince William Sound, Alaska. The region was sparsely populated and loss of life and structures low; although, 114 people died. Liquefaction events were mostly confined to the extensive lateral spreading that occurred.

Figure 2.3: Span collapse of the "Million Dollar" bridge due to lateral spreading after the 1964 "Good Friday" earthquake (http://neic.usgs.gov/neis/eq_depot/usa/1964_03_28.html).

Figure 2.4: Ground deformation due to lateral spreading after the 1964 "Good Friday" earthquake (http://neic.usgs.gov/neis/eq_depot/usa/1964_03_28.html).

2.1.2.2.3   Loma Prieta Earthquake, California 1989

The October 17, 1989, Loma Prieta earthquake, magnitude 7.1, was very important not only because of the extensive data that was collected and correlated but also because of unprecedented media coverage; it happened on live TV during the third game of the world series. The Marina District of San Francisco which was built on top of uncompacted rubble and debris from the 1906 earthquake experienced significant liquefaction damage.

Figure 2.5: Liquefaction induced damage in the Marina District, San Francisco after the Loma Prieta earthquake (http://libraryphoto.er.usgs.gov/earth1.htm).

Figure 2.6: Structures damaged in the Marina District of San Francisco. The first story of this three-story building was damaged because of liquefaction; the second story collapsed. What is seen is the third story. Loma Prieta earthquake 1989 (http://libraryphoto.er.usgs.gov/earth1.htm).

2.1.2.2.4   Hyogo-Ken Nanbu Earthquake, Kobe, Japan 1995

The magnitude 6.9 Hyogo-Ken Nanbu earthquake, on January 17, 1995, caused extensive liquefaction as well as over 5,000 deaths. At the time Kobe was the sixth largest port in the world. The port, built on artificial islands, suffered widespread liquefaction.

Figure 2.7: Damage at Kobe port due to liquefaction of the underlying fill after the 1995 Hyogo-Ken Nanbu earthquake (http://www.ce.washington.edu/~liquefaction/).
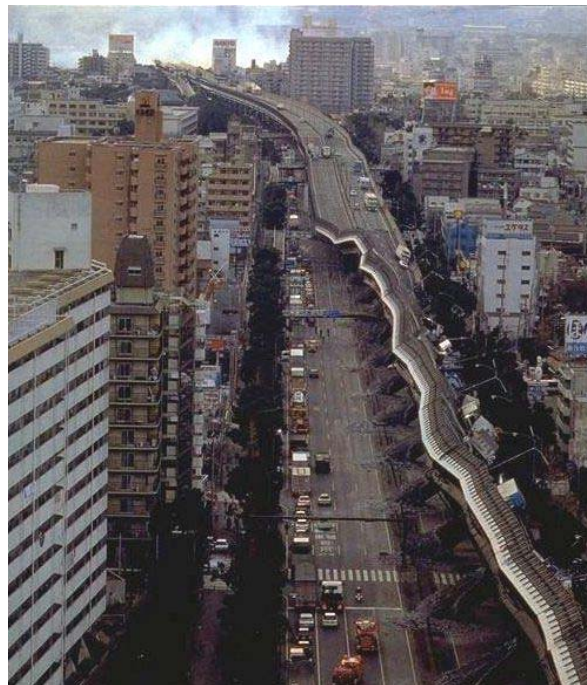
Figure 2.8: Overturned expressway in Kobe due to lateral spreading after the 1995 Hyogo-Ken Nanbu earthquake (http://www.ce.washington.edu/~liquefaction/).

2.1.3   Subsurface Stresses

At a point within a soil mass, stresses will be developed as a result of the soil lying above the point and by any structural or other loading imposed onto that soil mass (McCarthy 1998). These stresses along with pressure caused by water within the soil define the strength of a soil mass. In liquefaction analysis, as with most other geotechnical analyses, subsurface stresses are used to identify existing strength conditions as well as define conditions for failure for a given soil mass.

2.1.3.1   Vertical Stresses

Vertical stress is created by vertical loads. There are two types of vertical loads. One is due to the weight of the soil itself, and the other is produced by structural elements placed on the soil such as buildings or vehicles. A review of vertical stress, its definition and calculation, is presented in McCarthy (1998). Vertical stress is important in a liquefaction analysis because it defines the effective stress in a soil mass, which is reviewed in the next section.

2.1.3.2   Effective Stress

In 1925, Karl Terzaghi introduced the theory of effective stress. He stated, "All measurable effects of a change of stress [in a soil mass], such as compression, distortion and a change of shearing resistance are due exclusively to changes in effective stress." Effective stress is defined by the equation:

$$\sigma' = \sigma - u$$

where σ' is the effective stress, σ is the total or vertical stress, and u is the neutral stress or pore water pressure. A detailed overview of effective stress is explained in Holtz and Kovacs (1996).

Neutral stress or pore water pressure is caused by fluid in the soil, normally water, and is thus present in any soil that contains water. Liquefaction is governed by the pore water pressure in the soil and its effect on effective stress. In liquefaction susceptible soils, which are saturated, loosely deposited, cohesionless soils, the pore spaces in the soil mass are filled with water. When loose saturated cohesionless soils are subjected to vibrations, such as an earthquake, there is a tendency for the soil to decrease in volume, or densify. If drainage is unable to occur, the decrease in volume causes an increase in pore water pressure, and if the pore water pressure builds to the point at which it is equal to the vertical stress, the effective stress becomes zero, and the soil loses its strength, and it develops a liquefied state (Seed and Lee 1966).

2.1.4   Liquefaction-Related Phenomena

Mogami and Kubo (1953) first used the term liquefaction to describe the lowering of effective stress due to excess pore pressures generated during undrained loading conditions of saturated cohesionless soils. While this loss of strength is common to all liquefaction phenomena, in recent years liquefaction events have come to be separated into two main groups: flow liquefaction and cyclic mobility (Kramer 1996).

14

While both flow liquefaction and cyclic mobility are caused by a lowering of effective stress, the conditions under which they happen and the damage caused by each can be vastly different.

2.1.4.1   Flow Liquefaction (Kramer 1996)

Flow liquefaction produces the most dramatic effects of all the liquefaction-related phenomena – tremendous instabilities known as flow failures. Flow liquefaction can occur when the shear stress required for static equilibrium of a soil mass (the static shear stress) is greater than the shear strength of the soil in its liquefied state. Once triggered the large deformations produced by flow liquefaction are actually driven by static shear stresses. The cyclic stresses may simply bring the soil to an unstable state at which its strength drops sufficiently to allow the static shear stresses to produce flow failure. Flow liquefaction failures are characterized by the sudden nature of their origin, the speed at which they develop, and the large distance over which liquefied materials often move. Flow slide failures are shown in Figures 1.9 and 1.10.

2.1.4.2   Cyclic Mobility (Kramer 1996)

Cyclic Mobility is another phenomenon that can also produce unacceptably large permanent deformations during earthquake shaking. In contrast to flow liquefaction, cyclic mobility occurs when the static shear stress is less than the shear strength of the liquefied soil. The deformations produced by cyclic mobility failures develop incrementally during earthquake shaking. In contrast to flow liquefaction,

the deformations produced by cyclic mobility are driven by both cyclic and static shear stresses. These deformations, termed lateral spreading, can occur on very gently sloping ground or on virtually flat ground adjacent to bodies of water (Fig. 1.11). When structures are present, lateral spreading can cause significant damage (Fig 1.12 and 1.13).

A special case of cyclic mobility is level-ground liquefaction. Because static horizontal shear stresses that could drive lateral deformations do not exist, level-ground liquefaction can produce large, chaotic movement known as ground oscillation during earthquake shaking but produces little permanent lateral soil movement. Level ground liquefaction failures are caused by upward flow of water that occurs when seismically induced excess pore pressures dissipate. Depending on the length of time required to reach hydraulic equilibrium, level-ground liquefaction failure may occur well after ground shaking has ceased. Excessive vertical settlement and consequent flooding of low-lying land and the development of sand boils (Fig. 1.14) are characteristic of level-ground liquefaction.

Figure 2.9: Flow failure at Lake Merced, CA 1957

(http://www.ce.washington.edu/~liquefaction/).

Figure 2.10: Flow failure at Sheffield Dam after 1925 Santa Barbara earthquake

(http://www.ce.washington.edu/~liquefaction/).

Figure 2.11: Lateral spreading of very flat ground toward the Motagua River after the 1976 Guatemala earthquake (http://www.ce.washington.edu/~liquefaction/).

Figure 2.12: Ground failure showing lateral spread after 2001 Nisqually earthquake Olympia, Washington (http://peer.berkeley.edu/nisqually/geotech/liquefaction/lateralspread/).

Figure 2.13: Lateral spread of embankment after 2001 Nisqually earthquake Olympia, Washington. The drop seen varies between 3 to 4 feet (http://peer.berkeley.edu/nisqually/geotech/liquefaction/lateralspread/).

Figure 2.14: One of many sand boils that developed after 1979 El Centro earthquake in California (http://www.smate.wwu.edu/teched/geology/eq-general.html).

2.1.5 Evaluation of Liquefaction Hazards

Liquefaction, both flow and cyclic mobility, can cause large amounts of damage at a site. Because of this, the liquefaction hazards present at a site must evaluated in order to determine the severity of these hazards or whether any hazards exist at all. In order for a hazard to exist, a site must meet a set of criteria that outline optimum conditions for liquefaction to occur. These criteria are the earthquake potential, soil saturation, and liquefaction susceptible soil.

2.1.5.1 Earthquake Potential

In order for liquefaction to occur there must be a load placed on the soil. In most cases this load is in the form of an earthquake. Determining whether an earthquake will occur at a site is a complicated procedure that is outlined in seismic hazard analysis. There is both a deterministic seismic hazard analysis (DSHA) and a probabilistic seismic hazard analysis (PSHA). DSHA is used in worst case scenario analyses where a set of parameters are chosen then analyzed. PHSA uses a set of probability equations to account for variability in earthquake size, location, and rate of occurrence. This flexibility makes PHSA the preferred method of seismic hazard analysis. A detailed overview of seismic hazard evaluation is presented in Kramer (1996).

2.1.5.2 Soil Saturation

Liquefaction occurs only in saturated soils, so depth to groundwater (either free or perched) influences liquefaction susceptibility (Kramer 1996). In a dry soil,

the pore water pressure (u) will be zero, the effective stress (σ') will equal the total

stress (σ), and the strength of the soil will not be influenced. Therefore, liquefaction

susceptibility decreases with increasing groundwater depth. The effects of

liquefaction are most commonly observed at sites where the groundwater table is

within a few meters of the ground surface (Kramer 1996).

2.1.5.3   Liquefaction Susceptible Soil

Along with the saturation described in the previous section, the soil itself also

has a set of optimum criteria for liquefaction. Geologic processes that sort soil into

uniform grain size distributions and deposit them in loose states produce soils with

high liquefaction susceptibility. Consequently, fluvial deposits, and colluvial and

aeolian deposits are susceptible to liquefaction (Kramer 1996). After Ishihara (1984,

1985, and 1993) discovered that nonplastic silts liquefy, plasticity characteristics

instead of grain size alone were found to influence liquefaction. In 1979, Wang

outlined these characteristics:

Fraction finer than 0.005 mm $\leq$ 15%

Liquid limit, LL $\leq$ 35%

Natural water content $\geq$ 0.9 LL

Liquidity index $\leq$ 0.75

Any soils that show these properties may liquefy.

21

2.1.6 Lab Evaluation of Liquefaction Susceptibility

Once the soil at a site is deemed susceptible to liquefaction with the criteria described in the previous sections, analysis of the liquefaction problem can begin. Although field testing (described in section 1.1.7) is more common in practice, there are lab tests to determine the liquefaction potential of the soil. While these tests are rare outside of academic circles, the data is useful in analysis of liquefaction potential. Of these tests, cyclic triaxial testing is the most widely used followed by cyclic simple shear and cyclic torsional testing.

2.1.6.1 Cyclic Triaxial Testing

Cyclic triaxial testing is very similar to static triaxial testing in that a carefully prepared sample, wrapped in a membrane, is placed in a pressurized chamber and loaded axially. However, in cyclic triaxial testing the axial load is cyclic, where the load is applied as a sine function versus time. During the test, load, displacement (strain), and pore pressure is measured. A typical cyclic triaxial setup is shown in Figure 1.15.

Data from cyclic triaxial testing produces a number of cycles to liquefaction, N_L. Initiation of liquefaction is defined by Seed and Lee (1966) as the point at which the increase in pore pressure is equal (u_{excess}) to the initial effective confining pressure (σ'_3) (chamber pressure). This is usually expressed as a ratio $r_u = u_{excess} / \sigma'_3$, so when $r_u = 1.00$ liquefaction has occurred. Kramer (1996) presents a synopsis of this test and its use in analysis. Typical data from a cyclic strength test is shown in Figure 1.16.
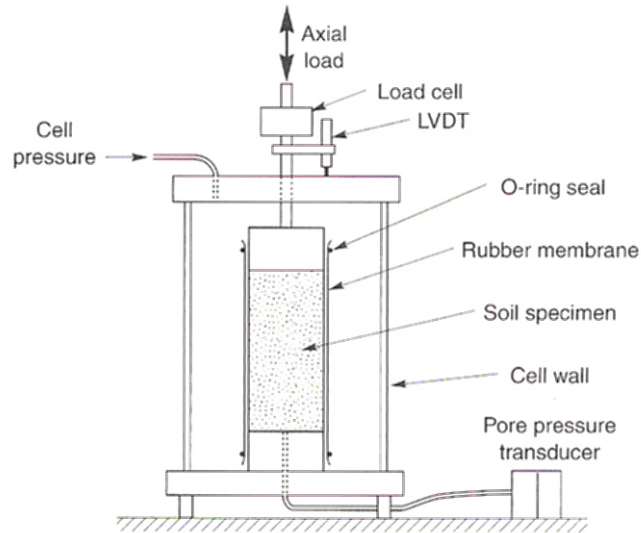
Figure 2.15: Typical cyclic triaxial test setup (Kramer 1996).
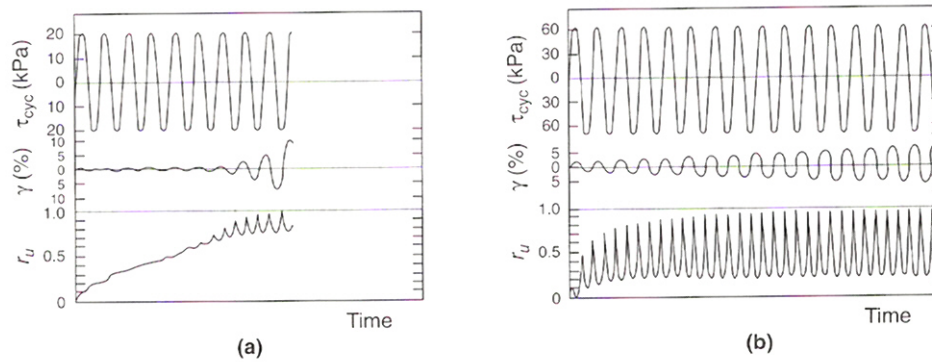
Figure 2.16: Typical cyclic testing data for (a) a loose sand and (b) a dense sand. Notice that the loose specimen has reached initial liquefaction (r_u = 1.00) on 10th loading cycle, while, despite a much higher loading, the dense sample has not reached liquefaction after 17 cycles (Kramer 1996).

2.1.6.2 Cyclic Simple Shear

An alternative to the cyclic triaxial test is the cyclic simple shear test. It is able to reproduce earthquake conditions more accurately than cyclic triaxial testing. Data from the test is reduced in the same manner as cyclic triaxial. An overview of the cyclic simple shear test can be found in Kramer (1996). A typical setup of the cyclic simple shear test is shown in Figure 1.17.
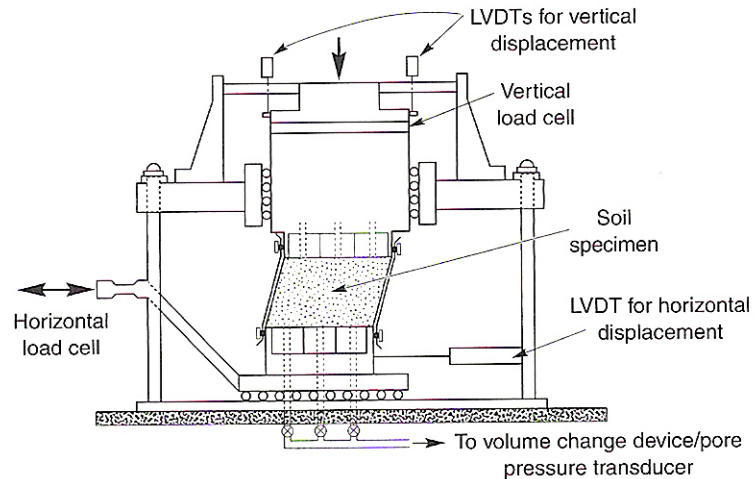
Figure 2.17: Typical cyclic simple shear test setup (Kramer 1996).

2.1.6.3 Cyclic Torsional Shear

Another laboratory liquefaction testing option is the cyclic torsional shear test. This test is used because it creates more even strains in the sample, which are more easily measured than in other tests. More on cyclic torsional testing can be found in Ishibashi, Kawamura, and Bhatia (1985). Figure 1.18 shows the mechanics of this test.
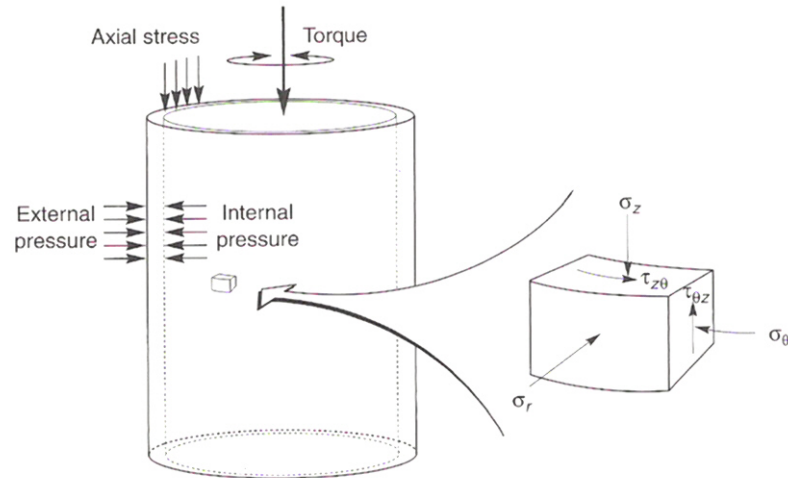
Figure 1.18: Mechanics of a cyclic torsional test (Kramer 1996).

2.1.7   Field (In-Situ) Evaluation of Liquefaction Susceptibility

The most common way to evaluate liquefaction hazards in engineering practice

is to correlate data gathered from the field. There are many types of in-situ tests that

can be performed; however, the Standard Penetration Test (SPT) and the Cone

Penetration Test (CPT) have become the standard by which liquefaction resistance is

evaluated. This is due to the large amounts of data that have been collected and

correlated with these tests and the many unknown factors associated with other in-situ

testing methods. Youd and Idriss et al (2001) provides detailed information on many of

the current evaluation methods using field testing data.

2.1.7.1   Evaluation Using Standard Penetration Test (SPT) Data

The SPT is the most common geotechnical engineering field test and has

been for many years. It has the largest case history database of any in-situ test. The

information gained from the test can be used not only for liquefaction analysis but for

many other soil analyses. As a result, the majority of field evaluations are done using

SPT blow count data. SPT measures the number of blows (N) to advance a SPT split

spoon sampler one foot into the ground. An overview of the SPT can be found in

McCarthy (1998).

Seed and Idriss (1971) were the first to correlate SPT blow count data with a

liquefaction resistance. The procedure for this evaluation is well known and is the

universal method for calculating liquefaction resistance of soils. While a brief

overview of this procedure is provided in the following sections, an in depth review

may be found in Youd and Idriss et al (2001).

2.1.7.1.1   Evaluation of Cyclic Stress Ratio (CSR)

The CSR is calculated from the projected earthquake obtained by using

the procedures described in section 1.1.5.1. Seed and Idriss (1971) formulated the

following equation for calculation of the cyclic stress ratio:

$$CSR = (\tau_{av} / \sigma'_{vo}) = 0.65(a_{max} / g)(\sigma_{vo} / \sigma'_{vo})r_d$$

where a_{max} = peak horizontal acceleration at the ground surface generated by the

earthquake; g = acceleration of gravity; τ_{av} = is the average cyclic shear stress

generated by the earthquake; σ_{vo} and σ'_{vo} are the total and effective vertical

overburden stresses, respectively; and r_d = stress reduction coefficient (Youd and

Idriss, et al (2001). The latter coefficient provides an approximate correction for

flexibility of the soil profile. The National Center for Earthquake Engineering

Research (NCEER) committee recommends the following equations developed by

Liao and Whitman (1986) for calculating the average values of r_d.

26

$$r_d = 1.0 - 0.00765z \qquad \text{for } z \leq 9.15 \text{ m}$$

$$r_d = 1.174 - 0.0267z \qquad \text{for } 9.15 \text{ m} < z \leq 23 \text{ m}$$

where z is the depth below the surface in meters at the location where the stress is being evaluated (Finn 2002).

2.1.7.1.2 SPT Liquefaction Assessment Chart (Finn 2002)

Seed and Idriss (1979, 1982, 1985) developed correlations between the SPT, N, and the CSR to cause liquefaction during earthquakes of magnitude M=7.5 on the basis of field data from many earthquake events (Fig. 1.19). Sites were considered to have liquefied based on observed surface features, such as sand boils and lateral spreading of the ground.

Seed et al (1985) drew a curve separating liquefied from non-liquefied sites, liquefied sites plot above the curve and non-liquefied sites plot below the curve. They noted that this curve corresponded to critical resistance stress ratios, CRR, for sands with 5% or less fines content (FC). They also noted increases in CRR for silty sands compared to clean sands having the same $(N_1)_{60}$. The increases depended on FC. Note that both CSR and CRR are shown on the curve in Figure 1.19. CSR refers to the value obtained in the calculation in Section 1.1.7.1.1. CRR refers to the value obtained by plotting SPT blow count on the $(N_1)_{60}$ axis, drawing a vertical line to the CRR curve then drawing a horizontal line to the CSR axis.

These increases in CRR were approximated by two additional CRR curves for FC = 35% and FC = 15%. These critical CRR curves are also shown in Fig. 1.19. All curves are shown dotted where they are not adequately restrained by field

data. The original Seed curve for clean sands with FC $\leq$ 5% was aligned through

the origin. After reviewing the available data, the NCEER Committee proposed a

modification to the Seed curve for FC $\leq$ 5%. The modification, shown by the lower

dotted portion of the CRR curve, is tangent to the original Seed curve at curve at

$(N_1)_{60} = 10$ and cuts the vertical CSR axis at a stress ratio of $\tau_{av}/\sigma'_{vo} = 0.05$.
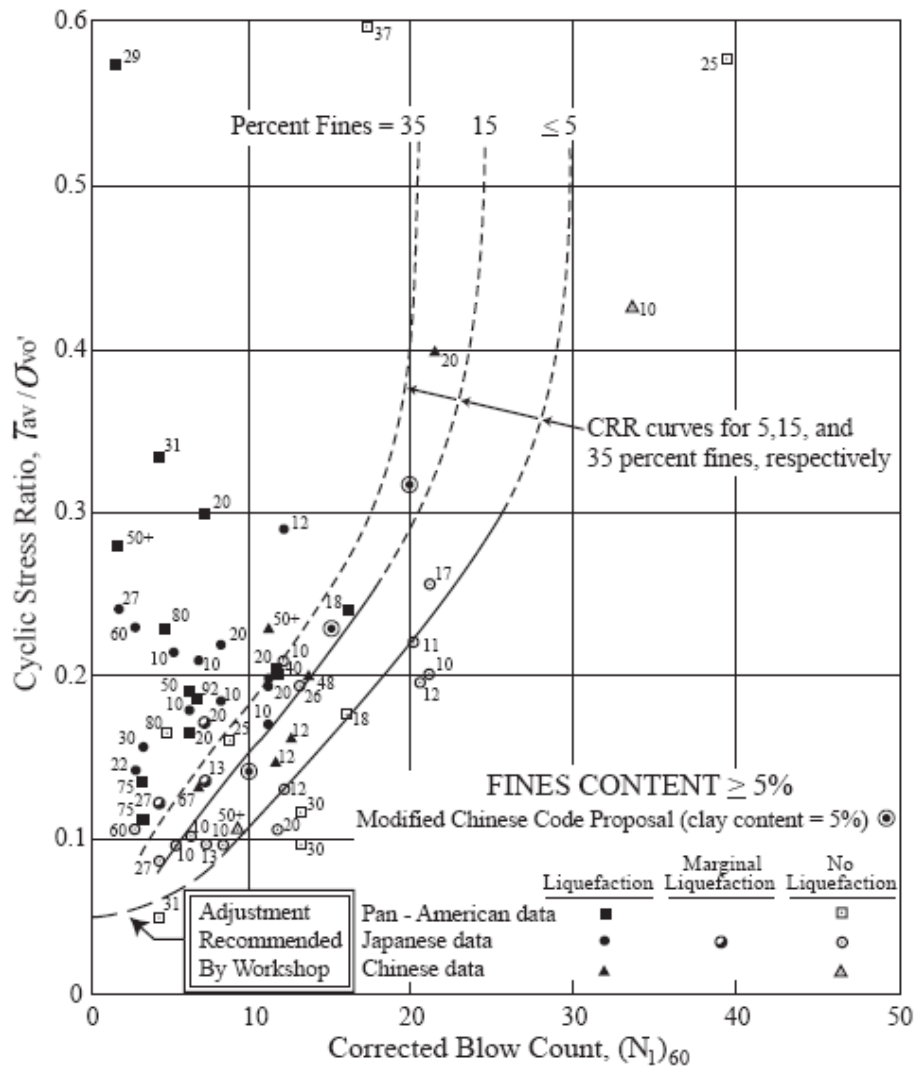
Figure 2.19: Simplified base curve recommended for calculation of CRR from

SPT data along with empirical liquefaction data (Youd and Idriss et al 2001).

Each site was characterized initially by the N value and the CSR from the earthquake calculated using CSR equation. However, to compare the ground conditions at site with those at another, it is necessary to standardize the measured penetration values to a standard driving energy and effective overburden pressure. Seed normalized the SPT to an energy level of 60% of the free-fall potential energy of the hammer and an effective overburden pressure of 100 kPa (nominally 1 tsf). Therefore, the field conditions for the site response data presented in Fig. 1.19 are characterized by the normalized SPT (N) value, $(N_1)_{60}$.

The NCEER Committee recommends that the hammer energy should be measured frequently at each site where the SPT is used. If not, the correction for energy level may be made using the data in Figure 1.20.

Country	Hammer type	Hammer release	Estimated rod energy (%)	Correction factor for 60% rod energy
Japan[a]	Donut	Free-fall	78	78/60 = 1.30
	Donut	Rope and pulley with special throw release	67	67/60 = 1.12
USA	Safety	Rope and pulley	60	60/60 = 1.00
	Donut[b]	Rope and pulley	45	45/60 = 0.75
Argentina	Donut	Rope and pulley	45	45/60 = 0.75
China	Donut	Free-fall[c]	60	60/60 = 1.00
	Donut	Rope and pulley	50	50/60 = 0.83

[a] Japanese SPT results have additional corrections for borehole diameter and frequency effects.
[b] Prevalent method in the USA today.
[c] Pilcon-type hammers develop an energy ratio of about 60%.

Figure 2.20: Energy ratios for different SPT procedures (Finn 2002).

A commonly used correction factor, C_N, for the effects of effective overburden pressure on measured N values is that proposed by Liao and Whitman (1986),

$$C_N = (P_a / \sigma'_{vo})^{0.5}$$

where σ'_{vo} is expressed in the same units as the atmospheric pressure P_a. Then $(N)_{60}$ at σ'_{vo} is corrected to $(N_1)_{60}$ at 100 kPa by:

$$(N_1) = C_N(N)_{60}$$

The NCEER Committee recommends an upper value of 1.7 for C_N.

2.1.7.1.3 NCEER Corrections for Fines Content (Finn 2002)

Idriss and Seed developed the alternative approach to CRR corrections for FC given by Youd and Idriss et al (2001) that was adopted by the NCEER Committee. The correction for converting $(N_1)_{60}$ to the clean sand equivalent $(N_1)_{60\_CS}$ is as follows:

$$(N_1)_{60\_CS} = \alpha + \beta(N_1)_{60}$$

$$\alpha = 0 \qquad\qquad\qquad \text{for FC} \leq 5\%$$

$$\alpha = \exp[1.76 - (190/FC^2)] \quad \text{for } 5\% < FC < 35\%$$

$$\alpha = 5.0 \qquad\qquad\qquad \text{for FC} \geq 35\%$$

$$\beta = 1.0 \qquad\qquad\qquad \text{for FC} \leq 5\%$$

$$\beta = [0.99 + (FC^{1.5}/ 1000)] \quad \text{for } 5\% < FC < 35\%$$

$$\beta = 1.2 \qquad\qquad\qquad \text{for FC} \geq 35\%$$

These equations give essentially the same curve for FC = 35% as the Seed et al curve in Fig. 1.19, but the curve for FC = 15% plots to the right of the original Seed et al curve.

2.1.7.1.4 Earthquake Magnitude Scaling Factor, K_m

The CRR curve in Figure 1.19 is normalized to an earthquake magnitude of M = 7.5. Earthquakes of other magnitudes may be scaled using the scaling factor, K_m, according to the equation:

$$CRR_M = K_m \times CRR_{7.5}$$

K_m may be estimated by using the values from Figure 1.21. The "Idriss (1995)" values, defined by the equation $K_m = 10^{2.24} / M^{2.56}$, are recommended by NCEER as the lower bound for earthquake magnitude scaling factors.

Magnitude (*M*)	Seed and Idriss (1982)	Idriss (1995)	Ambraseys (1988)
5.5	1.43	2.20	2.86
6.0	1.32	1.76	2.20
6.5	1.19	1.44	1.69
7.0	1.08	1.19	1.30
7.5	1.00	1.00	1.00
8.0	0.94	0.84	0.67
8.5	0.89	0.72	0.44

Figure 2.21: Various earthquake magnitude scaling factors (Finn 2002).

2.1.7.1.5   Effective Overburden Scaling Factor, K_σ

Tests have shown that resistance against liquefaction increases with increasing effective confining stress. To account for this the correction factor, K_σ, is used. Values of K_σ are defined by the equation:

$$K_\sigma = (\sigma'_{vo} / P_a)^{f-1} \text{ (Hynes and Olsen 1999)}$$

where f is an exponent that depends on the in-situ state of the soil. The NCEER committee adopted the Hynes and Olsen (1999) recommendations for f; for relative densities between 40-60%, $0.7 \le f \le 0.8$; for relative densities between 60-80%, $0.6 \le f \le 0.7$. A graph of this is shown in Figure 1.22.

2.1.7.1.6   Design CRR (CRR_D)

Taking into account the corrections for earthquake magnitude and confining pressure, the CRR_D for a given $(N_1)_{60}$ is defined as:

$$CRR_D = CRR \times K_m \times K_\sigma$$

The CRR_D may now be compared to the CSR to get a factor of safety (FS):

$$FS = CRR_D / CSR$$
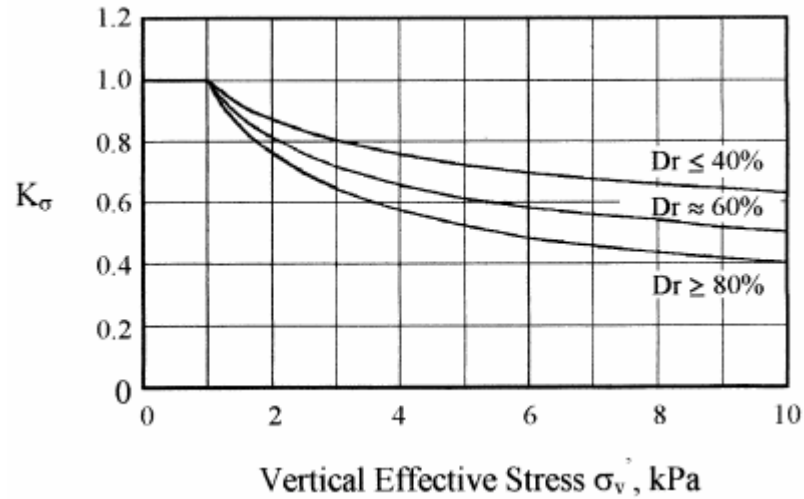
Figure 2.22: Correction factors Ks, for the effects of effective confining pressure recommended for practice (Finn 2002).

2.1.7.2   Evaluation Using Cone Penetration Test (CPT)

The primary advantage of the CPT is that a nearly continuous profile of penetration resistance is developed for stratigraphic interpretation (Youd and Idriss et al 2001). The results from the test are more repeatable than other tests, and it provides a more detailed definition of soil layers. The ability to detect thin sand layers is particularly advantageous in liquefaction evaluation. Despite these advantages, SPT data is usually used to verify CPT data in liquefaction analysis.

The chart correlating normalized CPT cone tip resistance and the CSR (Fig. 1.23) was developed by Robertson and Wride (1998). The cone tip resistance, q_{c1N}, and the CRR for CPT evaluation have many of the same correction factors as SPT evaluation, and the procedure to get a factor of safety follows along the same lines. More on the cone tip resistance vs. CSR graph and evaluation using CPT can be found in Youd and Idriss et al (2001) and Robertson and Wride (1998).

33
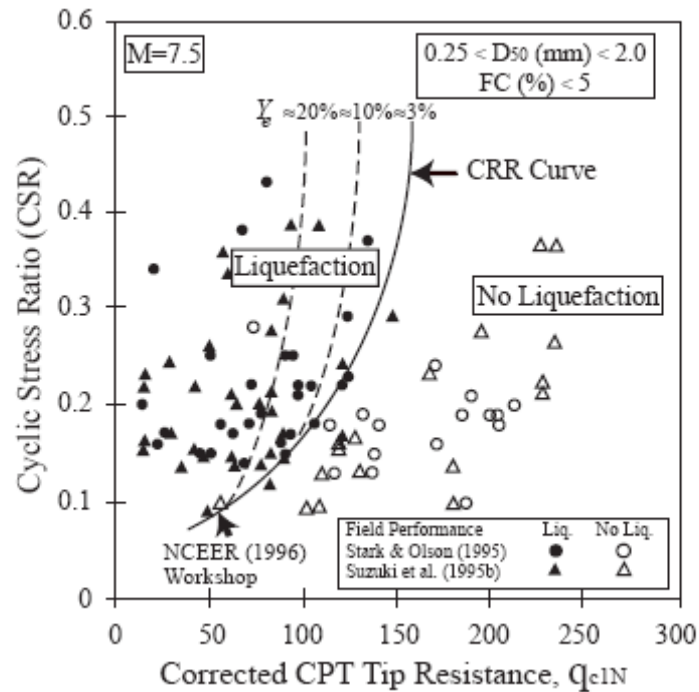
Figure 2.23: Curve recommended for calculation of CRR from CPT data (Youd and Idriss et al 2001).

2.2   Ground Modification

Once a liquefaction hazard has been identified at a site ground modification techniques may be considered as a means to reduce liquefaction susceptibility. These techniques involve changing the properties of the soil mass in order to improve engineering characteristics. Numerous techniques exist, but for liquefaction, a large concern is whether a structure is in place or yet to be built. While options on a preconstruction site cover a wide array of proven ground modification techniques, choices are restricted when a structure is already in place.

2.2.1 Preconstruction Ground Modification

Numerous ground modification techniques may be employed on a preconstruction site. Choosing a technique depends on the specific site conditions present at the time of construction. While many techniques are available, one or more events must occur for the mitigation of liquefaction to occur. The soil may be compacted, stabilized, or given a drainage path. These properties are usually accomplished using compaction, grouting, or drainage.

2.2.1.1 Compaction

Compaction collapses the void spaces within the soil, so that when earthquakes occur, pore pressure will not build high enough to cause loss of strength. Compaction is the most common solution to liquefaction susceptible site, and there are many methods to compact sandy deposits. These include both mostly vibratory and dynamic compaction techniques, but compaction grouting may also be used. In this process, stiff grout is used to create a grout bulb underground which displaces and compacts the soil surrounding it. However, this is a complicated and expensive process. Because of its familiarity and lower cost, vibration techniques are far more likely to be used for compaction. More on these methods can be found in Hausmann (1990) and Henn (1996).

2.2.1.2 Chemical, Permeation, and Jet Grouting

Chemical, permeation, or jet grouting may also be used to stabilize soil. These methods do not compact soil instead stabilization is done by either filling the

pore spaces in the soil using chemical or permeation grouting or by mixing the soil with cement using jet grouting. These processes strengthen the soil making it less susceptible to liquefaction. An in depth review of different grouting techniques can be found in Hausmann (1990) and Henn (1996).

2.2.1.3   Drainage

In recent years, the use of vertical drains to mitigate liquefaction hazards has gained acceptance. These drains, sometimes called earthquake drains, facilitate drainage of excess pore pressure during earthquakes. They consist of either columns in the soil filled with gravel or geosynthetic drains. The high permeability of the drains allows water to flow out freely when excess pore pressures are induced in the soil mass. A summary of this subject can be found in Adalier and Elgamal (2004) and Rollins et al (2004).

2.2.2   Under-Building Ground Modification

A problem in mitigating liquefaction hazards is improving ground conditions under an existing building. Very few techniques can be used in this situation, none of which have extensive research or database information to prove that they work effectively. Grouting has been done through the foundation of building in order to compact and stabilize the soil beneath, but this can cause damage to the underlying infrastructure and cause the building to be shut down while the work is performed. Drains have also been installed through foundations, but this can be impractical for the same reasons as grouting with the added threat of flooding. The lack of current

36

research in this area leaves no practical solutions to mitigating liquefaction hazards under existing buildings.

2.3   Summary

Since the awareness of its occurrence in the 1964 Niigata earthquake, liquefaction has been observed and researched around the world. Its susceptibility and the failure modes it creates have been studied, leading to the formulation and refinement of evaluation techniques to identify hazards. Ground modification techniques can be used on preconstruction sites to mitigate hazards. Ground modification under existing structures, however, creates a dilemma in the mitigation of liquefaction. Lack of research in this area has left engineers with only a few options when preventing in-place structures from being damaged by liquefaction. This justifies the need for current research in this area. The research covered in this paper addresses this issue by testing a soil additive to determine if it has the properties to remediate liquefaction.

CHAPTER 3: LABORATORY TESTING METHODS AND PROCEDURES

3.1   Overview of Laboratory Tests

In order to evaluate how hydrogel effects the strength, pore pressure, and permeability properties of Ottawa sand samples, laboratory tests were conducted on Ottawa sand samples containing varying percentages of hydrogel. To test the strength and pore pressure response of sand samples treated with hydrogel consolidated undrained (CU) triaxial tests were used. The flex wall permeameter test was run to assess changes in permeability hydrogel created in Ottawa sand samples. The triaxial and permeameter tests completed the main scope of this project and after their completion two secondary tests were performed to further evaluate the effects of hydrogel on Ottawa sand samples. These tests were an uplift pressure test to measure the uplift pressure hydrogel expansion created and a "cyclic mobility test" in which the effect of hydrogel was observed under unconfined dynamic loading. These secondary tests were improvised from available equipment and do not follow any ASTM standard. This chapter presents a summary of testing procedures; a detailed overview of equipment use is presented in Appendix D.

3.2 Sample Preparation for Consolidated Undrained Triaxial and Flex Wall Permeameter Testing

3.2.1 Sample Preparation Similarities

Sample preparation for CU triaxial testing and flex wall permeameter testing followed the same procedure. This is due to the similarities in testing setup between the two tests. Both tests involve setting a cylindrical sample, 2.8" in diameter, into a pressurized cell. In triaxial testing, the cell is equipped with a loading piston, used to load the sample during testing. The flex wall permeameter cell does not include this piston.

3.2.2 Sample freezing

The use of Ottawa sand in this project presented difficulties in sample preparation. Ottawa sand is a cohesionless soil, but it also has the disadvantage of being uniformly graded. This combination made for a soil that was susceptible to densification and collapse with small vibrations even when confined by testing membranes. During sample preparation, small vibrations were unavoidable when connecting tubing, placing the top cap and o-rings, and assembling the cell.

These problems with collapse and densification of samples led to sample freezing as an alternative preparation procedure. Frozen samples could be handled and placed in the triaxial and permeameter cells without worry of collapse and densification. Due to the available equipment, a new procedure had to be developed for the sample freezing process.

To freeze the samples, they were prepared in a mold. The mold was made of pieces of a Shelby tube cut to length. This length determined the height of the sample. The height of the sample was controlled by the test being run. ASTM recommends a height to diameter ratio of 2:1 for triaxial testing and 1:1 for permeability testing. To accommodate these height requirements the molds were cut to 6" for CU triaxial testing and 3" for flex wall permeameter testing. These molds were then covered on one end with a latex membrane which was secured with a rubber band (fig. 3.1). This membrane allowed for water to be added to the sample without having it drain away.

Figure 3.1: Latex membrane secured over the mold with rubber bands during mold preparation. Notice there are no wrinkles under the rubber band.

3.2.3   Funneling Method

To mimic a liquefiable soil, all samples, both with and without hydrogel, were made as loose as possible. A loose sample state was achieved by using a funnel to place the sand or sand/hydrogel mixture. This funneling method involved a large funnel connected to a piece of ¼" tubing. Sand or sand/hydrogel mixture was placed in the funnel and allowed to flow through the tube into the mold. The end of the tube was held within ¼" of the top of the sample as it was poured. This method created looser samples than just pouring sand alone.

3.2.4   Preparing a Sand Sample

Testing began by testing sand samples with no hydrogel added. This established a baseline to which samples with hydrogel added could be compared. Samples containing no hydrogel were prepared differently than samples that contained hydrogel. The hydrogel did not have to be mixed into the sand and there was no worry of the expansion hydrogel undergoes as it absorbs water.

To create a sand sample, a mold was prepared with membrane covering one end. Enough dry sand to overfill the mold was placed into a large beaker (1500g for triaxial tests, 600g for permeability tests). The mold was placed into the freezer, membrane down. The sand was placed in the funnel and funneled into the mold, dry. Once the mold was overfull with sand, the top of the mold was struck off. The sample is then made wet for freezing, a procedure outlined in Section 3.2.6.

3.2.5   Preparing a Sand/Hydrogel Sample

3.2.5.1   Preparing the Hydrogel

For testing, dry hydrogel needed to be small enough to fit into the pore spaces of the sand sample. Hydrogel, as purchased for this project, was in granular form with grain sizes of 1-2mm. These granules were too large to fit into the pore spaces therefore they had to be made smaller. To do this the hydrogel granules were crushed in a blender then sifted through a #200 (0.075mm mesh opening) sieve. Only the particles passing the #200 sieve were used in sample preparation as these particles were small enough to fit in the pore spaces of a sample.

3.2.5.2   Sand/Hydrogel Mixing

Creating samples that contained both sand and hydrogel required the two substances to be mixed together. This was achieved by first determining the amount of hydrogel to be added to the sample. The amount of hydrogel added is expressed as a percentage:

% hydrogel = (dry weight of hydrogel / dry weight of sand) x 100

The dry sand (1500g for triaxial, 600g for permeability) was evenly separated into separate beakers (5 for triaxial, 3 for permeability). Then the dry hydrogel was evenly separated into each of the beakers, on top of the sand. Each beaker was tilted to ~45$^\text{o}$, in hand, and slowly turned 5 revolutions until no hydrogel can be easily seen. Through trial and error this method was found to be the best way to evenly distribute hydrogel throughout the sample.

Once mixing was complete, a mold, prepared with a membrane (fig. 3.1), was placed into the freezer, membrane down. Each beaker of the sand hydrogel mixture was placed into the funnel and the mixture was funneled into the mold, dry. The mold was struck off once overfull. Water was then added to the sample as described in Section 3.2.6.

3.2.6 Wetting the Sample for Freezing

In order for the sample to freeze and the sand or sand/hydrogel particles to stabilize the sample must be wet with water. When the water in the sample freezes, particles in the sample will be surrounded by frozen water and locked into place. This allows the sample to be manipulated without collapse or densification.

Wetting the sample used long hypodermic needles to inject the samples with deaired water. The needle was inserted into the top of the sample after it had been struck off in the freezer. Insertion was done very carefully to cause as little disturbance to the sample as possible and thus avoid densification. The needle was inserted close to the bottom of the sample and water was injected slowly to prevent liquefaction from occurring at the injection point. Using one injection point, the sample was filled with water until water flowed from the top, and then the sample was allowed to freeze at -36^oF for at least three hours. After freezing, a large bulb of frozen water would be seen on top of the sample caused by expansion of water during freezing. This bulb was struck and grinded off using a rasp. This method of wetting the sample worked well for samples containing no hydrogel. However, this procedure did not work with samples that contained hydrogel.

3.2.6.1   Hydrogel Expansion

As wetting occurred in sand/hydrogel samples and the hydrogel began to absorb water and expand. This caused the sand hydrogel mixture to expand out of the top of the mold (fig. 3.2). It was suspected that because the sample was allowed to expand, that hydrogel was not being forced into the pore spaces in the sample. Instead, hydrogel particles were freely expanding in place (fig. 3.3) pushing soil particles apart. Therefore, a mold that would confine the sample was made to alleviate this problem (fig. 3.4). This mold, called a "confining mold", would not allow soil particles in the sample to displace and would, in turn, force hydrogel into the pore spaces of the sample.
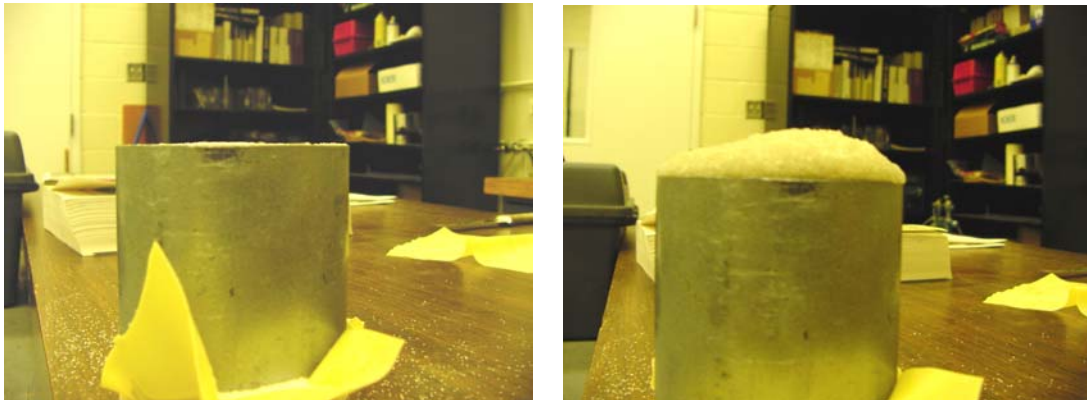
Figure 3.2: Sample expansion due to hydrogel. Sample before expansion (left). Sample after expansion (right).

Figure 3.3: In place expansion of hydrogel. Dark spots are individual hydrogel particles. This indicates hydrogel is not being forced into sample void spaces.

Figure 3.4: Confining mold used in sample preparation.

3.2.6.2 The Confining Mold

The confining mold uses a steel plate, called the "confining plate", to confine the sample from the top of the mold. This plate has many holes drilled though it to allow for the injection of water using the hypodermic needle. The plate is held in place by tightening a thumbscrew to it. The thumbscrew is connected to a crossbar, which is connected to two threaded rods, which are connected to a base plate that the sample mold rests on. Nuts on the threaded rods allow for the cross bar to be moved up and down to accommodate either the triaxial or permeability molds. The base plate, threaded rods, and crossbar assembly collectively is called the "confining frame".

3.2.7 Preparing a Sand/Hydrogel Sample Using the Confining Mold

To prepare a sample using the confining mold, hydrogel and a sand/hydrogel mixture was prepared as outlined in Section 3.2.5. Then, before placing the mold in the freezer, the crossbar was fit to the sample mold. The sample mold was placed on the base plate, and the confining plate was placed on top of the sample mold. The crossbar was then moved into place using the nuts on the threaded rod. This was done to be sure that the thumb screw could be tightened to the confining plate.

The confining mold was then disassembled and the confining frame was placed in the freezer with the cross bar swung out of the way. The sample mold (with membrane attached to one end) was then centered on the base plate. The sand/hydrogel mixture was funneled in and struck off. The confining plate was placed on top of the sample, the crossbar swung into place, and the thumb screw tightened. The placement

46

of the confining plate and movement of the crossbar and screw were done very carefully to create as little disturbance as possible. The sample was then wet using the holes drilled through the confining plate until water flowed from the top. Once the sample was wet, it was left to freeze.

3.2.8   Discussion on Confined Molds

3.2.8.1   Problems with Dry Spots

Wetting the sample became very difficult as the sample tried to expand but could not. As the hydrogel expanded, the pore spaces in the sample were filled, either with hydrogel or sand that was displaced into voids by hydrogel. This caused the soil to become the very tightly packed in the mold making needle penetration and water injection very difficult. As a result, dry spots were often found on the samples after extraction. Dry areas could be seen on the outside of the sample as non-frozen sand sloughed off. It had to be assumed, that if dry spots occurred on the outside, they would occur on the inside. The problem only increased as the percentage of hydrogel increased. As more hydrogel was introduced, the sample would try to expand more, making water injection increasingly difficult. This was particularly evident in a 100% hydrogel sample, where the needle could not even be inserted into the sample after it began to expand. Dry spots were counter-acted using more injection points, sometimes up to ten, and while this did not completely solve the problem, a saturated sample could be achieved in one out of two samples.

3.2.8.2 Water Expansion during Freezing

Water expansion during freezing caused another problem with confined molds. The force due to water expansion overcame the confining force of the molds. This bent and deformed the mold frames, rendering them unusable. Water expansion also caused small cracks in the sample. This was due to water freezing from the outside of the sample in. As water in the center of the sample froze, its expansion would cause the frozen areas around it to displace, resulting in cracks (fig. 2.7). The cracks were noticed after extraction of the sample but occurred during the freezing process. Evidence of which was seen by the displacement that caused the deformation of the mold frames.
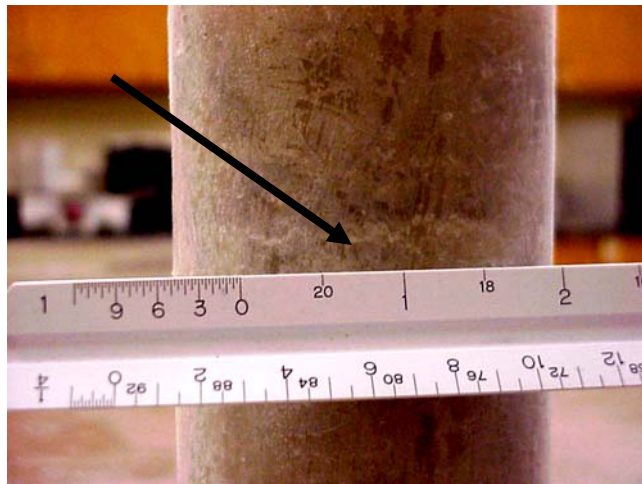
Figure 3.5: Crack due to water expansion in confined mold (arrow points to crack).

3.2.8.3   Advantage of Confined Molds

Despite these problems with the confined mold, it did stop the free expansion hydrogel in the sample (fig. 2.8). The individual hydrogel particles that could be seen in the sample before the use of confined molds could no longer be seen, suggesting that the hydrogel was forced into the pore spaces of the sample.

Figure 3.6: Comparison of visible hydrogel particles (dark spots) before confined molds (left) and after confined molds (right), showing hydrogel being forced into void spaces.

3.2.9   Post Freezing Procedure

Once the sample had frozen, the sample and mold (or confining mold) were removed from the freezer. The sample was extracted from the mold using a Shelby tube extractor. The samples were trimmed to remove areas of frozen water or to level the top of the sample using a rasp. The samples were then weighed and their height and diameter measured. Five measurements were taken for both height and diameter and averaged to obtain an average height and diameter.

3.3 Sample Setup in the Triaxial and Flex Wall Permeameter Cells

Because of the similarities in the triaxial and permeameter test cells, placing the sample in the cell and some pre-test procedures were the same for both tests. Before beginning to place the sample in either cell, all tubing should be connected and flushed with deaired water and porous stones should be saturated. Detailed procedures for deairing lines and sample placement are given in Section D.5.4 of Appendix D.

3.3.1 Sample Thawing

While the sample is frozen it was placed into the appropriate testing cell. All membranes, porous stones, filter paper, o-rings, and tubing were properly placed. Once the sample was in place, the test cell was assembled and the cell was filled with deaired water. All lines to the sample were closed and a cell pressure was placed on the cell. This pressure (40 psi) will drive air in the sample into solution as the sample thaws. This helped in sample saturation. Once the cell had been pressurized the sample was left to thaw for 3 hours.

3.3.2 Flushing the Sample

Once the sample was thawed, deaired water was flushed through the sample to remove any excess air. To do this a back pressure 2 psi below the cell pressure was placed on the bottom of the sample and a pressure 3 psi below cell pressure was placed on the top. This created a 1 psi pressure gradient between the top and bottom of the sample allowing water to flow from the bottom to the top of the sample. Once no air

bubbles were seen exiting the top of the sample this process was complete and all lines to the sample were closed.

3.3.3   Sample Saturation

Once the sample was run through with deaired water it was saturated. In order to accurately measure pore pressures, the sample must be very near to 100% saturation or compressing air bubbles in the sample will dissipate the energy transferred by the pore pressure. After thawing, saturation could take anywhere from 5 minutes to 5 hours. The saturation time depended largely on how much hydrogel is in the sample. Because the hydrogel is not fully saturated from injected water, it will soak up water from the back pressure reservoir. The more hydrogel in the sample, the more water it will soak up. The degree of saturation was measured using Skempton's "B" Coefficient (Holtz and Kovacs 1981), and during this study, only "B" values of at least 0.98 were used. "B" values are a measure of how saturated the sample is; for example, a "B" value of 0.98 would correspond approximately to 98% saturation. Observed "B" values may initially be too low and need to be increased. Values can be increased by increasing the cell and back pressure to the sample and than rechecking the "B" value in 15-20 minutes. The increased pressure will drive more air into solution, and the additional time will allow it to do so.

B = Δ pore pressure / Δ cell pressure, so to measure the B value, a 5 psi change in the cell pressure was induced. The change in pore pressure corresponding to the change in cell pressure was recorded and the B value was calculated. If the B value

was too low the cell pressure was increased by 5 psi and the B value was checked again in 15-20 minutes. Once a B value of 0.98 was reached testing began.

3.4   Consolidated Undrained Triaxial Testing

Once the sample was adequately saturated, triaxial testing could proceed. Consolidated undrained triaxial tests were run while measuring pore pressure, displacement, and load. Tests were run using a Brainard-Kilman S-600 triaxial load frame and triaxial cell. Pressures were regulated on a Brainard-Kilman S-500 triaxial/permeability panel board with an E-114 pressure transducer. Sensor readings were taken electronically with an Optim Electronics Megadac and Total Control Software (TCS) for DOS. The Megadac was set to take five readings per second, and the strain rate on the load frame was set to 0.01in/sec. With the readings from the sensors, pore pressure and load could be plotted against deformation from each test. These plots showed the effect of hydrogel on pore pressure and strength under triaxial loading.

3.4.1   Triaxial Consolidation

Triaxial tests were consolidated before testing. Sample consolidation will drive excess water out of the sample.   Removing excess water in the sample will also remove access pore pressures that have increased during sample saturation. By controlling the amount of pore pressure relived from the sample during consolidation, effective stress can be controlled. Consolidation will reduce the pore pressures in the sample that have increased during saturation which will allow testing to start at a pre-determined pore pressure. This will allow for accurate pore pressure measurements during testing.

52

For this study triaxial testing samples were consolidated by driving all excess pore pressure from the sample at the cell pressure needed to attain saturation. Therefore effective stress in the sample was equal to the cell pressure. For triaxial tests this pressure is called the total consolidation pressure and is denoted as σ_{3c}. Consolidation was conducted by opening the top drainage line from the sample, and allowing the sample to drain freely (no back pressure) under the cell pressure until equilibrium was reached. Change in volume due to consolidation was not measured. When sample consolidation was finished triaxial testing began measuring pore pressure, load, and deformation.

3.5 Flex Wall Permeameter Testing

Flex wall permeameter test was conducted to measure if sample permeability changed with the addition of hydrogel. As hydrogel expands and fills the pore spaces, permeability should be reduced because there is less room for water to move through the sample. This phenomenon should happen with any substance that fills the pore spaces in soil. But the degree to which this happens was tested. Because all samples were created to simulate hydrogel having already been put in place, hydrogel was assumed to stay in place as water was run through the sample. Therefore no hydrogel was assumed to be in the effluent and the permeability of a hydrogel/water mixture was not considered. Flexible wall permeameter testing followed ASTM D 5084: Standard Test Methods for Measurement of Hydraulic Conductivity of Saturated Porous Materials Using a Flexible Wall Permeameter. An ELE International, Tri-Flex 2 Permeability Test System was used connected to a Durham-Geo S-500 Triaxial/Permeability Panel with auxiliary board.

Data was recorded by hand on a data sheet. Auxiliary board operation is outlined in Durham-Geo S-500 Triaxial/Permeability Panel owner's manual.

3.5.1   Flex Wall Permeameter Consolidation

Consolidation of permeability samples will drive out excess water and allow for the accurate measurement of water entering and exiting a sample. For flex wall permeameter testing, soil samples were consolidated to a 5 psi effective confining pressure. The initial effective confining stress is set using the difference between the cell pressure (regulator 1) and the back pressure (regulator 2). The consolidation pressure is called the effective consolidation pressure and is denoted as σ'_{3c}.

Consolidation is achieved by opening the back pressure line to the sample and allowing water to drain out until equilibrium is achieved. Volume change due to consolidation was not measured. When sample consolidation had finished flex wall permeameter testing began measuring influent and effluent with time.

3.6   Unit Weight Calculations for CU Triaxial and Flex Wall Permeameter Tests

After testing was completed, unit weights were calculated for both triaxial and permeameter tests. Once a test had been run the sample was dumped into a large foil baking pan. Any soil or hydrogel particles left on the membrane, top cap, or base plate were also washed into the pan. The sample was then dried in an oven overnight and the dry weight of the sample was determined. The dry unit weight was then calculated using height and diameter measurements taken after the sample was extracted from the mold and trimmed. The water content of the sample was also calculated using the dry and wet

weights (obtained after sample extraction). The pre-test dry unit weight is called the initial unit weight denoted by $\gamma_{d\ initial}$. The calculated dry unit weight is a pre-test unit weight and does not account for volume change during testing.

3.7   The Uplift Pressure Test

The uplift pressure test was an improvised run to evaluate the uplift pressure the expansion of hydrogel exerts. To do this, a sand/hydrogel triaxial sample was formed in the triaxial mold on triaxial load frame platen. This sample was not frozen and was created directly on the load frame. The mold was never removed from the sample. The mold was centered under the load cell before funneling the sand/hydrogel mixture (because the load platen was manufactured with recesses to accommodate bolt heads the base plate of the confining frame was used as a flat surface). Once the sample had been struck off, the confining plate was placed on top of the mold and 6" bolt was placed between the confining plate and the load cell (fig. 3.7). This bolt allowed room for the injection of water and transferred load from the plate to the cell. The initial load reading was recorded. Deaired water was then injected into the sample with as many injection points as necessary until the water flowed from the top of the sample. The sample was allowed to sit for 15-20 min. and the load reading was recorded. Water was then injected again until overflowing and allowed to sit for 15-20 min. and the load reading was recorded. This process was repeated until there was no load change observed after water injection. The using the load readings and the cross sectional area of the sample, an uplift pressure was calculated. A Boart Longyear E-210 load cell and S-400 digital readout was used to run the test.

Figure 3.7: Uplift pressure test setup. Notice the bolt, transferring load from the load cell to the top plate (arrow points to bolt).

3.8   The Cyclic Mobility Test

The cyclic mobility test was a test run to observe the effects of hydrogel under an unconfined dynamic load. Because cyclic testing equipment normally used to induce dynamic loads in earthquake research, i.e. cyclic triaxial, cyclic simple shear, cyclic torsional, or shake table, were not available to this project, a test was improvised using a flow table and mold described in ASTM C 230/C 230M: Standard Specification for Flow Table for Use in Tests of Hydraulic Cement (fig. 3.8). This table used a motor to drop a table repeatedly over a set distance a chosen number of times a minute. This table provided the dynamic load necessary to test the effects of hydrogel in unconfined samples.

Samples were prepared in the mold described in ASTM C 230/C 230M. Sand or sand/hydrogel mixture was funneled into these molds and confined using the confining

plate and a large c-clamp (fig. 3.9). The samples were not frozen. Pictures of the sample were taken before testing started. The flow table apparatus was then started using 25 drops/min. When 25 drops were completed pictures were taken of the failed sample (fig. 3.10).

Figure 3.8: Flow table and mold used in cyclic mobility testing.

Figure 3.9: Top plate secured with c-clamp during sample preparation for cyclic mobility testing.

Figure 3.10: A sample before and after cyclic mobility testing. The picture on the left shows the sample before testing and the picture on the right, after testing.

CHAPTER 4: LABORATORY TESTING RESULTS

4.1 Consolidated Undrained Triaxial Testing

4.1.1 Overview

Consolidated undrained triaxial tests were performed with measurements of pore pressure, load, and displacement. These measurements allowed the pore pressure and strength response of Ottawa sand (untreated samples) and Ottawa sand/hydrogel (treated samples) samples to be observed. The raw testing data for all triaxial tests are presented in Appendix D. Treated tests were run with varying percentages of hydrogel in order to evaluate the effect of hydrogel on the strength and pore pressure response of Ottawa sand samples. Percentages used were 0.043%, 0.085%, 0.01%, 0.25%, and 0.50% percent hydrogel. A 100% hydrogel sample was also tested in order to establish a bound for sample response. The treated samples were then compared with untreated samples and the 100% hydrogel sample. "Jumps" or discontinuities in plots are due to piston seating or mechanical error of the loading frame.

4.1.2 Definition and Selection of Percent Hydrogel

Percent hydrogel refers to the amount of hydrogel each sample contains. For sand/hydrogel samples, percent hydrogel = wt. of hydrogel / wt. of Ottawa sand. 0% hydrogel samples refer to samples that contain no hydrogel and the 100% hydrogel sample contains no sand.

Selection of the percent hydrogel used during testing began by estimating the

void spaces within a sample. Using the void ratio and taking into account the

that hydrogel will undergo expansion when saturated, it was believed that 0.085%

hydrogel would fill the voids in the sample. Therefore, sand/hydrogel testing began

with this percentage (0.10% hydrogel used in SANDHYDRO1 is 0.085% rounded to

the nearest tenth decimal place. When this test was run, a balance with the precision to

measure the small amounts of hydrogel used in creating a 0.085% hydrogel had not

been obtained). Then this percentage was decreased by one half (0.043%) to see if

differences in pore pressure and strength response could be seen. The initial 0.085%

hydrogel was re-evaluated as confined molds were used for sample preparation. It was

believed that if the samples were confined, expanding hydrogel would be forced into

smaller void spaces. Therefore 0.25% and 0.50% hydrogel samples were tested.

4.1.3   Effect of Unit Weight on Triaxial Results

4.1.3.1   Variation of Unit Weight During Sample Preparation

Unit weights measured for this project were a pre-test unit weight. Changes

in sample volume during consolidation were not measured; therefore, unit weight

measurements refer to the dry unit weight of the sample as prepared in the mold and

are denoted as $\gamma_{d\ initial}$. During sample preparation, pre-determined weights of sand

were not used to fill the molds (i.e. 2 lbs of sand was not used to exactly fill the 6"

tall, 2.8" diameter mold). Instead 1500g of sand was prepared for all samples.

Hydrogel was then added to the 1500g of sand to achieve the percentage of hydrogel

desired. The mold was filled to over-full and then struck off. With this method of

mold filling, variability in sand placement in the mold affected the amount of sand the sample contained. Therefore, the weight of sand in the mold fluctuated from sample to sample. This caused the unit weight (weight per unit volume) of the sample to vary (Table 4.1). There was a 14.7 pcf difference between the highest and lowest unit weights achieved.

Table 4.1: Sample information for consolidated undrained triaxial testing. SAND"X" is an untreated sample. SANDHYDRO"X" is a treated sample.

Test Name	% Hydrogel	Confined	B Value	Initial Dry Unit Weight (γ_d initial) (pcf)[1]	Consolidation Pressure σ_{3c} (psi)
SAND1	0.00	no	0.95	102.9	80
SAND5	0.00	no	0.98	103.0	45
SAND6	0.00	no	0.98	103.8	45
SAND7	0.00	no	0.96	102.9	45
SAND8	0.00	no	0.96	101.9	45
SAND9	0.00	no	0.98	98.6	45
SAND10	0.00	no	0.98	98.8	45
SAND11	0.00	no	0.99	102.5	49
SAND12	0.00	no	1.00	97.1	45
SANDHYDRO1	0.10	no	0.98	89.1	45
SANDHYDRO2	0.085	no	0.99	93.0	45
SANDHYDRO3	0.085	no	0.98	93.6	45
SANDHYDRO4	0.085	yes	1.00	98.6	45
SANDHYDRO5	0.043	yes	1.00	95.7	49
SANDHYDRO6	0.250	yes	0.99	95.7	47
SANDHYDRO7	0.500	yes	1.00	96.4	45
HYDRO	100.00	yes	1.00	N/A	45

NOTES: 1 – Unit weight before testing.

4.1.3.2 Importance of Unit Weight

Unit weight is important to triaxial testing because it affects both the pore pressure and strength response of the sample. Due to reasons stated in Section 4.1.3.1, consistency in unit weight could not be achieved, which is illustrated by the 14.7 pcf difference between the highest achieved and lowest unit weights. So, all testing data had to be reviewed with the understanding that unit weight varied and affected results.

4.1.3.3 Effect of Unit Weight on Pore Pressure and Strength

Unit weight affects the pore pressure response of the sample. As the unit weight is decreased the pore pressure response is increased and vice versa as illustrated in Figure 4.1.   This figure shows a more than 50% increase in peak pore pressure with a 5.4pcf decrease in unit weight. This phenomenon is explained by the amount of water the sample is able to hold. Because a loosely configured sample (low unit weight) has more pore spaces, it can hold more water. During triaxial testing these pore spaces collapse causing pore pressure increase, and effective stress decrease. The decrease in effective stress decreases the strength of the sample. Therefore, pore pressure measurement was of great importance. This, in turn, makes the unit weight of the soil significant in this study.

Effect of Unit Weight on Pore Pressure for Ottawa Sand
σ_{3c} = 49psi
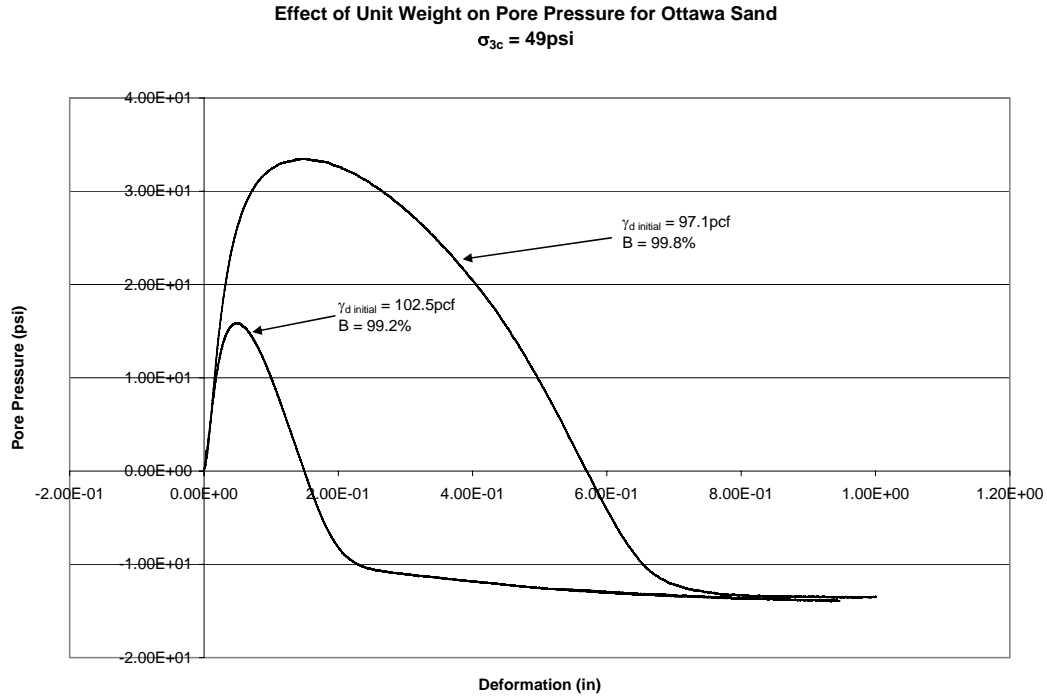
Figure 4.1: Effect of unit weight on pore pressure for Ottawa sand during triaxial testing. Pore pressure vs. deformation from tests SAND11 (fig. 3.17) and SAND12 (fig. 3.19) are shown. σ_{3c} = 49psi. SAND11 has been zeroed.

4.1.4   Importance of the "B" Value

Skempton's "B" Coefficient or "B" value (labeled as B on plots) is another important factor to consider when viewing test results. As mentioned in Chapter 3 Section 3.5.4.4, all tests were run with B > 0.98. The "B" value is a measure of sample saturation, if the value is high, the sample is more saturated than if it is low. The "B" value obtained is approximately equal to the percent saturation in the sample, although the actual percent saturation of the sample may be higher than the "B" value (Holtz and Kovacs 1981). Sample saturation is important in obtaining pore pressure and strength measurements because of water in the soil. If the pore spaces in the soil are not

completely filled with water, accurate pore pressure and strength measurements will not be obtained. This is due to the compressibility of air; small pockets of air in the sample will absorb energy during triaxial loading. Therefore, all of the energy created by the load will not be transferred to the water resulting in lower pore pressures.

4.1.5   Consolidation Pressure

Samples in triaxial testing were consolidated at σ_3 which provided an adequate B value. This pressure was not constant throughout testing and therefore the consolidation pressure (σ_{3c}) varied from test to test. Because the consolidation pressure was high for triaxial testing (80-45psi) samples could not be considered loose during testing. Volume change during consolidation was not measured and, as a result, unit weights or void ratios during testing are unknown.

4.1.6   Shear Strength Properties of Ottawa Sand

4.1.6.1   Overview

Shear strength of soils is governed by the equation $S = c + \sigma'\tan\phi$, where S is the shear strength, c is soil cohesion, σ' is the effective stress, and ϕ is the internal angle of friction. For cohesionless soils c is zero; therefore, the shear strength of sand is a function of the effective stress and internal angle of friction.

4.1.6.2　Pore Pressure Response of Untreated Samples

      The pore pressure response of untreated samples tested are presented in

Figure 4.2.　Sample information is presented in Table 4.1.　Figure 4.1 shows the

change in pore pressure with sample deformation.　As can be seen in the plots, pore

pressure initially increases and peaks somewhere between 1.0% and 2.5% strain.　As

strains increase, the pore pressure decreases and eventually becomes negative at large

strains.　Differences in the strains at which changes in pore pressure occur between

samples is attributed to variation in relative density during testing and B value.
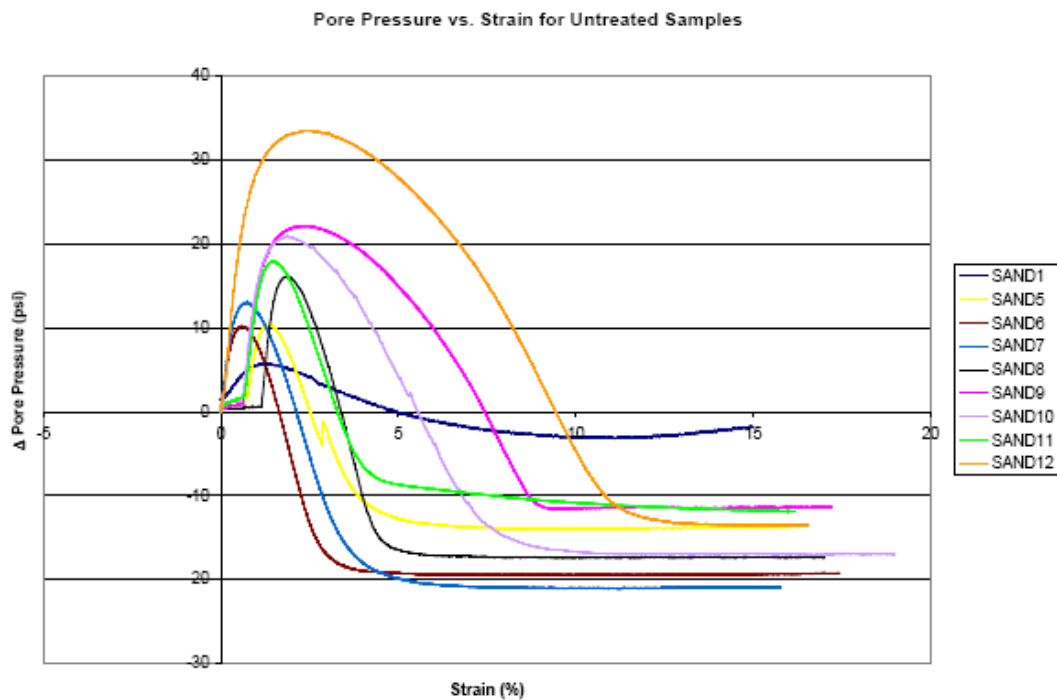
Figure 4.2: Pore Pressure vs. Strain for untreated samples from consolidated undrained triaxial testing.　Sample information is shown in Table 4.1.

4.1.6.3   Sample Dilation

Negative pore pressures are caused by sample dilation. Dilation is an increase in sample volume and is caused by soil particles moving around one another as the soil is compressed during loading. This event is expected in triaxial testing of sand consolidated to high pressures.

4.1.6.4   Strength Response of Untreated Samples

Figure 4.3 show deviator stress vs. strain for untreated samples. The stress vs. strain response shows an initial peak or "bump" at 1 to 2% strain where the samples yield plastically. This yielding corresponds to the rise and peak in pore pressure seen in Figure 4.2. The initial rise of pore pressure at low strains lowers effective stress within the sample causing a reduction in strength seen as the plastic yielding. Figure 4.3 also shows the samples undergoing strain-hardening once the sample yields plastically. Strain-hardening occurs as the samples begin to dilate and pore pressures begin to fall, raising effective stress and strength. At high strains the samples have failed as the stress-strain curve levels out. Variations in strain where events occur are attributed to differences in the relative density of the sample during testing.

Figure 4.4 presents q/p' vs. strain for untreated samples. Peak q/p' corresponds to maximum obliquity (maximum inclination of the Mohr failure envelope) for the sample tested. Peak q/p' also coincides with the maximum ratio of shear stress at failure / effective stress at failure. The plane at failure is on the plane of maximum obliquity. Therefore, peak q/p' represents failure for untreated samples.

Figure 4.4 shows that SAND1-8 and SAND11 have peaked and failed by 10% strain.

SAND9, 10, and 12 are continuing to fail becoming asymptotic to a peak and are also

considered to fail at 10% strain.
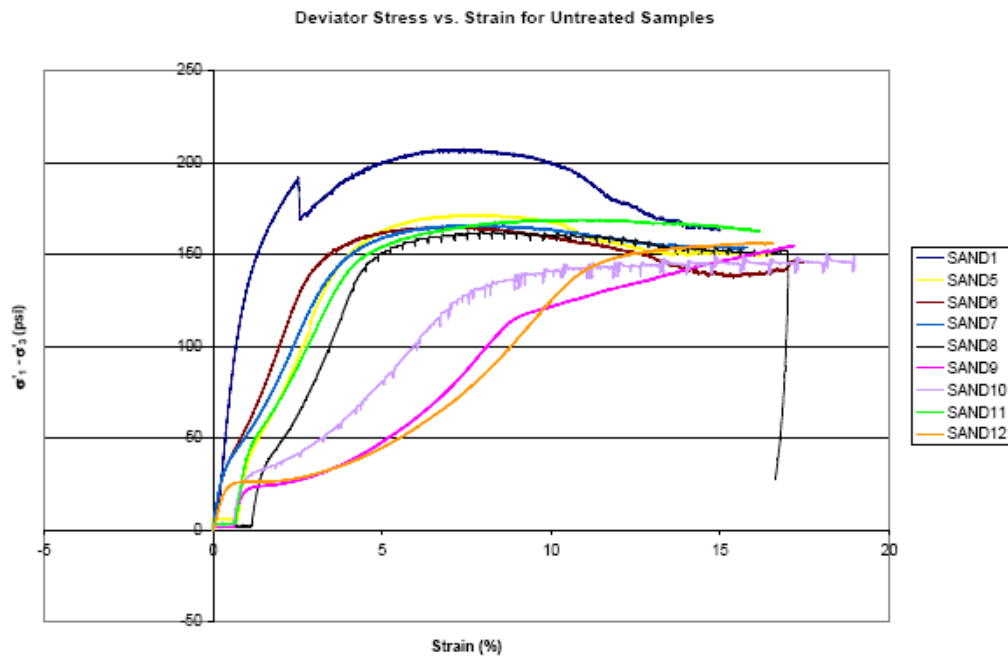
Figure 4.3: Deviator Stress vs. Strain for untreated samples form consolidated undrained triaxial testing. Sample information is shown in Table 4.1

q/p' vs. Strain for Untreated Samples
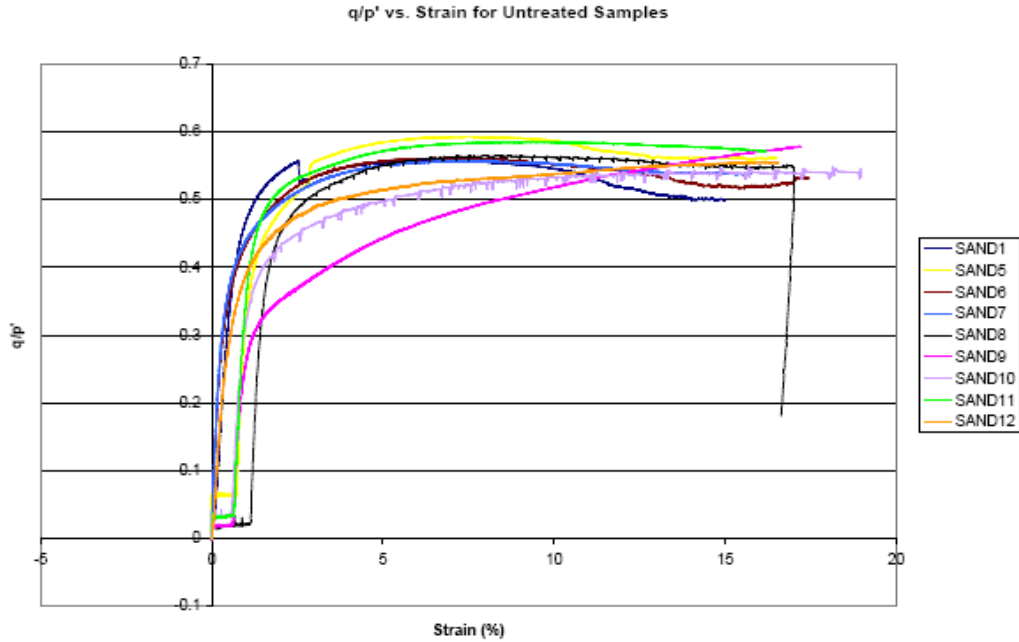
Figure 4.4: q/p' vs. Strain for untreated samples form consolidated undrained triaxial testing. Sample information is shown in Table 4.1

4.1.6.5   Internal Angle of Friction

To determine the internal angle of friction for Ottawa sand samples, a p-q plot was drawn for all untreated samples and is presented in Figure 4.5. The p-q plot shows the stress path for the sample as it is stressed in axial compression. As the sample fails the stress path follows along a failure plane defined by a and Ψ. These parameters relate to c and ϕ for the sample: $c = a / \cos\phi$ and $\sin\phi = \tan\Psi$. For sand c $= a = 0$. Figure 4.5 shows a best fit failure plane for all untreated samples with $\Psi = 26.5^o$ establishing ϕ for Ottawa sand in this project at ~30°.

68
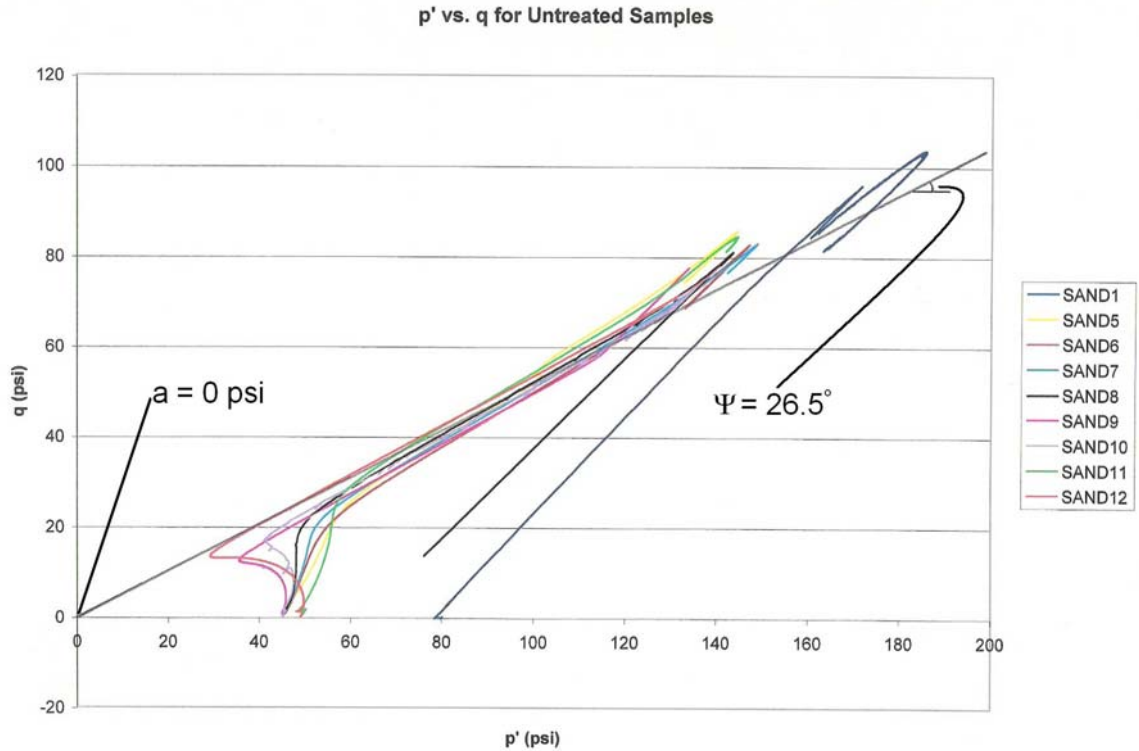
Figure 4.5: p-q Plot for untreated samples from consolidated undrained triaxial testing. Sample information is shown in Table 4.1.

4.1.7 Shear Strength Properties with Variation in Percent Hydrogel

4.1.7.1 Overview

Samples containing hydrogel (treated samples) are also defined by the shear strength equation: $S = c + \sigma'\tan\phi$. The cohesion of hydrogel was not evaluated during testing and therefore cohesion was not considered to contribute the strength of treated samples. This is a conservative approach since trends seen in σ' and ϕ do not change if cohesion is added to the strength equation. Cohesion only shifts the trends by the value of c. Since it is assumed that c does not add to the shear strength of treated samples, their strength is controlled by the internal angle of friction and the effective stress.

69

4.1.7.2 Pore Pressure Response of Treated Samples

Figure 4.6 shows the change in pore pressure vs. strain for untreated samples. SANDHYDRO4, SANDHYDRO5, SANDHYDRO6, and SANDHYDRO7 were used to create this plot. These samples were prepared using the confining mold. This plot shows variations in pore pressure responses with changes in percent hydrogel. Variations in the peak pore pressure between samples is attributed to variations in relative density during testing.

The effect of sample dilation on pore pressure changes between samples. By comparing SANDHYDRO6 with SANDHYDRO7 it can be seen that the effects of dilation are being lessened with the increasing percentage of hydrogel. The more hydrogel is added to the sample, the more the pore pressure response becomes like that of a 100% hydrogel sample (Fig. 4.7).

A comparison between SANDHYDRO7 and the 100% hydrogel sample (Fig.4.7) shows that at 0.50% hydrogel the sample reacts like 100% hydrogel. This establishes the highest percentage of hydrogel that can be added to the soil before it acts as hydrogel. Since the pore pressure response of the 0.50% hydrogel sample and the 100% hydrogel sample are the same, the addition of more hydrogel will not affect the response further.

Bryan Shiver
10/19/03

Pore Pressure vs. Strain for Treated Samples
Samples Prepared with the Confined Mold
SANDHYDRO4 and SANDHYDRO6 have been zeroed
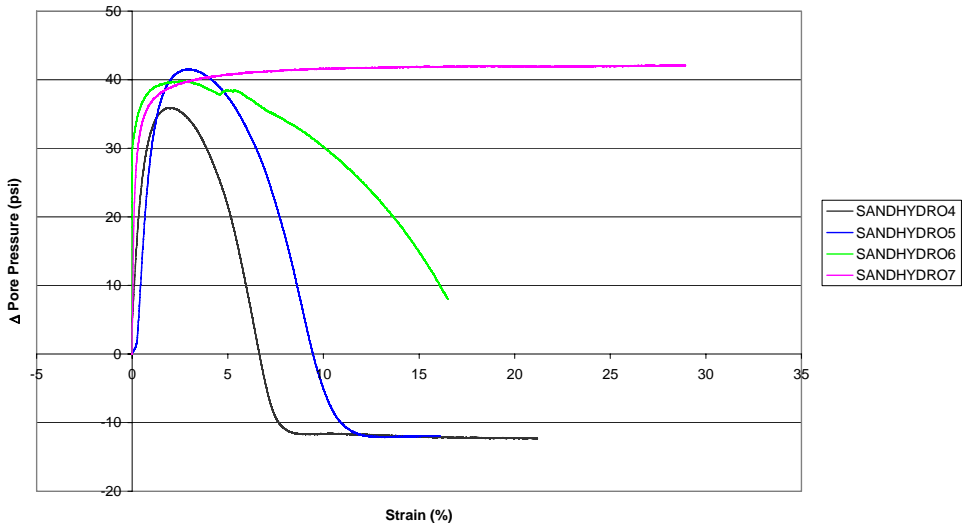
Figure 4.6: Change in Pore Pressure vs. Strain for treated samples from consolidated undrained triaxial testing. Sample information is present in Figure 4.1.

Bryan Shiver
10/1/03
B = 0.996

Pore Pressure vs. Strain
HYDRO: 100% Hydrogel; σ_{3c} = 45psi
Sample Prepared with the Confined Mold
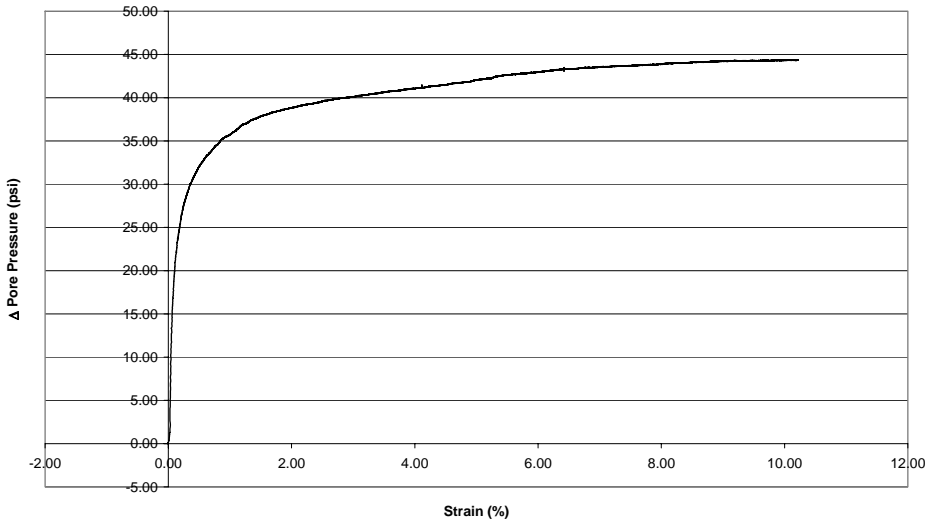
Figure 4.7: Change in Pore Pressure vs. Strain for 100% Hydrogel sample from consolidated undrained triaxial testing. Sample information is present in Figure 4.1.

71

4.1.7.3 Variation in Internal Angle of Friction with Variation in Percent Hydrogel

p'-q plots were drawn for treated samples prepared in the confined mold. These plots are presented in Appendix D. From the p'-q plots, ϕ was calculated for each treated sample. Figure 4.8 presents ϕ vs. percent hydrogel and shows how the internal angle of friction changes as hydrogel is added to Ottawa sand.

This plot shows that while ϕ varies with percent hydrogel, this variation is considered acceptable for testing and is attributed to differences in relative density of samples during testing. The variation in percent hydrogel is bounded in Figure 4.8, representing an acceptable range of 28 – 33 degrees. Therefore, hydrogel is not considered to effect ϕ in Ottawa sand samples.
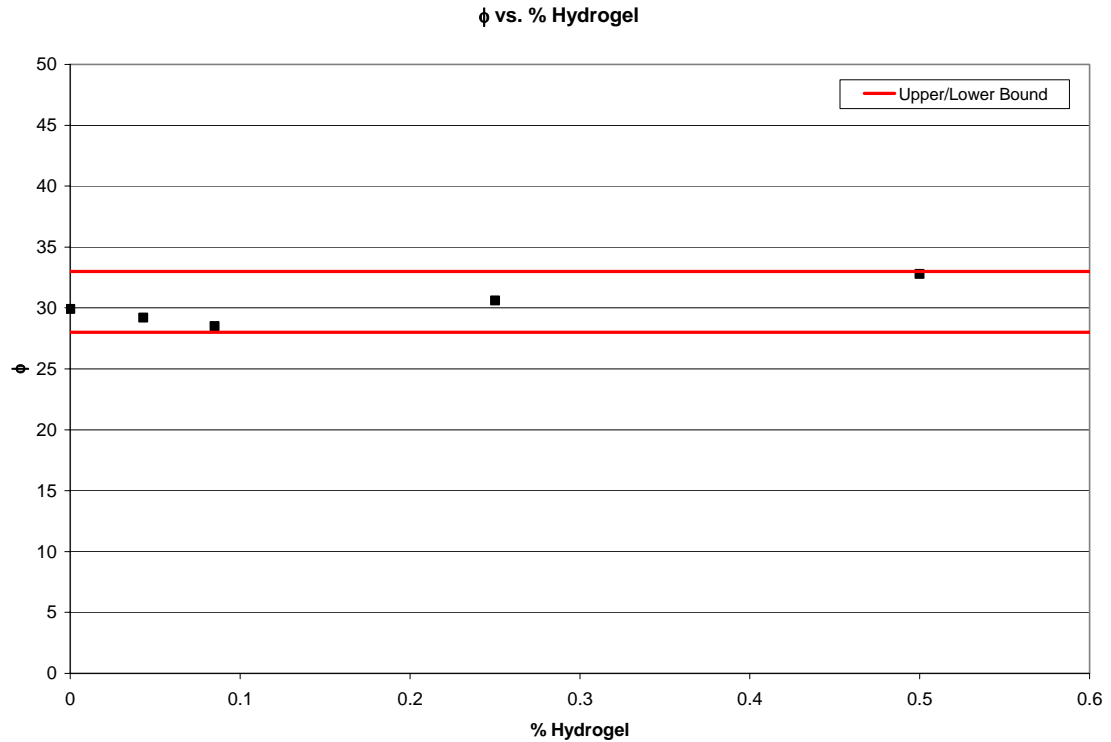
Figure 4.8: φ vs. Percent Hydrogel from consolidated undrained triaxial testing.

4.1.7.4 Variation in Effective Stress with Variation in Percent Hydrogel

Since φ does not change with the addition of hydrogel to Ottawa sand samples, changes in effective stress was evaluated. This is done by evaluating changes in Skempton's "A" Coefficient with changes in percent hydrogel. Skempton's "A" Coefficient defined by the equation: $A = \Delta$ pore pressure/Δ deviator stress. A defines the effective stress at any strain for a sample. When $A < 1$ effective stress is positive, when $A = 1$ effective stress is zero, and when $A > 1$ effective stress is negative.

A vs. strain was plotted for all samples tested. These plots are presented in Appendix D. Peak A (A_{max}) taken from these plots and compared to percent

hydrogel. Peak A corresponds to the peak pore pressure and represents the point where effective stress is lowest for the samples tested. Figure 4.9 shows peak A vs. percent hydrogel. This plot shows effective stress being decreased as percent hydrogel is increased.
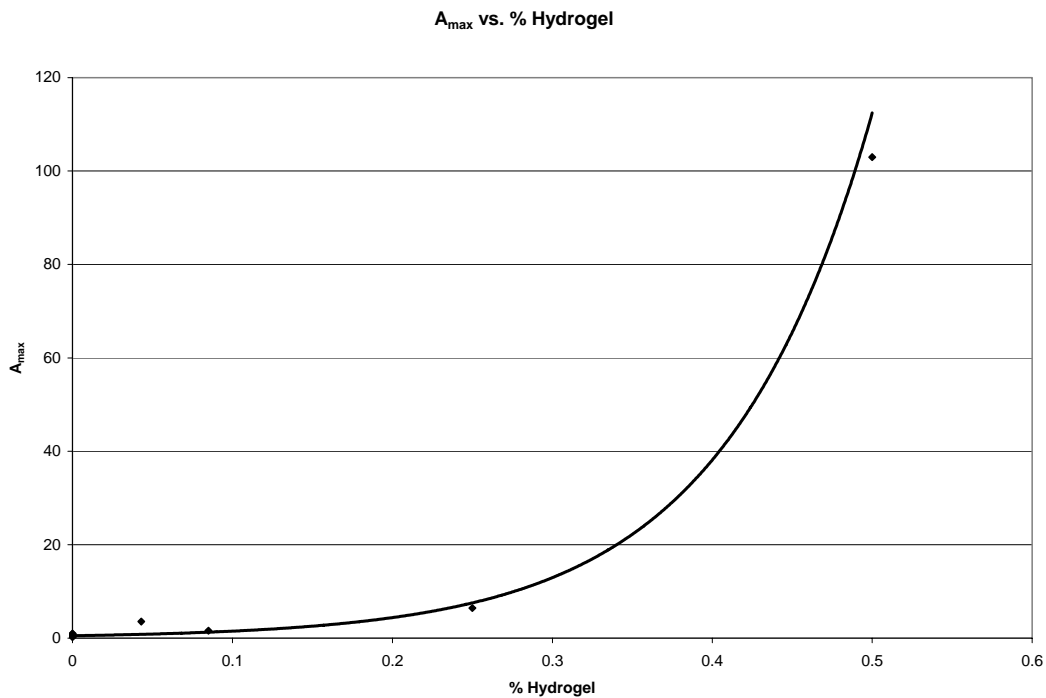
Figure 4.9: Peak A vs. Percent Hydrogel from consolidated undrained triaxial testing.

The reduction of effective stress with the addition of hydrogel to Ottawa sand samples is also illustrated by the reduction in q/p' seen in Figure 4.10. Samples were considered to fail at 10% strain. This plot shows a more than 30% ((0.55 – 0.35) / 0.55) decrease in the shear strength at failure at 0.50% hydrogel.

q/p'@10% Strain vs. % Hydrogel
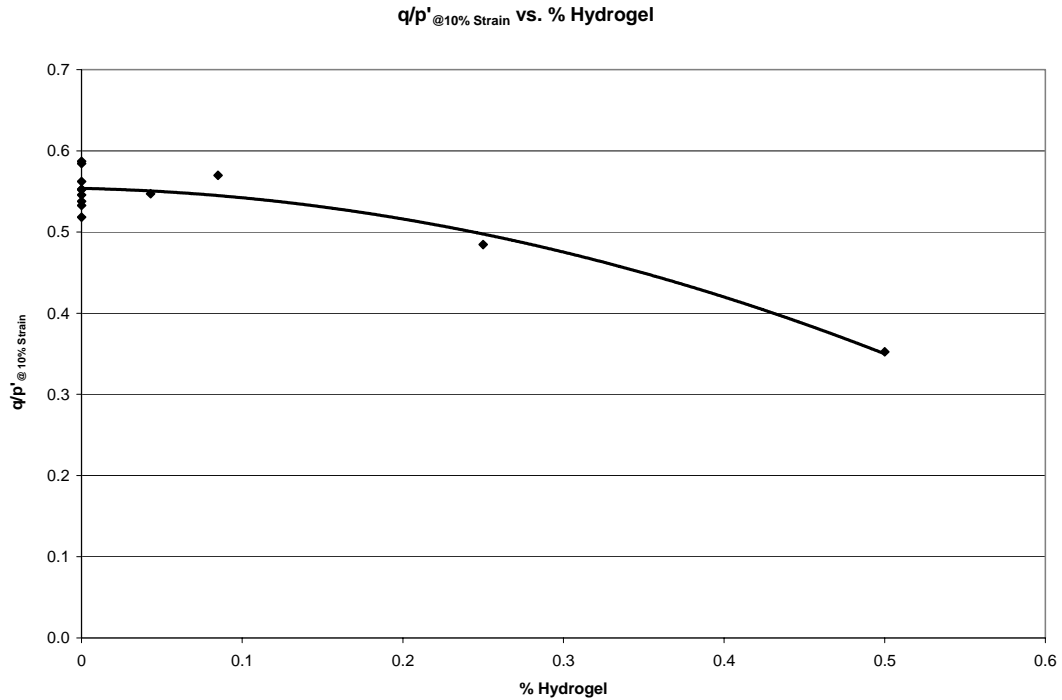
Figure 4.10: q/p' at 10% Strain vs. Percent Hydrogel from consolidated undrained triaxial testing.

4.2   Flex Walled Permeameter Testing

4.2.1   Variables in Permeability Testing

Variables for permeability testing are the same as the variables for consolidated undrained triaxial testing:

Percent Hydrogel – Percent hydrogel was chosen for the same reasons presented in Section 3.1.2 and is define in the same manner.

Unit Weight – Denser (high unit weight) samples have less void spaces and therefore have a lower permeability.

"B" Value – Saturation is important for permeability testing. For example, if one drop of water goes into the sample, one drop should come out. If the sample is not

saturated, the drop of water going in will be used to fill a void space that is not filled with water, and its effect will never be observed coming out.

4.2.2   Permeability vs. Percent Hydrogel

Figure 3.39 shows average permeability of confined mold tests against percent hydrogel. Permeability values were calculated by taking the average permeability of the tests run on each sample. Two tests at each percentage of hydrogel used were run. The percentages of hydrogel used were: 0.085%, 0.17%, 0.26%, 0.34%, and 0.68%. The 0.0% hydrogel samples were not confined because they do not need to force any hydrogel into pore spaces. There were five separate 0.0% hydrogel samples run, and only the average of these five tests are shown on the plot.

4.2.3   Permeability Response with Variation of Percent Hydrogel

Hydrogel fills the pore spaces within Ottawa sand samples. This implies that as the amount of hydrogel increases, water flow through the sample will decrease. As hydrogel percentage increases, an increasing amount of void space is taken up by it. This creates less room for water to move through, thereby reducing permeability.

Results from permeability testing show that hydrogel does reduce the permeability of Ottawa sand samples. This can be seen in Figure 3.39. At approximately 0.30% hydrogel, a pronounced reduction in permeability is observed. The reduction in permeability from 0.0% hydrogel sample to 0.68% hydrogel is approximately 5.5 orders of magnitude.

In Figure 3.39, the samples at 0.0%, 0.085%, 0.17%, and 0.26% hydrogel show a decrease in permeability of approximately one order of magnitude. This is expected, as hydrogel begins to fill more pore spaces. Then between 0.26% and 0.34% hydrogel the permeability decreases by four orders of magnitude. The comparison between 0.34% and 0.68% hydrogel only shows a one order of magnitude reduction. This large drop in permeability and subsequent leveling out between the 0.26%, 0.34%, and 0.68% hydrogel samples suggests that at a percentage of hydrogel between 0.26% and 0.34% all the void spaces have been filled. This is confirmed by the small change in permeability between 0.34% and 0.68% samples. This shows that there are no more void spaces to be filled at 0.34% or 0.68% hydrogel, or the change in permeability would be greater. This testing showed that, for this project, 0.34% hydrogel constituted filled void spaces within loose Ottawa sand samples.
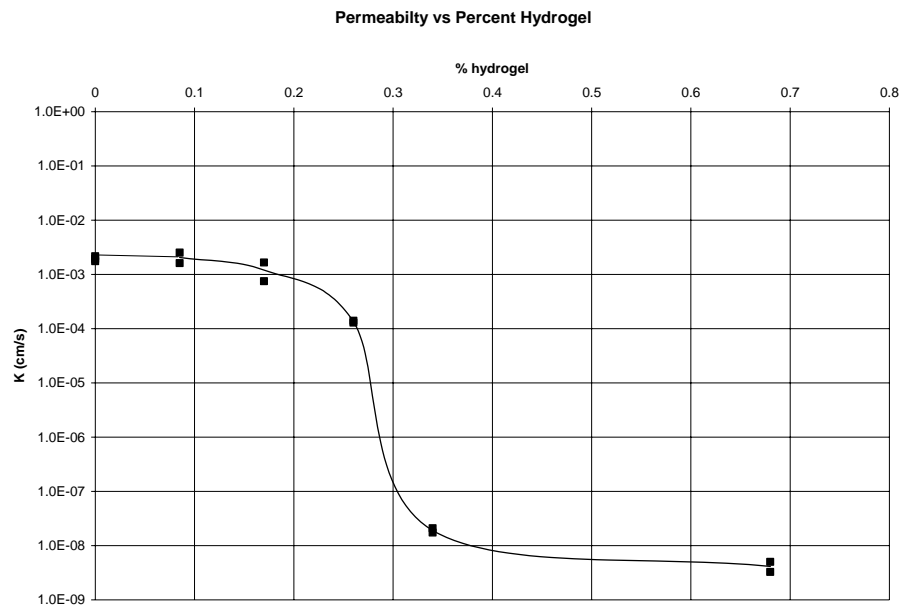
Figure 4.11: Results from permeability testing showing average permeability vs. percent hydrogel.

4.3 Uplift Pressure Test

The Swell Test was performed measuring uplift pressure generated by a hydrogel sample. After determining, from triaxial results, that 0.50% hydrogel was the largest percentage a sample could hold before displaying the properties of a 100% hydrogel sample, the swell test was run. 0.50% was chosen as a worst-case scenario which would produce an upper bound for swell pressure. Only one swell test on a 0.50% sample was run. The test was conducted over an approximately two hour period taking readings every fifteen minutes.

4.3.1 Uplift Pressure Test Data and Response

Initial Load (from digital readout) – 3.8 lbs.

Final Load (from digital readout) – 21.6 lbs.

Sample Diameter = 2.88"

Change in Load = 21.6 lbs. – 3.8 lbs. = 17.8 lbs.

Uplift Pressure = Change in Load / Sample Cross Sectional Area

Sample Cross Sectional Area = $(\pi * (2.88")^2) / 4 = 6.51$ in^2

<u>*Uplift Pressure*</u> = 17.8 lbs. / 6.51 in^2 = **2.73 psi (0.20 tsf)**

These data shows a 2.73 psi (0.20 tsf) uplift pressure at 0.50% hydrogel.

4.4 Cyclic Mobility Testing

Cyclic Mobility tests were run using the flow table described in ASTM C230/C230M: Standard Specification for Flow Table for Use in Tests of Hydraulic Cement, using 25 drops per test. No data were measured during the tests, instead, the

condition of the sample after testing was observed and pictures were taken. Varying

percentages of hydrogel were added to the samples tested to see if it restricted either flow

liquefaction or cyclic mobility. Samples were tested using 0.0%, 0.06%, 0.12%, 0.18%,

0.26%, 0.34%, and 0.68% hydrogel.

4.4.1 Cyclic Mobility Response with Variation in Percentage of Hydrogel

Before and after pictures of cyclic mobility tests are presented in Figures 4.6 –

4.13. Testing started with 0.0% percent hydrogel to establish that the soil would

liquefy on the flow table (figs. 4.6 – 4.7). The total collapse and the standing water

observed with the 0.0% sample along with 0.06% (fig. 4.8) and 0.12% (fig. 4.9)

hydrogel samples were considered to indicate a state of flow liquefaction. This

indicated that at low hydrogel percentages, liquefaction was not inhibited.

Beginning with the 0.18% (fig. 4.10) sample and continuing with 0.26% (fig.

4.11) sample, no standing water was observed, but sample collapse and spread was still

observed. These samples were considered to fail in lateral spread. Therefore, these

percentages stopped flow liquefaction, but cyclic mobility was still occurring.

The 0.34% (fig. 4.12) and 0.68% (fig. 4.13) sample also showed no standing

water and some collapse and spread of the samples. However, these samples are

believed to fail in shear due to the dynamic load and not because of liquefaction.

Figures 4.12 and 4.13 show that the 0.34% and 0.68% samples have failed leaving a

pile containing large chunks of the sand hydrogel mixture. This type of failure gives no

indication that liquefaction has occurred. However, this failure does suggest that these

samples have collapsed due to dynamic loading and the unconfined sample setup.

Figures 4.14 and 4.15 present graphs comparing percent hydrogel and sample spread. Figure 4.14 shows the sample diameter after failure (final average diameter) versus percent hydrogel. Figure 4.15 shows this diameter as a percentage of the original 4" sample diameter (% spread) versus percent hydrogel:

% spread = ([(final average diameter – initial diameter)/initial diameter] x 100 =

[(8.4" – 4.0")/4.0"]*100 = 110.0%)

Sample spread was estimated from testing pictures. Two diameter measurements were taken for each sample and averaged. Sample diameter at the base before testing was 4", and the drop table diameter was 10". Both graphs show a decrease in sample spread as hydrogel percentage increases indicating that hydrogel is lessening the effects of liquefaction and stabilizing the sample.

While the curves presented in figures 4.14 and 4.15 show a decrease in liquefaction susceptibility with increasing percent hydrogel, they also show a decrease in the efficiency that larger percentages of hydrogel have on lessening the effects of liquefaction. The curves become asymptotic to a final average diameter/% spread (~6.3"/~37%) at approximately 0.50% hydrogel. This indicates that larger percentages of hydrogel will have negligible effects and are not needed.

Figure 4.12: Cyclic mobility testing pictures. 0.0% hydrogel before testing (scale = one inch).

Figure 4.13: Cyclic mobility testing pictures. 0.0% hydrogel after testing. Standing water and collapse indicate flow liquefaction (scale = one inch).

Figure 4.14: Cyclic mobility testing pictures. 0.06% hydrogel before and after testing. Standing water and collapse indicate flow liquefaction.

Figure 4.15: Cyclic mobility testing pictures. 0.12% hydrogel before and after testing.

Standing water and collapse indicate flow liquefaction.

Figure 4.16: Cyclic mobility testing pictures. 0.18% hydrogel before and after testing. Collapse, smaller spread, and no standing water indicating lateral spread.

Figure 4.17: Cyclic mobility testing pictures. 0.26% hydrogel before and after testing.
Large chunks indicating liquefaction is being reduced, but lateral spread is still occurring in
outer edges. The clamp in the top left picture and mold in top right picture are both used in
sample preparation.

Figure 4.18: Cyclic mobility testing pictures. 0.34% hydrogel before and after testing. Small spread and large chunks indicate shear failure, not liquefaction, has occurred.

Figure 4.19: Cyclic mobility testing pictures. 0.68% hydrogel before and after testing.

Small spread and large chunks indicate shear failure, not liquefaction, has occurred.

Percent Hydrogel vs. Final Average Diameter
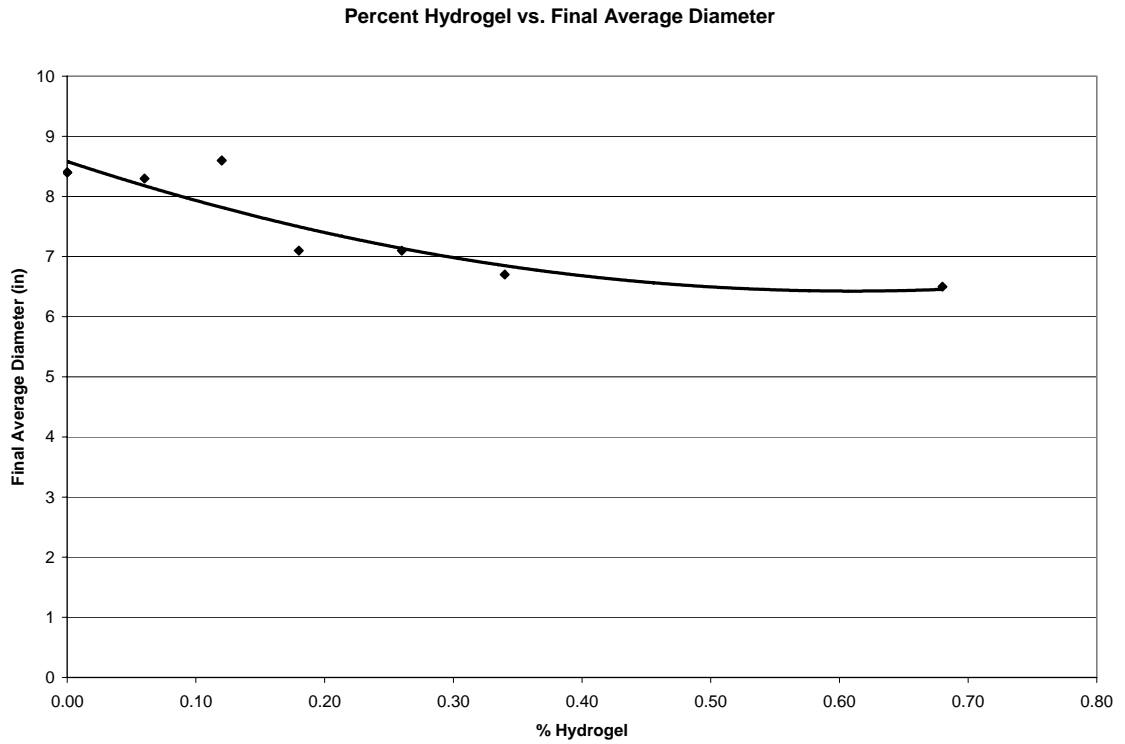
Figure 4.20: Percent hydrogel vs. final average diameter results from cyclic mobility testing, showing increase in sample stability with increasing percent hydrogel.

Percent Spread from Original Sample Diameter (4") vs. Percent Hydrogel
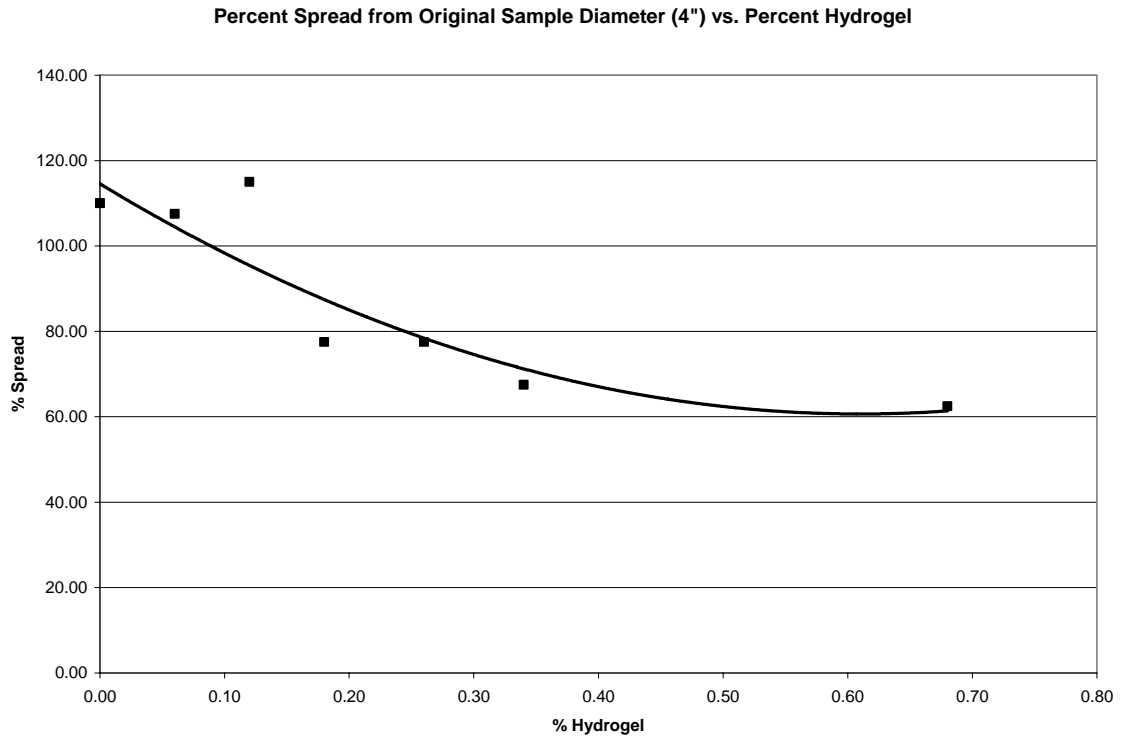
Figure 4.21: Percent spread from original 4" diameter sample vs. percent hydrogel results from cyclic mobility testing. Note the decrease in spread denoting an increase in sample stability.

CHAPTER 5: CONCLUSIONS FROM LABORATORY TESTING
RESULTS

5.1   Consolidated Undrained Triaxial Testing

5.1.1   Peak Pore Pressure

An overview of pore pressure response for triaxial testing is shown in Chapter 4, Section 4.1. Figure 5.1 and 5.2 presents the pore pressure response for untreated and treated samples respectively. These tests confirm that hydrogel is having little effect on the peak pore pressure response of Ottawa sand samples. While peak pore pressure differs from test to test these differences are attributed to differences in unit weight of the samples during testing.

This trend is attributed to the confined nature of triaxial testing. Unlike cyclic mobility testing (Section 5.4), a sample in triaxial testing is loaded from all sides. This does not allow the sample to collapse to a state of lowest stress as it is loaded. The combination of the axial and confining load squeezes water out of the hydrogel particles. This water is then free to contribute to the pore pressure response of the sample as if the hydrogel was not there. There is no indication that this phenomenon is affected by increasing or decreasing the amount of hydrogel in the sample.   Therefore, because water can be squeezed out of hydrogel particles during triaxial testing, hydrogel has no effect on the peak pore pressure response of samples tested.

Pore Pressure vs. Strain for Untreated Samples
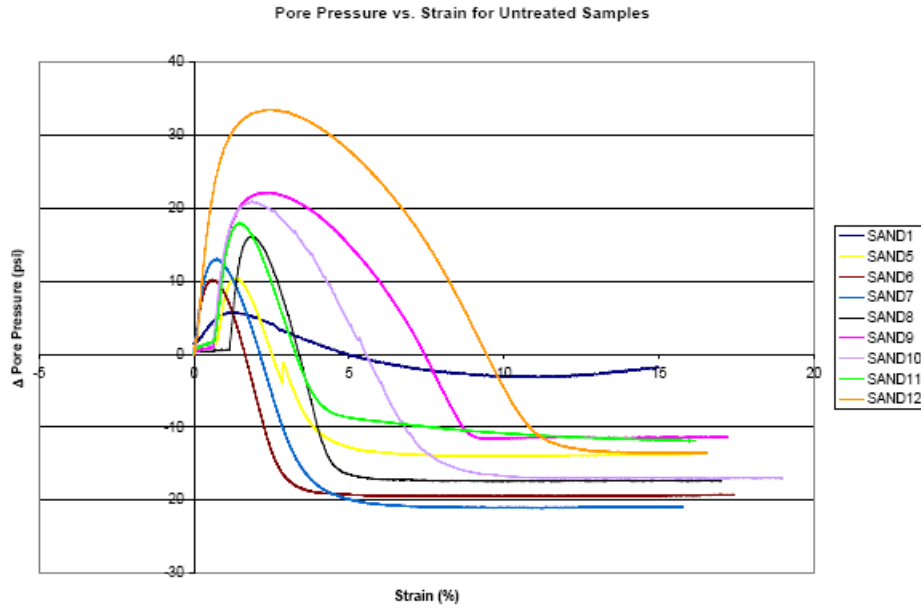
Figure 5.1: Pore Pressure vs. Strain for untreated samples from consolidated undrained triaxial testing. Reprinted from Chapter 4, Figure 4.2.

Bryan Shiver
10/19/03

Pore Pressure vs. Strain for Treated Samples
Samples Prepared with the Confined Mold
SANDHYDRO4 and SANDHYDRO6 have been zeroed
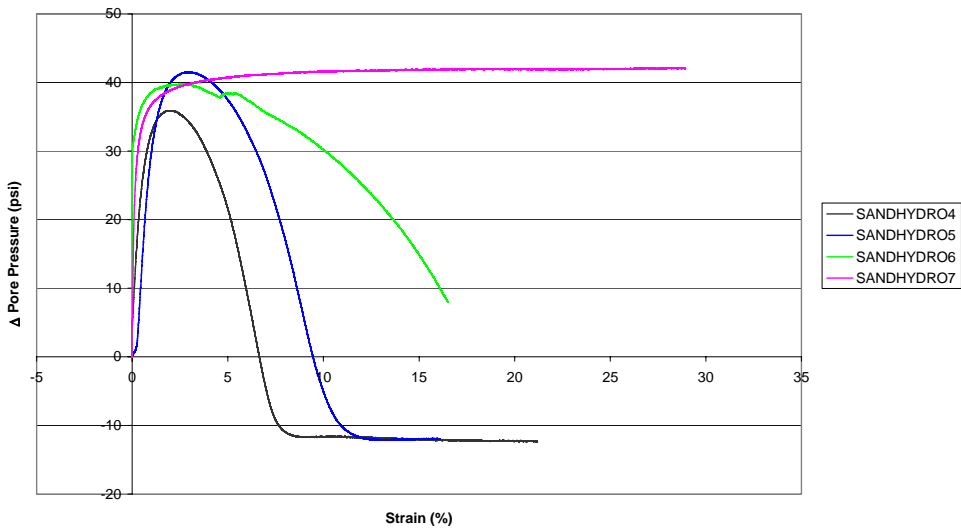
Figure 5.2: Change in Pore Pressure vs. Strain for treated samples from consolidated undrained triaxial testing. Reprinted from Chapter 4, Figure 4.6.

5.1.2 Sample Dilation

While hydrogel has little effect on the peak pore pressure response, it does affect sample dilation. Dilation is an increase in sample volume as the sample is loaded. As the sample compresses and soil particles move, they must eventually move around one another causing a volume increase. The effect of sample dilation can be seen in pore pressure versus deformation graphs as a decrease in pore pressure. Figures 5.1 and 5.2 suggest that as hydrogel percentage increases, the samples dilate less, and eventually act as a 100% hydrogel sample (Fig. 5.3).

As the hydrogel percentage is increased, it begins to take up more space in the sample as it is saturated and expands which causes a change in the way the sample reacts as it is loaded. At higher percentages of hydrogel, the properties of the soil are eclipsed by the properties of hydrogel. Instead of reacting as hydrogel suspended in a soil matrix, it acts as soil suspended in a hydrogel matrix. This creates a state in which hydrogel has overtaken the sample. This effect is increased as the percentage of hydrogel is increased.

The permeation of hydrogel properties in Ottawa sand samples is exemplified by sample dilation. Because hydrogel is compressible, it does not dilate; therefore, the effect of dilation is lessened as the percentage of hydrogel is increased. Testing gives evidence that 0.50% hydrogel causes an Ottawa sand sample to react as a 100% hydrogel sample and have no sample dilation.

Bryan Shiver
10/1/03
B = 0.996

Pore Pressure vs. Strain
HYDRO: 100% Hydrogel; σ_{3c} = 45psi
Sample Prepared with the Confined Mold
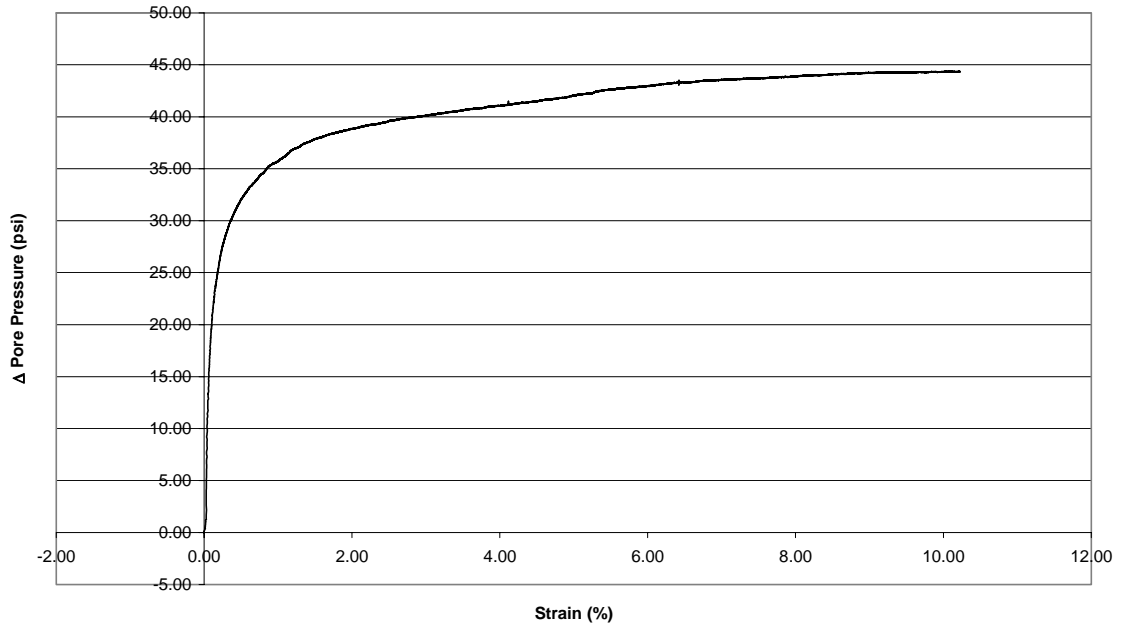
Figure 5.3: Change in Pore Pressure vs. Strain for 100% Hydrogel sample from consolidated undrained triaxial testing. Reprinted from Chapter 4, Figure 4.7.

5.1.3   Shear Strength Response

The strength of the samples is lessened by increasing percentages of hydrogel. This can be seen in Figures 5.4 and 5.5. These figures show that as hydrogel percentage is increased effective stress during sample loading is decreased causing a 30% decrease in the shear strength at 10% strain. This trend illustrates that samples containing 0.50% hydrogel no longer respond as sand, instead hydrogel has overtaken the sample creating a soil that responds as hydrogel.
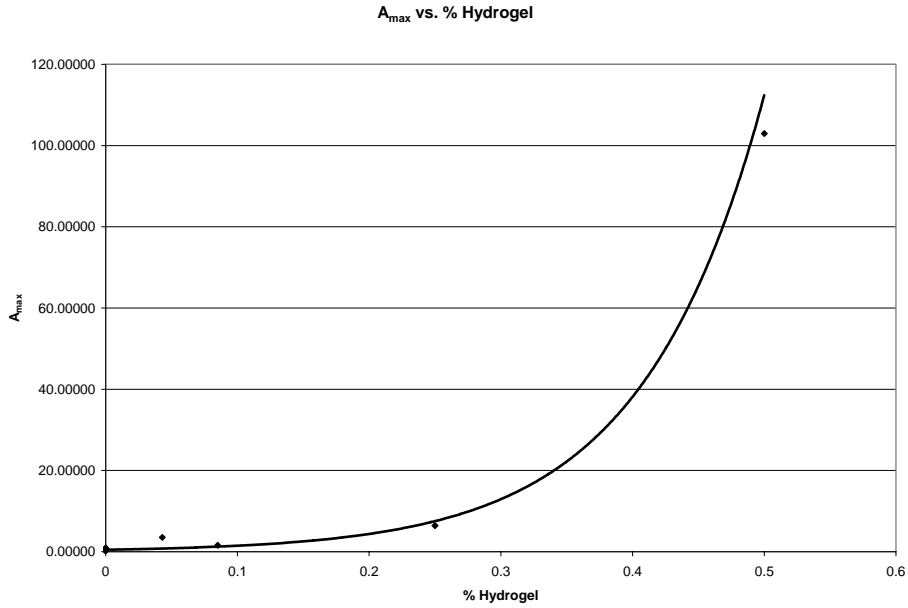
Figure 5.4: Peak A vs. Percent Hydrogel from consolidated undrained triaxial testing. Reprinted from Chapter 4, Figure 4.9.
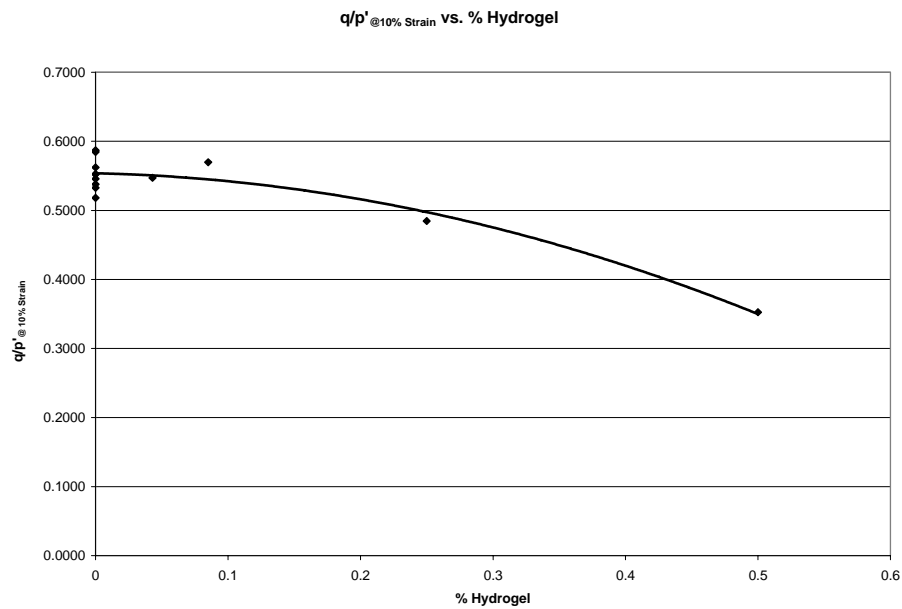
Figure 5.5: q/p' at 10% Strain vs. Percent Hydrogel from consolidated undrained triaxial testing. Reprinted from Chapter 4, Figure 4.10.

5.2 Permeability Testing

The results from permeability testing are presented in Chapter 4, Section 4.2. Testing showed a 5.5 order of magnitude drop in permeability over the entire range of samples tested (0.0% - 0.68% hydrogel) and in particular, a reduction of four orders of magnitude between samples containing 0.26% and 0.34% hydrogel. This indicates that hydrogel has its greatest effect on lowering permeability in the sample at the 0.26% - 0.34% hydrogel range.

As hydrogel expands, it fills the void spaces within the sample which creates less room for water to flow. Hydrogel is assumed to stay in place as water is passed through the sample; therefore, the permeability of a hydrogel/water mixture is not considered in this study. Since water cannot travel though sand particles or hydrogel particles, it must flow through the void spaces. As these void spaces fill with hydrogel, two events occur that lower permeability. First, water must take a longer path around the hydrogel. Second, hydrogel particles may surround a pocket of water, trap it in place, and not allow it to contribute to the permeability. In either case, permeability is decreased.

Figure 5.6, shows the permeability is reduced as the hydrogel percentage is increased. This reduction is small (~ one order of magnitude) at lower percentages of hydrogel (0.0% - 0.26%). Then, between 0.26% and 0.34% hydrogel, a four orders of magnitude reduction occurs. Once 0.34% hydrogel is reached, further increase in hydrogel does not lower permeability substantially.

This trend is explained by hydrogel filling the pore spaces in the soil. At lower percentages of hydrogel, the pore spaces begin to be filled with expanding hydrogel;

however, water can still flow through contiguous voids. But, as the pore spaces approach a completely filled state, a large reduction in permeability occurs. Once the pore spaces are entirely filled, higher percentages of hydrogel have only a small effect on permeability because the excess is not being used to close more flow paths. According to this logic and data from testing, pore spaces within a sample are mostly filled at approximately 0.34% hydrogel with a reduction in permeability of five orders of magnitude.
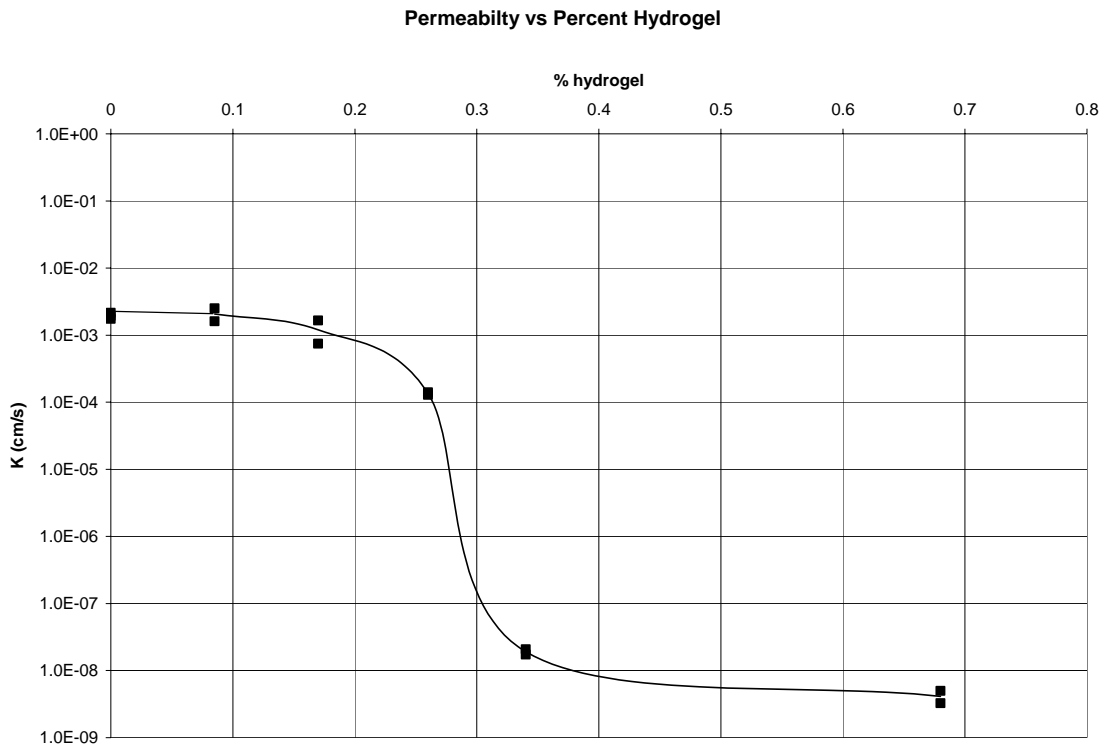
Figure 5.6: Results from permeability testing. Average Permeability vs. Percent Hydrogel. Reprinted from Chapter 3, Figure 3.39

97

5.3 Cyclic Mobility Testing

Chapter 4, Section 4.4 outlines the results from cyclic mobility testing. These results suggest a decrease in liquefaction susceptibility with increasing percentage of hydrogel. As the percentage of hydrogel increases, the samples move from a flow liquefaction state, to a state of cyclic mobility, to shear failure. This implies that hydrogel is inhibiting liquefaction in unconfined Ottawa sand samples. In these samples hydrogel is soaking up and trapping the water in the pore spaces of the soil. Once trapped, the water does not contribute to the pore pressure in the soil. This is due to the unconfined test setup. In this setup the sample is allowed to collapse to a state of lowest stress as it is loaded. Therefore, the stress never becomes large enough to squeeze water out of the hydrogel particles. If water cannot be squeezed from the hydrogel particles, it cannot contribute to the pore pressure in the sample, thereby lowering the pore pressure. As pore pressure is negated by increasing percentages of hydrogel, liquefaction susceptibility is diminished.

For this test, hydrogel is acting as a sponge in the sample, soaking up excess water, and holding it in place. The water is tied up in the hydrogel polymer and is not able to transfer pressure to the soil. Instead of the soil reacting as if it is full of water, it reacts as if it is full of hydrogel particles. The hydrogel particles act as a semi-solid in the soil and do not transfer fluid pressure to particles surrounding it. The hydrogel has essentially lessened the amount of water that is available to influence effective stress in the sample creating effective stress levels which do not induce liquefaction.

This effect can be seen in Chapter 4, Figures 4.6 – 4.13. As the percentage of hydrogel increases, less water can be seen after failure. Since the samples were of

uniform size and approximately an equal amount of water filled the volume of each

sample (hydrogel was not allowed to expand during sample preparation), hydrogel must

be influencing free water in the sample. The free water is bound by the hydrogel

particles which causes an increase in the effective stress of the soil as it is loaded. Figure

5.7 illustrates this phenomenon. It suggests that as percent hydrogel is increased, the

sample spread is decreased. This implies that sample stability increases with an increase

in percent hydrogel.

Figure 5.7 also establishes a limit to the effect that increasing percentages of

hydrogel has on sample stability. The curve shown in figure 4.1 becomes asymptotic to

~37% percent spread illustrating that sample stability will not be increased by adding

increasing amounts of hydrogel.   This curve illustrates that 0.50% hydrogel is the

effective limit that hydrogel has on sample stability with a 38% reduction in sample

spread. Increases to sample stability at percentages higher than 0.50% hydrogel will be

insignificant.

Percent Spread from Original Sample Diameter (4") vs. Percent Hydrogel
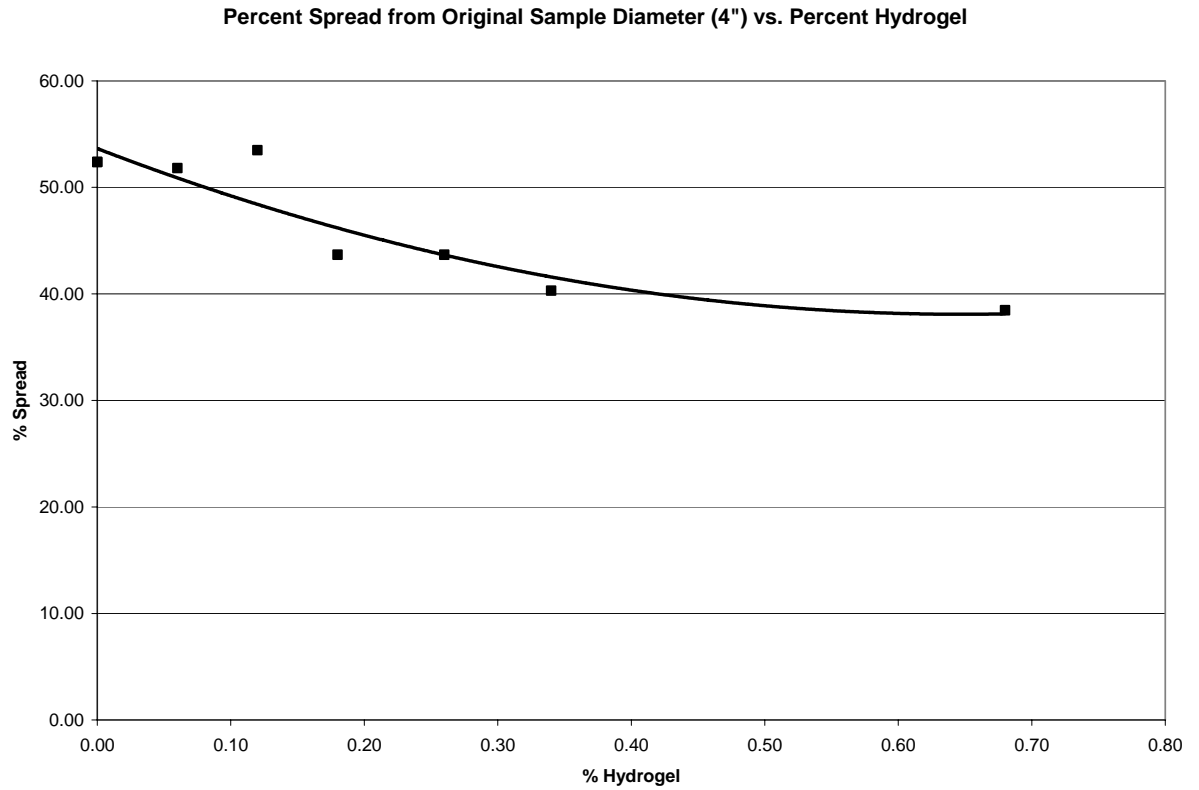
Figure 5.7: Results from cyclic mobility testing. Percent spread from original 4" sample vs. percent hydrogel. Note the decrease in spread denoting an increase in sample stability (Reprinted from Chapter 3, Figure 3.48).

SUGGESTIONS FOR FURTHER RESEARCH

1. The response of samples containing hydrogel under dynamic loading conditions needs to be explored to more accurately simulate earthquake loads. This could include cyclic triaxial, cyclic simple shear, or cyclic torsional testing.

2. In order to penetrate the pore spaces of in-situ soils, hydrogel must be inserted into the soil unsaturated. Ways of keeping the hydrogel unsaturated until it reaches the pore spaces of the soil and ways to insert the particles under a building need to be developed.

3. Hydrogel has been used commercially in agriculture and horticulture applications. These applications should be evaluated for their effectiveness in engineering purposes.

3. Hydrogel is adversely affected by salts. This effect needs to be measured and analyzed to protect against degradation in coastal areas.

4. Confining pressure may affect the ability of hydrogel to absorb and retain water. The extent of this effect should be investigated.

5. Polymers degrade over time. Degradation of hydrogel due to natural processes must be evaluated.

6. There is much debate in the polymer chemistry field concerning the degradation of non-toxic polyacrylamide into its monomer, acrylamide, which is a neurotoxin and a suspected carcinogen. Most notably, the World Health Organization (WHO) is monitoring and sponsoring research on the use of polyacrylamide in agriculture and its relation to acrylamide found in food. If polyacrylamide is deemed unsafe in the future, it would be a problem for this project.

7. Alternatives to polyacrylamide hydrogel may exist. Any substance found should be analyzed.

8. Triaxial testing on samples containing hydrogel should be expanded to include tests run at varying confining pressures. This will allow for the analysis of Mohr-Coulomb failure planes for samples containing different percentages of hydrogel. From these failure planes, comparisons could be made between cohesion, c, internal angle of friction, ϕ, and percent hydrogel.

REFERENCES

Adalier, K., and Elgamal, A. (2004). "Mitigation of liquefaction and associated ground

deformations by stone columns." *Engineering Geology*, 72, 275-291.

Bray, J. D., et al (2001). "Soil liquefaction and ground failure: lateral spread." *Some

Observations of Geotechnical Aspects of the February 28, 2001,

Nisqually Earthquake in Olympia, South Seattle, and Tacoma, Washington*,

http://peer.berkeley.edu/nisqually/geotech/liquefaction/lateralspread/ (Nov. 10,

2004).

Finn, W. D. (2002). "State of the art for the evaluation of seismic liquefaction potential."

Computers and Geotechnics, 29, 329-341.

Hamada, M., and O'Rourke, T. D. (1992). *Case studies of liquefaction and lifeline

performance during past earthquakes*, National Center for Earthquake

Engineering Research, Buffalo, New York.

Hausmann, M. R. (1990). *Engineering principles of ground modification*, McGraw-Hill,

New York, New York.

Hays, W. W., ed. (1981). *Facing geologic and hydrologic hazards - earth science considerations*. United States Geological Survey Professional Paper 1240B, U.S. Government Printing Office, Washington D.C.

Henn, R. W. (1996). *Practical guide to grouting of underground structures*, ASCE, New York, New York.

Holtz, R. D., and Kovacs, W. D. (1981). *An Introduction to Geotechnical Engineering*, Prentice Hall, Englewood Cliffs, New Jersey.

Hynes, M. E., and Olsen, R. S. (1999). "Influence of confining stress on liquefaction resistance", *Proc., International Workshop on Physics and Mechanics of Soil Liquefaction*, Balkema, Rotterdam, The Netherlands.

Ishibashi, I., Kawamura, M., and Bhatia, S.K. (1985). "Torsional simple shear apparatus for drained and undrained cyclic testing." *Advances in the art of testing soils under cyclic loads*, ASCE, New York, New York, 51-73.

Ishihara, K (1985). "Stability of natural deposits during earthquakes." *Proc., 11th International Conference on Soil Mechanics and Foundation Engineering*, Vol. 1, 321-376.

Ishihara, K. (1984). "Post-earthquake failure of a tailings dam due to liquefaction of the pond deposit." *Proc., International Conference on Case Histories in Geotechnical Engineering*, University of Missouri, St. Louis, Missouri, Vol. 3, 1129-1143.

Ishihara, K (1993). "Liquefaction and flow failures during earthquakes." *Geotechnique*, 43(3), 351-415.

Johansonn, J. (2000). "Soil liquefaction web site." Department of Civil Engineering, University of Washington, http://www.ce.washington.edu/~liquefaction/ (Sep. 13, 2004).

Kramer, S. L. (1996). *Geotechnical earthquake engineering*, Prentice Hall, Englewood Cliffs, New Jersey.

Liao, S. S. C., and Whitman, R. V. (1986). *Catalogue of liquefaction and non-liquefaction occurrences during earthquakes*, Department of Civil Engineering, Massachusetts Institute of Technology, Cambridge, Massachusetts.

McCarthy, D. F. (1998). *Essentials of soil mechanics and foundations: basic geotechnics*, Prentice Hall, Englewood Cliffs, New Jersey.

Mogami, T., and Kubu, K. (1953). "The behavior of soil during vibration." *Proc., 3rd International Conference on Soil Mechanics and Foundation Engineering*, Zurich, Switzerland, Vol. 1, 152-155.

Optim Electronics (1996). *Optim Technical Information: TCS*, Optim Electronics

    Corporation, Germantown, Maryland.

Optim Electronics (1996). *Optim Technical Information: Megadac 3415AC*, Optim

    Electronics Corporation, Germantown, Maryland.

Robertson, P. K., and Wride, C. E. (1998). "Evaluating cyclic liquefaction potential using

    the cone penetration test." *Canadian Geotechnical Journal*, Ottawa, Ontario,

    35(3), 442-459.

Rollins, K., Anderson, J. K. S., Goughnour, R. R., McCain, A. K. (2004). "Liquefaction

    hazard mitigation using vertical composite drains." *Proc., 13th World Conference

    on Earthquake Engineering*, Vancouver, Canada, paper no. 2880, in press.

Seed, H. B., and Lee, K. L. (1966). "Liquefaction of saturated sands during cyclic

    loading." *Journal of the Soil Mechanic and Foundations Division: Proceedings of

    the American Society of Civil Engineers*, 92, No. SM6, 105-134.

Seed, H. B., and Idriss, I. M. (1971). "Simplified procedure for evaluating soil

    liquefaction potential." *Journal of Geotechnical Engineering*, ASCE, 97(9), 1249-

    1273.

Seed, H. B. (1979). "Soil liquefaction and cyclic mobility evaluation for level ground during earthquakes." *Journal of Geotechnical Engineering*, ASCE, 105(2), 201-255.

Seed, H. B., and Idriss, I. M. (1982). *Ground motions and soil liquefaction during earthquakes*, Earthquake Engineering Research Institute, Monograph, Oakland, California.

Seed, H. B., Tokimatsu, K., Harder, L. F., Chung, R. M. (1985). "The influence of SPT procedures in soil liquefaction resistance evaluation." *Journal of Geotechnical Engineering*, ACSE, 111(12), 1425-1445.

Terzaghi, K. (1925). *Erdbaumechanik auf bodenphysikalischer grundlage*, Leipzig F. Deuticke, Vienna.

United States Geological Survey (2004). "Earth science photographic archive." *Earthquakes*, http://libraryphoto.er.usgs.gov/earth1.htm (Nov. 12, 2004).

United States Geological Survey (2004). "Earthquake facts and lists." *Earthquake hazards program*, http://neic.usgs.gov/neis/eq_depot/usa/1964_03_28.html (Nov. 12 2004).

Wang, W (1979). *Some findings in soil liquefaction*, Water Conservancy and Hydroelectric Power Scientific Research Institute, Beijing, China.

Youd, T. L. (1991). "Mapping of earthquake-induced liquefaction for seismic zonation." *Proc., 4th International Conference on Seismic Zonation*, Earthquake Engineering Research Institute, Stanford University, Stanford, California, Vol. 1, 111-147.

Youd T. L., and Idriss, I. M. (2001). "Liquefaction resistance of soils: summary report from the 1996 NCEER and 1998 NCEER/NSF workshops on evaluation of liquefaction resistance of soils." *Journal of Geotechnical and Geoenviromental Engineering*, 127(10), 297-313.

APPENDIX A: TESTING EQUIPMENT INFORMATION

Triaxial Testing Equipment

Load Frame:

Brainard-Kilman S-600 Triaxial Load Frame; Serial Number: 1033

Brainard-Kilman E-410 Four Channel Readout; Serial Number: 1033

Test Cell:

Brainard-Kilman S-510 Triaxial Cell; Serial Number: 134

Panel Board:

Brainard-Kilman S-500 Triaxial/Permeability Panel Board; Serial Number: 1479

Brainard-Kilman E-400 Digital Readout; Serial Number: 715

Brainard-Kilman E-114 Pressure Transducer; Serial Number: 428

Range: 0 – 300 psi

Sensitivity: 0.1 psi

Excitation Voltage: 10.0 V DC at maximum 90 mA

Sensors:

Brainard-Kilman E-124 Pore Pressure Transducer; Serial Number: 332

Range: 0 – 150 psi

Sensitivity: 0.1 psi

Excitation Voltage: 10.0 V DC at maximum 90 mA

Brainard-Kilman E-214 Load Cell (0-1500lbs); Serial Number: 253

Range: 0 – 6000 lbs

Sensitivity: 1.0 lbs

Excitation Voltage: 10.0 V DC at maximum 90 mA

Boart Longyear E-312 Linear Displacement Transducer; Serial Number: 134

Range: 2.0 in

Sensitivity: 0.001 in

Excitation Voltage: 10.0 V DC at maximum 90 mA

Data Collection:

Optim Electronics, Megadac 3415AC with Total Control Software (TCS) for DOS

Toshiba Satellite Pro 460CDT Laptop; Model Number: PA1251U XCD; Serial

Number: Y7382545

Permeability Testing Equipment

Test Cell:

Three, ELE International, 25-0690 Tri-Flex 2 Permeability Test Cells; Serial

Numbers: 020808, 020804, 020801

Panel Board:

Durham Geo Enterprises S-500 Triaxial/Permeability Panel Board; Serial Number:

1752

Durham Geo Enterprises E-400 Digital Readout; Serial Number: 412

Durham Geo Enterprises E-116 Pressure Transducer; Serial Number: 312

Range: 0 – 300 psi

Sensitivity: 0.1 psi

Excitation Voltage: 10.0 V DC at maximum 90 mA

Durham Geo Enterprises S-502 Auxiliary Panel Board; Serial Number: 2131

Sensors:

Durham Geo Enterprises E-124 Pore Pressure Transducer; Serial Number: 1162

Swell Pressure Testing Equipment

Load Frame:

Brainard-Kilman S-600 Triaxial Load Frame; Serial Number: 1033

Brainard-Kilman E-410 Four Channel Readout; Serial Number: 1033

Sensors:

Brainard-Kilman E-210 Load Cell (0-500lbs); Serial Number: 138

Cyclic Mobility Testing Equipment

Apparatus described in ASTM C 230/C 230M: Standard Specification for Flow Table

for Use in Tests of Hydraulic Cement

Sensor Calibrations for Megadac 3125AC

Calibration for Brainard-Kilman E-124 Pore Pressure Transducer; Serial Number: 332

$y = 0.3275x + 3.4229$
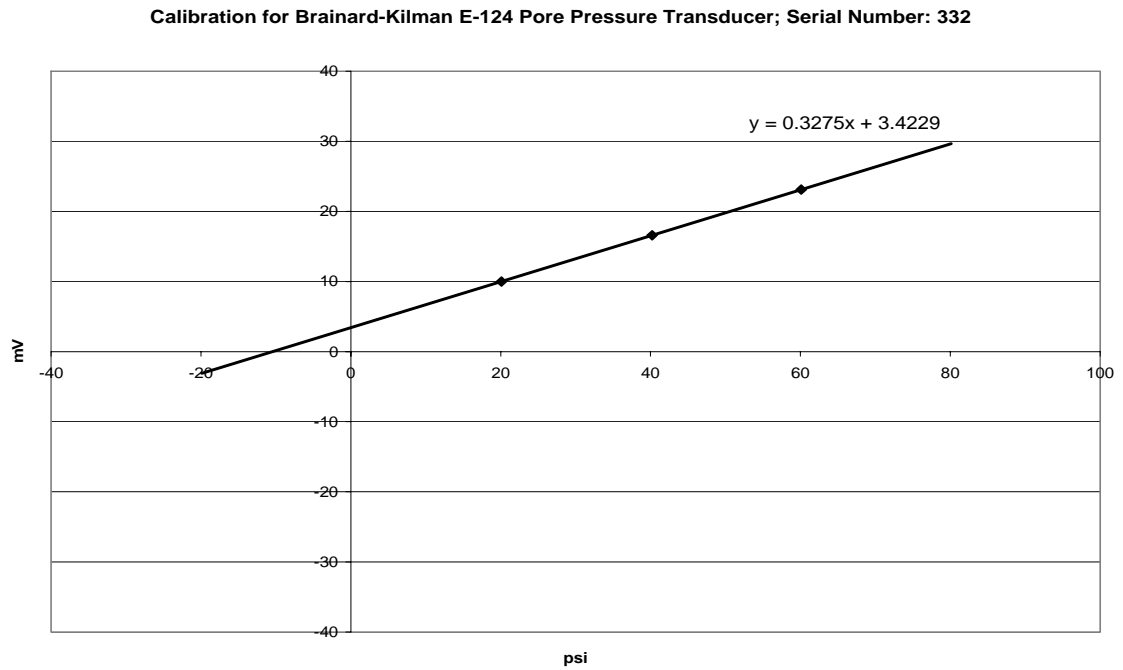
Figure A.1: Megadac calibration for Brainard-Kilman E-124 Pore Pressure

Transducer; Serial Number: 332.

Calibration for Brainard-Kilman E-214 Load Cell (0-1500lbs); Serial Number: 253

y = 0.0059x - 0.0257
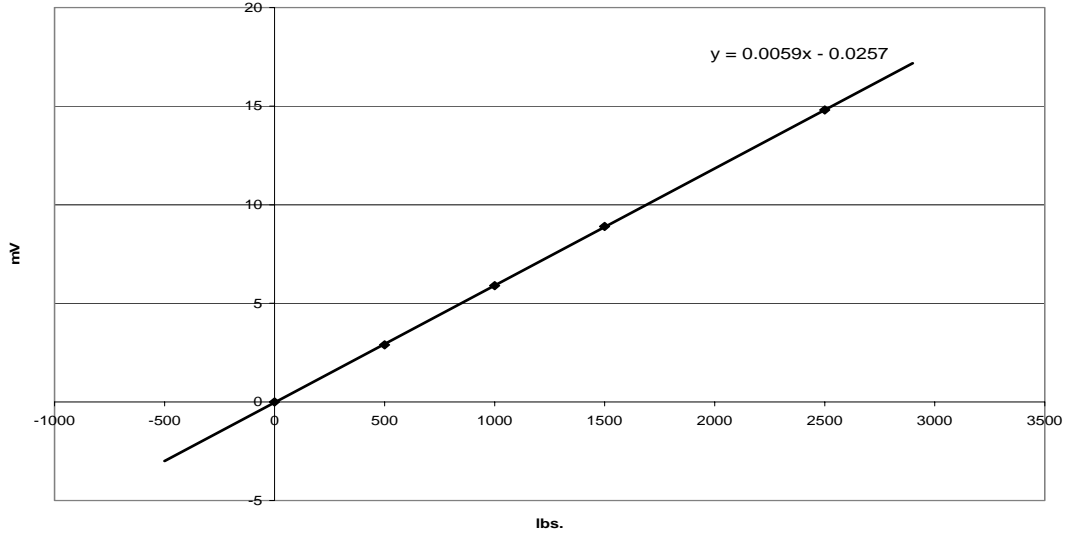
Figure A.2: Megadac calibration for Brainard-Kilman E-214 Load Cell (0-1500lbs); Serial Number: 253.

Calibration for Boart Longyear E-312 Linear Displacement Transducer; Serial Number: 134

y = 17.945x - 2.6
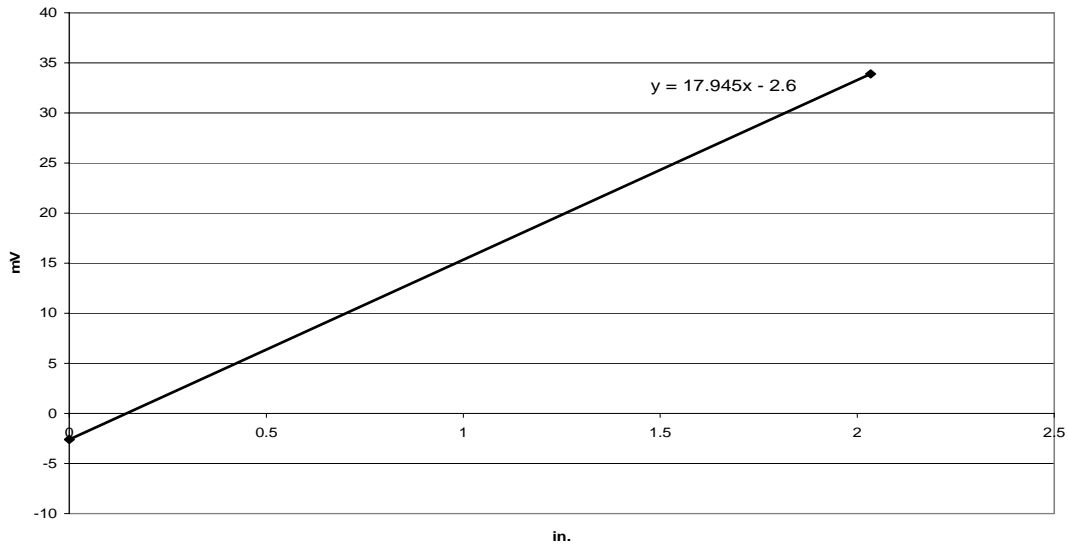
Figure A.3: Megadac calibration for Boart Longyear E-312 Linear Displacement Transducer; Serial Number: 134.

113

Third Party Sensor Calibrations

DURHAM GEO ◯|◖ SLOPE INDICATOR

2175 West Park Court
Stone Mountain GA 30087
Tel: 1-800-837-0864
Technical Assistance: Ext. 2012
Fax: (770)-465-7447

Calibration Certificate

Device Calibrated:	General Purpose Transducer
Range:	15.0 - 150.0 PSI
Model No:	E-114
Serial No:	428

Readout Model No:	E-400
Readout Serial No:	715
Channel No:	N/A
Equipment Condition:	Used, Good

Calibration Instrument:
Druck Pneumatic Calibrator 300 PSI Max
Serial No: 6011315012 (.01 Resolution)
Last Calibration Date: 10/17/03
Report #: SCC-14537

Service Used: **Precision Standards Intl.**
Equipment-Standard Used:
Ruska Dead-Weight Gage #14123
NIST #: SCC-9102

| Applied Pressure | Output | Before Calibration | | After Calibration | | | |
| | | Reading | Error | Reading | Reading | Deviation | Deviation |
(psi)	(mV)			#1	#2	#1	#2
0.00		0.0	0	0.0	0.0	0.00	0.00
15.00		15.0	0.00	14.9	15.0	-0.67	0.00
30.00		29.9	-0.33	30.0	30.0	0.00	0.00
45.00		44.7	-0.67	44.9	45.0	-0.22	0.00
60.00		59.6	-0.67	60.0	60.0	0.00	0.00
90.00		89.4	-0.67	90.1	90.1	0.11	0.11
120.00		119.4	-0.50	120.4	120.5	0.33	0.42
150.00		149.5	-0.33	150.9	150.9	0.60	0.60
					Total Error:	-0.67%	0.60%

Resolution:	.1 PSI
Temperature at time of calibration °C:	23
Error due to temperature change:	
Excitation Voltage:	10.00

| Offset 1 | (-) 15 | Offset 2 | (-) 11 | Break Pt | 1061 |
| Scale 1 | .2970 | Scale 2 | .2962 | | |

*NOTE: Readouts and transducers have been calibrated at the factory and are a matched pair. In general, pressure transducers, load cells and LDT's are not interchangeable.

Associated Equipment: S-500 - 1479

Location of Equipment at time of Calibration
Company Name: **Auburn University**
Physical Address: **201 Harbert Engineering Ctr**
Auburn University36849, AL

Phone Number: **(334) 844-6825**
Contact: **David J. Elton, Ph.D., P.E.**

Calibration performed by:
Steve Cash

Signature: *Steve Cash*

Calibration Date : **April 24, 2003**

Calibration Due Date : **April 23, 2004**

Traceable to NIST Standards.
This calibration conforms to the latest standards set by ASTM E4.

Report # E-114 #428.xls

Page 1 of 2

Figure A.4: Durham Geo Calibration Certificate for Brainard-Kilman E-114 Pressure Transducer; Serial Number: 428. Page 1 of 2.

Figure A.5: Durham Geo Calibration Certificate for Brainard-Kilman E-114 Pressure Transducer; Serial Number: 428. Page 2 of 2.

DURHAM GEO ⬤ SLOPE INDICATOR

2175 West Park Court
Stone Mountain GA 30087
Tel: 1-800-837-0864
Technical Assistance: Ext. 2012
Fax: (770)-465-7447

Calibration Certificate

Device Calibrated:	**General Purpose Transducer**
Range:	**15.0 - 200 psi**
Model No:	**E-116**
Serial No:	**321**

Readout Model No:	**E-405**
Readout Serial No:	**412**
Channel No:	**N/A**
Equipment Condition:	**New**

Calibration Instrument:
Druck Pneumatic Calibrator 300 PSI Max
Serial No: **6011315012** (.01 Resolution)
Last Calibration Date: **11/17/02**
Report #: **SCC-14537**

Service Used: **Precision Standards Intl.**
Equipment-Standard Used:
Ruska Dead-Weight Gage #14123
NIST #: **SCC-9102**

Applied Pressure	Output	Before Calibration		After Calibration			
		Reading	Error	Reading	Reading	Deviation	Deviation
(psi)	(mV)			# 1	# 2	# 1	# 2
0.00				0.0	0.0	0.00	0.00
15.00				15.0	15.0	0.00	0.00
30.00				29.9	29.9	-0.33	-0.33
45.00		New Equipment, No Prior Readings		44.9	44.9	-0.22	-0.22
60.00				59.9	59.9	-0.17	-0.17
90.00				89.9	89.9	-0.11	-0.11
120.00				119.9	119.9	-0.08	-0.08
150.00				150.0	149.9	0.00	-0.07
200.00				200.1	200.0	0.05	0.00
					Total Error:	-0.33%	-0.33%

Resolution:	**.1 PSI**
Temperature at time of calibration °C:	**23**
Error due to temperature change:	
Excitation Voltage:	**10.12**

Lo IN: (-) .00011   Hi IN: (+) .03894
Lo RD: 0000.0   Hi RD: 0150.0

*NOTE: Readouts and transducers have been calibrated
at the factory and are a matched pair. In general, pressure
transducers, load cells and LDT's are not interchangeable.

Associated Equipment: S-500-1752

Location of Equipment at time of Calibration

Company Name: **Durham Geo**
Physical Address: **2175 West Park Ct**
Stone Mtn, GA 30087

Phone Number: **800-837-0864**
Contact: **Steve Cash**

Calibration performed by:
Steve Cash

Signature: *Steve Cash*

Calibration Date :   **March 25, 2003**

Calibration Due Date :   **March 24, 2004**

Traceable to NIST Standards.
This calibration conforms to the latest standards set by ASTM E4.

Figure A.6: Durham Geo Calibration Certificate for Durham Geo Enterprises E-116

Pressure Transducer; Serial Number: 312. Page 1 of 2.

Figure A.7: Durham Geo Calibration Certificate for Durham Geo Enterprises E-116

Pressure Transducer; Serial Number: 312. Page 2 of 2.

117

DURHAM GEO 〰 SLOPE INDICATOR

2175 West Park Court
Stone Mountain GA 30087
Tel: 1-800-837-0864
Technical Assistance: Ext. 2012
Fax: (770)-465-7447

Calibration Certificate

Device Calibrated:	Pore Pressue Transducer
Range:	15.0 - 150.0 PSI
Model No:	E-124
Serial No:	332

Readout Model No:	E-410
Readout Serial No:	133
Channel No:	2
Equipment Condition:	Used, Good

Calibration Instrument:
Druck Pneumatic Calibrator 300 PSI Max
Serial No: 6011315012 (.01 Resolution)
Last Calibration Date: 10/17/02
Report #: SCC-14537

Service Used: **Precision Standards Intl.**
Equipment-Standard Used:
Ruska Dead-Weight Gage #14123
NIST #: **SCC-9102**

Applied Pressure	Output	Before Calibration		After Calibration			
		Reading	Error	Reading	Reading	Deviation	Deviation
(psi)	(mV)			# 1	# 2	# 1	# 2
0.00		0.0	0	0.0	0.0	0.00	0.00
15.00		14.9	-0.67	15.1	15.1	0.67	0.67
30.00		29.7	-1.00	30.0	30.1	0.00	0.33
45.00		44.4	-1.33	44.9	45.0	-0.22	0.00
60.00		59.4	-1.00	60.0	60.0	0.00	0.00
90.00		89.7	-0.33	90.1	90.2	0.11	0.22
120.00		119.8	-0.17	120.4	120.5	0.33	0.42
150.00		150.2	0.13	150.9	151.0	0.60	0.67
					Total Error:	0.67%	0.67%
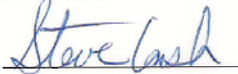
Resolution:	.1 PSI
Temperature at time of calibration °C:	23
Error due to temperature change:	
Excitation Voltage:	9.92
Offset 1	(-) 96
Scale 1	.3043

*NOTE: Readouts and transducers have been calibrated at the factory and are a matched pair. In general, pressure transducers, load cells and LDT's are not interchangeable.

Associated Equipment:

Location of Equipment at time of Calibration
Company Name: **Auburn University**
Physical Address: **201 Harbert Engineering Center**
Auburn University, AL 36849

Phone Number: **(334) 844-6825**
Contact: **David J. Elton, Ph.D., P.E.**

Calibration performed by:

Steve Cash

Signature: _Steve Cash_

Calibration Date : April 24, 2003

Calibration Due Date : April 23, 2004

Traceable to NIST Standards.
This calibration conforms to the latest standards set by ASTM E4.

Report # E-124 #332a.xls

Page 1 of 2

Figure A.8: Durham Geo Calibration Certificate for Brainard-Kilman E-124 Pore Pressure Transducer; Serial Number: 332. Page 1 of 2.
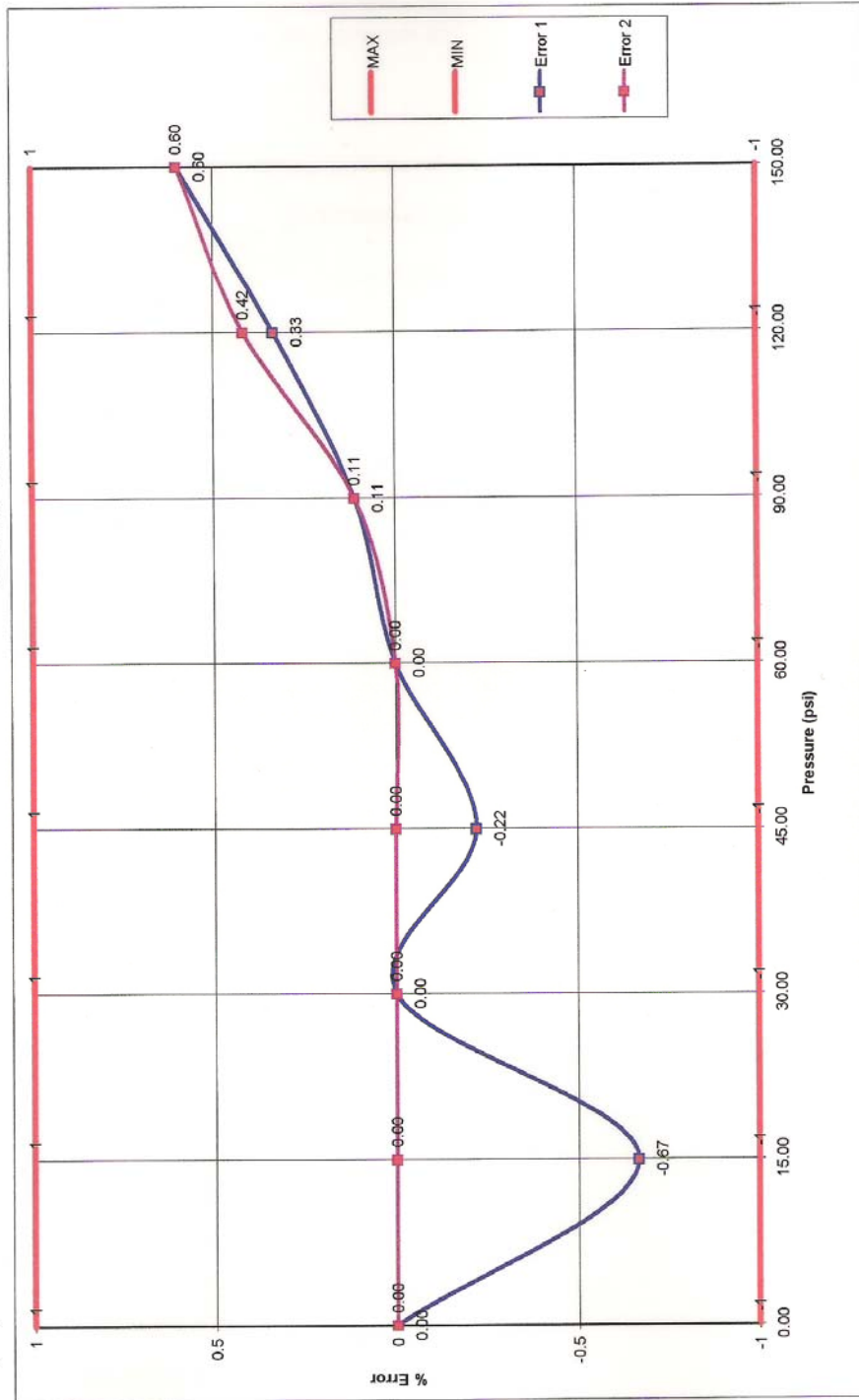
118
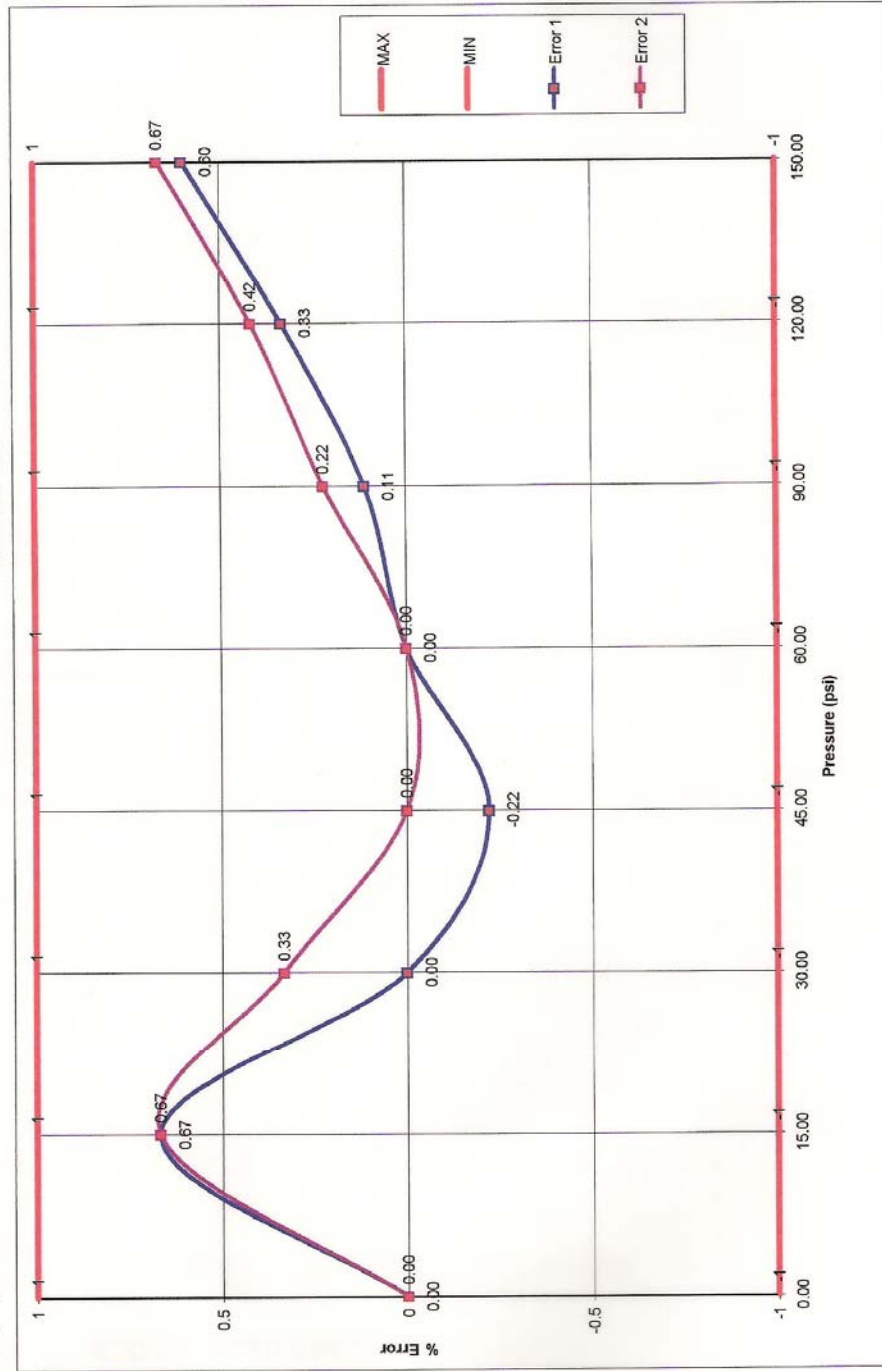
Figure A.9: Durham Geo Calibration Certificate for Brainard-Kilman E-124 Pore Pressure Transducer; Serial Number: 332. Page 2 of 2.

DURHAM GEO ⬤⬤ SLOPE INDICATOR

2175 West Park Court
Stone Mountain GA 30087
Tel: 1-800-837-0864
Technical Assistance: Ext. 2012
Fax: (770)-465-7447

Calibration Certificate

Device Calibrated:	Displacement Transducer
Range:	0.000 - 2.036
Model No:	E-312
Serial No:	134

Readout Model No:	E-410
Readout Serial No:	133
Channel No:	1
Equipment Condition:	Used, Good
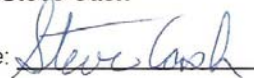
Instrument Information:
Starrett 0.0001 Div Micrometer
Serial No: T-465
Last Calibration Date: **Oct. 8 2002**
Service Used:
Precision Instruments Repair
Equipment-Standard Used:
Carl Ziess Calibrator #14380
Control Number: 4600339308

Increment	Output	Before Calibration		After Calibration			
		Reading	Error	Reading	Reading	Deviation	Deviation
(Inches)	(mV)			#1	#2	#1	#2
.000				0.000	0.000	0.00	0.00
0.0250				0.025	0.025	0.00	0.00
0.0500				0.050	0.050	0.00	0.00
0.1000				0.101	0.101	1.00	1.00
0.2000				0.200	0.200	0.00	0.00
0.3000		No Adjustment Necessary		0.300	0.300	0.00	0.00
0.4000				0.400	0.400	0.00	0.00
0.5000				0.500	0.501	0.00	0.20
1.0000				1.000	1.000	0.00	0.00
1.5000				1.499	1.500	-0.07	0.00
1.7500				1.750	1.750	0.00	0.00
2.0000				2.003	2.003	0.15	0.15
2.0360				2.033	2.033	-0.15	-0.15
					Total Error:	1.00%	1.00%

Resolution:	.001 "
Temperature at time of calibration ^{0}C:	23
Error due to temperature change:	
Excitation Voltage:	9.92

Offset 0   (+) 141
Scale 0   .5604

*NOTE: Readouts and transducers have been calibrated
at the factory and are a matched pair. In general, pressure
transducers, load cells and LDT's are not interchangeable.

Calibration performed by:
Steve Cash

Signature: *Steve Cash*

Associated Equipment:

Location of Equipment at time of Calibration

Company Name: **Auburn University**
Physical Address: **201 Harbert Engineering Ctr**
Auburn University, AL 36849
Phone Number: **(334)844-6825**
Contact: **David J. Elton, Ph.D., P.E.**

Calibration Date :   **April 29, 2003**

Calibration Due Date :   **April 28, 2004**

Traceable to NIST Standards.
This calibration conforms to the latest standards set by ASTM E4.

Figure A.10: Durham Geo Calibration Certificate for Boart Longyear E-312 Linear

Displacement Transducer; Serial Number: 134. Page 1 of 2.
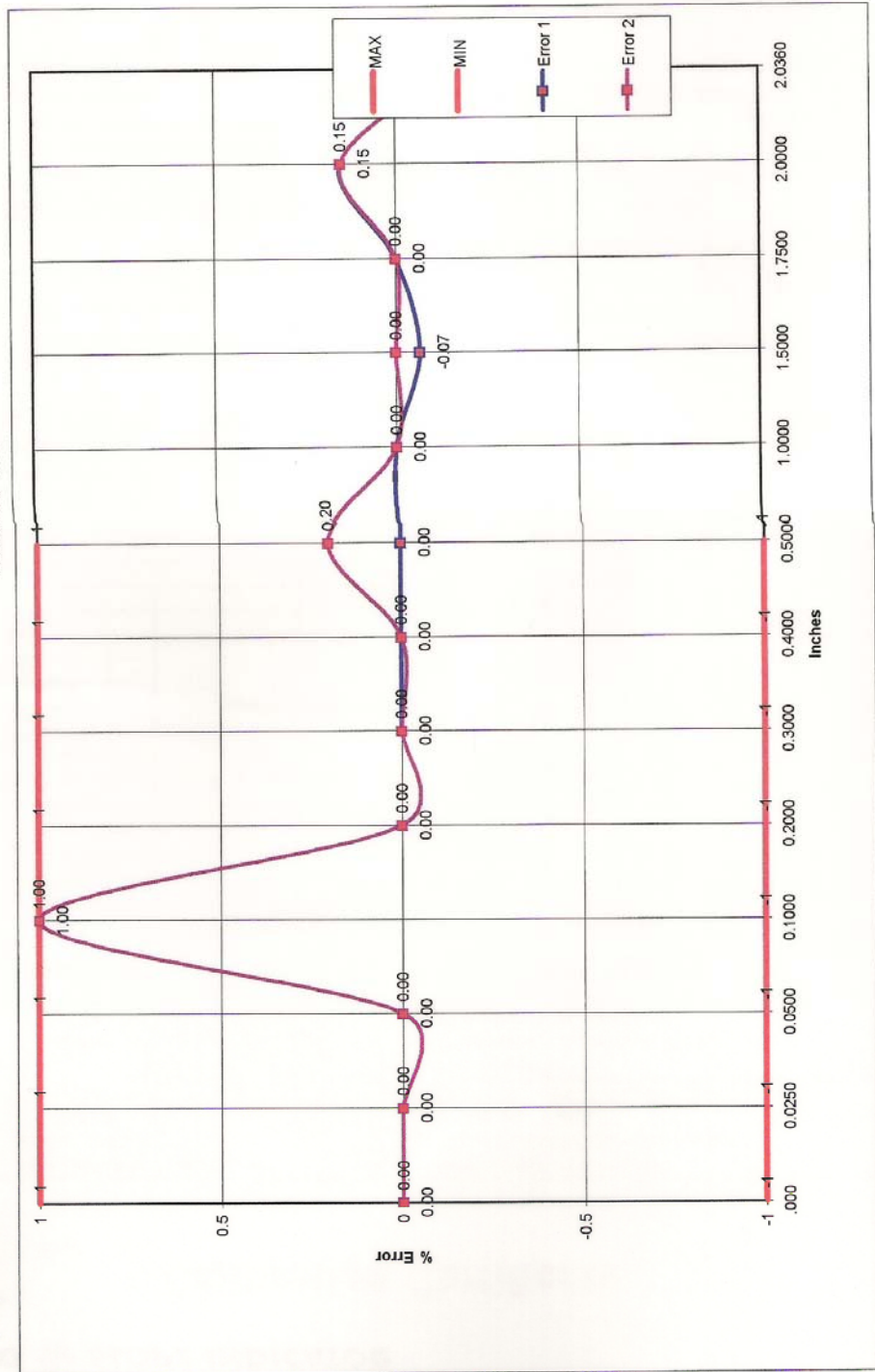
Figure A.11: Durham Geo Calibration Certificate for Boart Longyear E-312 Linear Displacement Transducer; Serial Number: 134. Page 2 of 2.

121

E-400

DIGITAL READOUT

ATTN: DAVE ELTON

SERIAL NO

SCALE FACTOR

POWER

INPUT

OUTPUT

110 V. AC
220 V. AC

BRAINARD-KILMAN
STONE MOUNTAIN, GA
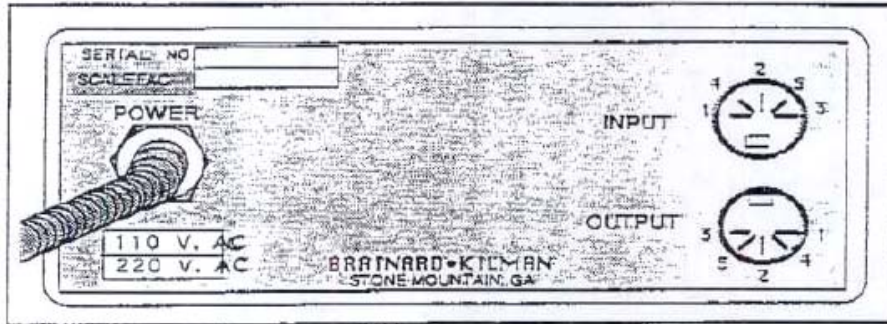
WARNING:
DISCONNECT POWER BEFORE REMOVING COVER!

COLOR KEY

TRANSDUCER INPUT: 5 PIN DIN SOCKET (180°)

WIRING CONFIGURATION - TRANSDUCERS

	LOAD CELL	PRESSURE	DISPLACEMENT	SOCKET PIN
SUPPLY –	RED	RED	RED	5
SUPPLY –	BLACK	BLACK	YELLOW	4
SIGNAL –	WHITE	GREEN	BLUE	2
SIGNAL–	GREEN	WHITE	GREEN	1

SUPPLY VOLTAGE 10.00V DC at maximum 90mA.

OUTPUT DATA: 5 PIN DIN SOCKET (180°)

OPTIONS SOCKET
PIN #

PIN 1=
PIN 2=
PIN 3=
PIN 4=
PIN 5=

NOTE: STANDARD OUTPUT SOCKET FITTED, NOT INTERNALLY CONNECTED UNLESS OPTIONS PURCHASED.

SERIAL NUMBER

SCALE FACTOR

TRANSDUCER SERIAL NO.

1-800-241-9468

10

Figure A.12: Wiring diagram for Durham Geo (formerly Brainard – Kilman and Boart Longyear) 5 Pin Socket transducers.

122

Contact Information

Equipment Service and Supplies:

Durham Geo Slope Indicator (formerly Brainard-Kilman and Boart Longyear)

2175 West Park Court

Stone Mountain, GA 30087

Phone: 800-837-0864

Phone: 770-465-7557

Fax: 770-465-7447

www.durhamgeo.com

LDS-Nicolet (formerly Optim Electronics)

8551 Research Way, M/S 140

Middleton, WI 53562

Phone: 608-821-6600

Fax: 608-821-6691

www.optimelectronics.com

Hydrogel:

The hydrogel used in this project is called "Soil Moist" and was obtained from:

JRM Chemical, Inc.

4881 NEO Parkway

Cleveland, OH 44128

(800) 962-4010

www.soilmoist.com

APPENDIX B: MEGADAC QUICK START GUIDE

B.1   Introduction

This guide will help in the setup of the Megadac 3415AC and Total Control Software (TCS) for DOS software for data collection. The procedures described in the guide were used to setup a Brainard-Kilman E-124 Pore Pressure Transducer, Boart Longyear E-312 Linear Displacement Transducer, and Brainard-Kilman E-214 Load Cell (0-1500lbs) for use in data collection for triaxial testing. However, these procedures may be used to setup any sensor. This guide is not a comprehensive manual for the Megadac or TCS software. The *Optim Technical Information: Megadac 3415AC* or *Optim Technical Information: TCS* should be consulted for more detailed information. *NOTE: Avolt/multi meter will be needed to calibrate sensors*.
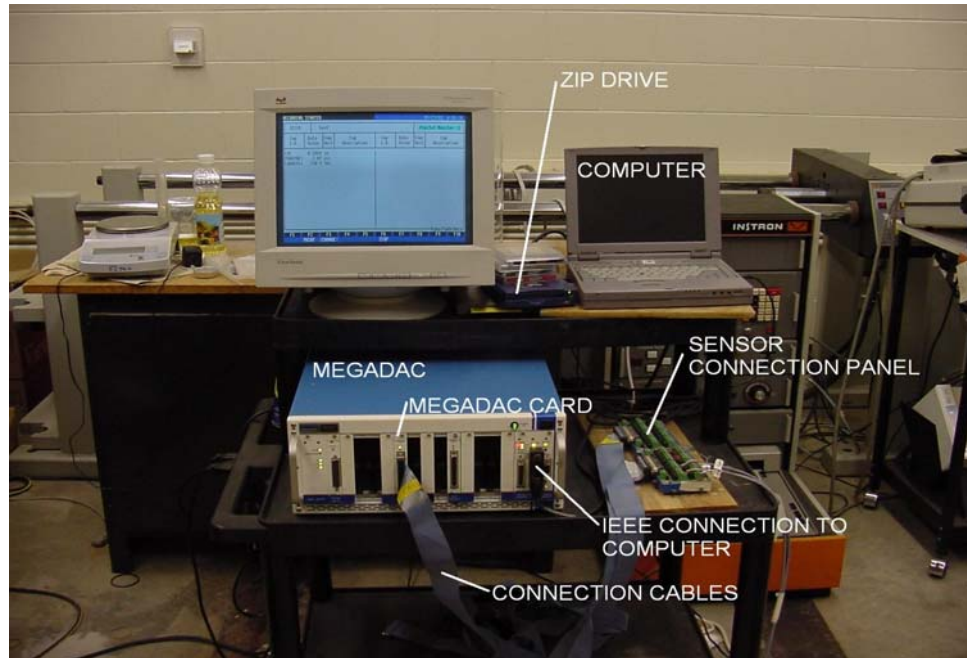
Figure B.1: Megadac setup with labeled components.

B.2   Megadac Setup

B.2.1   The Megadac

The Megadac (fig. B.1) is an electronic device used to capture and record data from sensors. The sensors are any device used to measure a value such as load, displacement, or pressure. Each sensor is recorded on a channel which the Megadac is programmed to monitor. This provides a continuous log of readings from these sensors during testing.

B.2.2   Sensor Connection Panel

Sensors are connected to the Megadac through the sensor connection panel (fig. B.1). Each sensor is connected to a different channel on the sensor connection panel.

Each channel provides excitation voltage to the sensor and also relays change in mV back to the Megadac.

B.2.3 The Megadac Card

The Megadac card (fig. B.1) relays the information from the channels on the sensor connection panel to the Megadac. Each card is able to monitor 8 channels. The card also controls the excitation voltage and gain for the sensors. *NOTE: The Optim technical manuals call Megadac cards modules*.

B.2.4 Connection Cables

The connection cables (fig. B.1) connect the sensor connection panel with the Megadac card.

B.2.5 IEEE Connection to Computer

The IEEE connection to computer (fig. B.1) provides a line of communication between the Megadac and the computer. This setup shows a connection to a laptop, other connection options may be used for different computers. Consult the *Optim Technical Information: Megadac 3415AC* for details.

B.2.6 Computer

Any computer (fig. B.1) that has the TCS for DOS software loaded on it.

127

B.2.7 ZIP Drive

In this setup, the laptop computer did not have the ability to transfer large files to a portable media (i.e. no cd burner). Therefore, the ZIP drive (fig. A.1) was installed, so large files could be transferred to portable media to share with other computers. *NOTE: If the computer in figure A.1 is being used, the ZIP drive must be installed on a parallel port. The USB ports will not work*.

B.3 Preparing to Record Data

B.3.1 Checking the Megadac Card

NOTE: All card instructions for the Megadac card apply only to cards labeled AD-1 808FB-1 (labeled on front tab). The Megadac card monitors and regulates the sensor channels for the Megadac. If the card is setup incorrectly, the Megadac will not work properly because sensor readings will not occur. So, it is worth the time to check it before starting. Before removing a card, be sure the Megadac is turned off. To remove a card, unscrew the small screw at the top and bottom of the card, and then lift up on the bottom tab and pull out.

Changes to the card are controlled by jumpers. Jumpers are the small, plastic and metal pieces that slide on and off metal studs on the card. Installing or removing them closes or opens a different circuit respectively.

B.3.1.1   Checking the Channel Address Jumpers

Each Megadac card monitors and controls a different set of 8 channels. Each card fits into a card slot on the Megadac which represents a fixed set of 8 channels. The first slot (far left) on the Megadac represents channels 000-007, the second, 008-015, and so on. The channel numbers for the Megadac slots cannot be changed. However, the card channel numbers can be changed. The card channel numbers and the slot channel numbers must match or the Megadac will not recognize it. Jumpers on the card can be adjusted (fig. B.2) so that the card channel numbers match the Megadac slot channel numbers. These jumpers are called the channel address jumpers (fig. B.3). *NOTE: The card may be labeled with channel numbers (under the top screw), but this does not mean that the card is setup for those channels, nor does it mean that the card must be used for those channels. If the channel address jumpers on the Megadac card match the channel numbers for the card slot to be used, no adjustment is necessary.*

J6 J5 J4 J3	J9 J8 J7 1 1 1	J9 J8 J7 1 1 0	J9 J8 J7 1 0 1	J9 J8 J7 1 0 0	On **J10** thru **J25** install two and only two jumpers
1 1 1 1	000-007	128-135	256-263	384-391	J10, J18
1 1 1 0	008-015	136-143	264-271	392-399	J10, J18
1 1 0 1	016-023	144-151	272-279	400-407	J11, J19
1 1 0 0	024-031	152-159	280-287	408-415	J11, J19
1 0 1 1	032-039	160-167	288-295	416-423	J12, J20
1 0 1 0	040-047	168-175	296-303	424-431	J12, J20
1 0 0 1	048-055	176-183	304-311	432-439	J13, J21
1 0 0 0	056-063	184-191	312-319	440-447	J13, J21
0 1 1 1	064-071	192-199	320-327	448-455	J14, J22
0 1 1 0	072-079	200-207	328-335	456-463	J14, J22
0 1 0 1	080-087	208-215	336-343	464-471	J15, J23
0 1 0 0	088-095	216-223	344-351	472-479	J15, J23
0 0 1 1	096-103	224-231	352-359	480-487	J16, J24
0 0 1 0	104-111	232-239	360-367	488-495	J16, J24
0 0 0 1	112-119	240-247	368-375	496-503	J17, J25
0 0 0 0	120-127	248-255	376-383	504-511	J17, J25

Where   1 = Jumper block installed
            0 = No jumper block

Figure B.2: Megadac card (AD-1 808FB-1) channel address jumper configurations, for different channel ranges. Channel ranges are listed in the center of the figure. The 1's and 0's represent where jumpers are either installed or removed. Jx, where x = 3-25, is an individual jumper (Optim 1996).
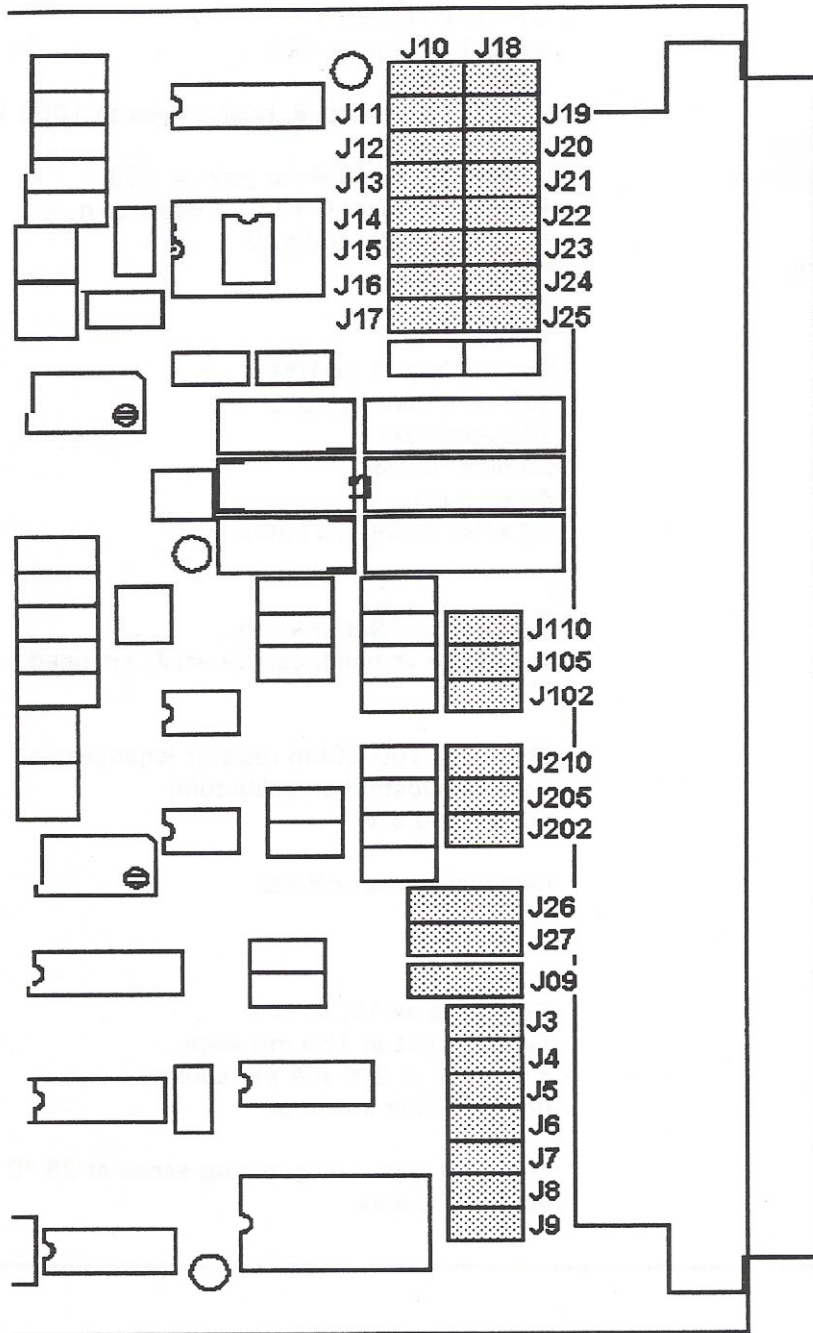
Figure B.3: Diagram showing jumpers on the back end of the Megadac AD-1 808FB-1 card. Jumpers labeled Jx, where x = 3-25, are channel address jumpers. Jumpers labeled J1x or J2x, where x = 10, 05, 02, are excitation voltage control jumpers (Optim 1996).

131
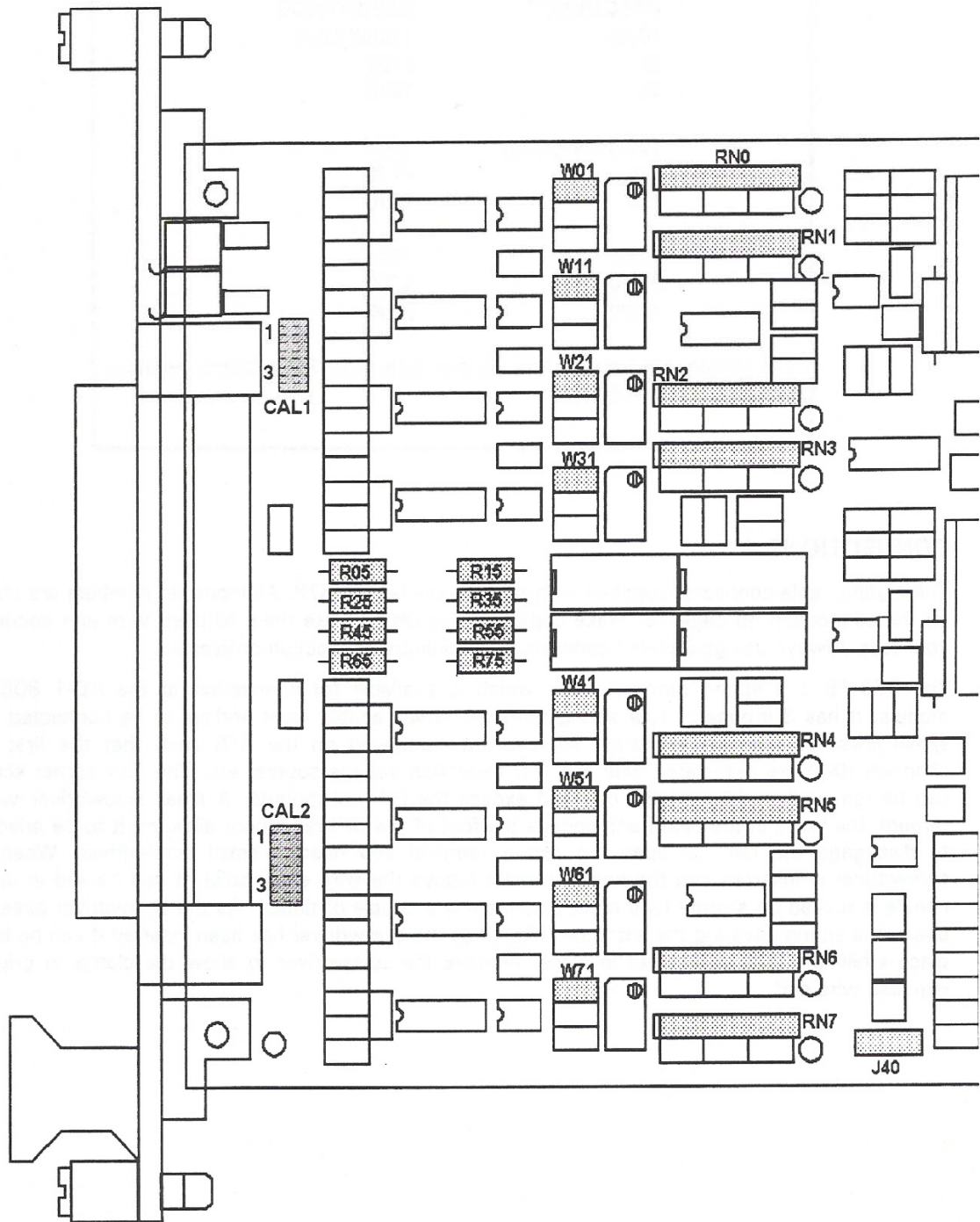
Figure B.4: Front end of the Megadac AC-1 808FB-1 card. Gain jumpers are labeled Wx1, where x = channel number (Optim 1996).

B.3.1.2   Setting the Excitation Voltage

Excitation voltage is supplied to the sensor through the Megadac card. It can be set to 10V, 5V, or 2V by moving the voltage control jumper. For voltage supply, the 8 channels on the card are split in half. The first 4 channels can be set to one voltage, while the last 4 channels can be set to another. Figure B.3 shows the voltage control jumpers. J1x, where x = 10, 05, 02, controls the first 4 channels and J2x, where x = 10, 05, 02, controls the last 4. The number represented by x on these jumpers designates the voltage to be used 10 = 10V, 05 = 5V, and 02 = 2V. Because the jumper controls 4 channels, all sensors on those channels must use the same excitation voltage.

B.3.1.3   Setting the Gain

The range and resolution of each channel is set by the gain. Gain on the Megadac card can either be set at 100 or 1 by installing or removing a jumper. If the sensors are recording a small range of values and greater resolution is required, the gain should be set at 100. If the opposite is true, gain should be set at 1. Figure B.4 shows the locations of the gain jumpers. Gain can be controlled on each channel separately. If the jumper is installed, gain = 100, if it is removed, gain = 1.

B.3.2   Sensor Connection

Sensor connection involves connecting bare ends of sensor wire to screw down clamps on the sensor connection panel. If the sensor has loose wires this is fine, but if the sensor has a plug on the end, an adaptor plug wired to a piece of wire

will have to be made (adaptor plugs and wires for this project were five pronged

female adaptors connected to a thin, grey, five wire, wire). The ends of the wires will

have to be stripped. Figures B.5, B.6, B.7 show more detail on sensor connection.

This project used wiring for a four wire bridge, other wiring options can be found in

Optim Technical Information: Megadac 3415AC. NOTE: Be sure the Megadac is

turned off before connecting sensors.
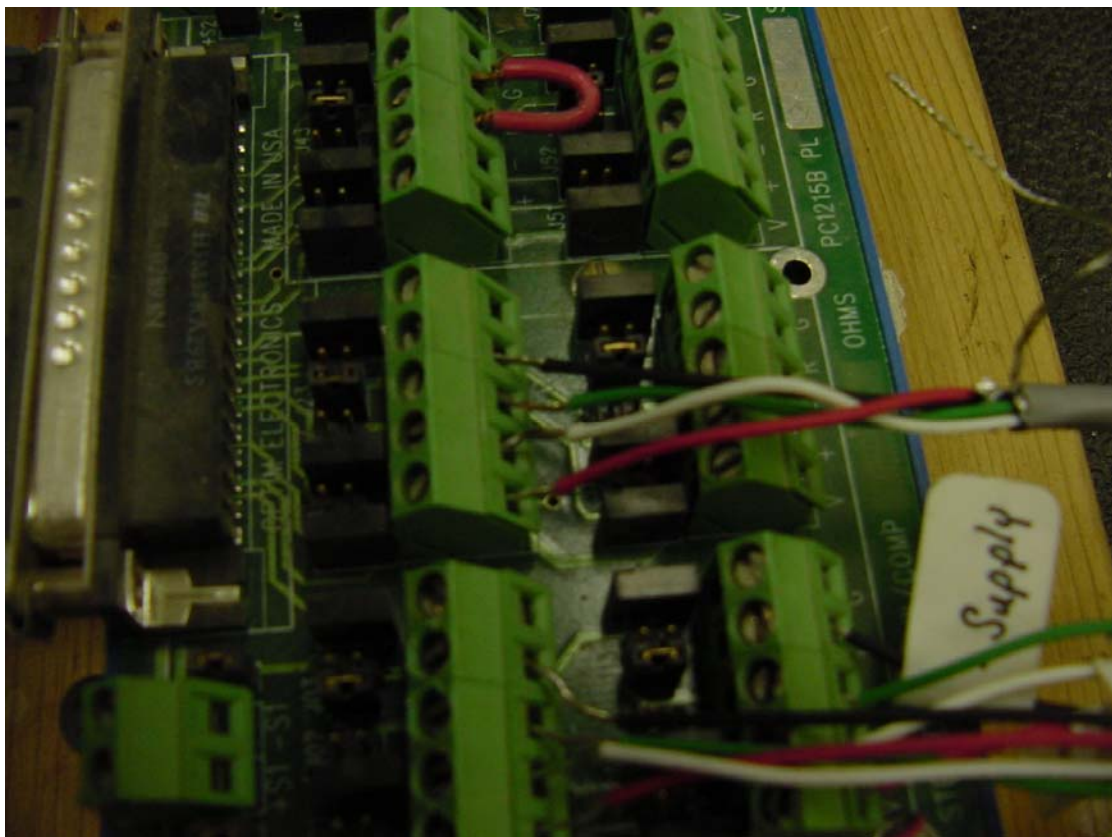
Figure B.5: Picture from the left end of the sensor connection panel for the Megadac,

showing sensor wiring for this project.
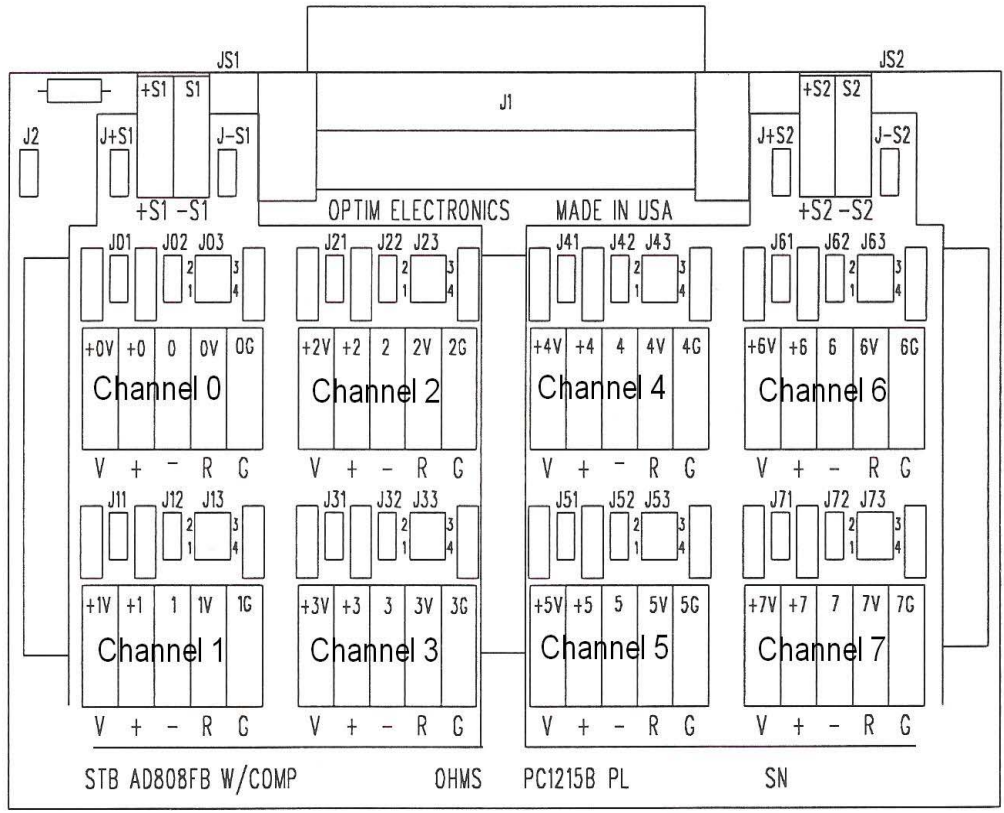
Figure B.6: Overhead diagram of the Megadac sensor connection panel. Channel numbers and order are labeled (Optim 1996).
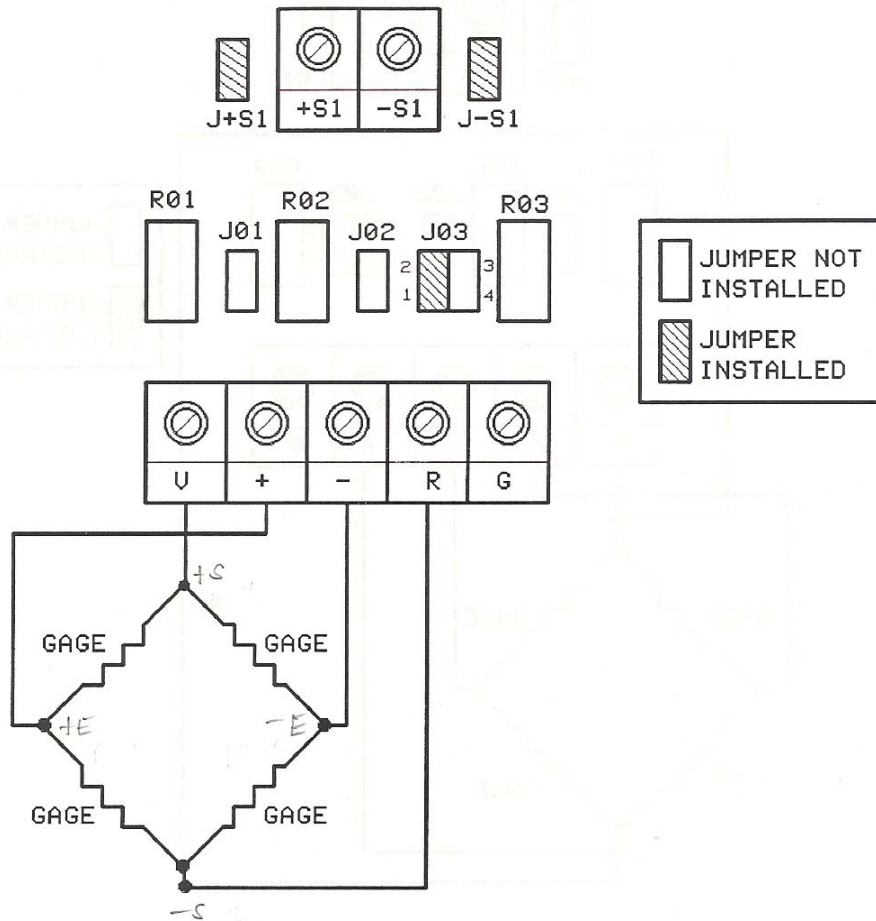
Figure B.7: Detail diagram of channel 0 from the Megadac sensor control panel. Illustrates wiring for a four wire bridge (Optim 1996).

B.3.3   Sensor Calibration

Sensors operate by supplying an excitation voltage, and then as a change occurs in the sensor, a change is voltage is outputted to a readout. The voltage output is converted to a measured unit through calibration. For example, a linear displacement transducer is excited using 10V. When the transducer is displaced 0", a voltmeter connected to the output reads 0mV. When the transducer is displaced 1", the voltmeter reads 5mV. Therefore, a change of 5mV equals a change of 1".

When the measured unit is plotted against mV, the relationship is linear. The slope of the line created in the plot, mV/unit, must be inputted into the TCS software. This slope, called sensitivity in TCS, tells the TCS program what value corresponds to an output mV.

In order to calibrate a sensor, its output mV must be plotted against a known change in the sensor. For example, a pore pressure transducer is connected to a triaxial cell. If the triaxial cell is completely filled with water, cell pressure = pore pressure. This allows you to measure output mV at different pressures to create a pressure versus mV plot.

Calibration is performed using a voltmeter. *NOTE: Voltmeter should be set to read DC volts. The voltmeter probes must touch bare wire to obtain a reading.* Once the sensors are connected turn the Megadac on. Place the black voltmeter probe on wire going into R clamp (fig. B.7). Place the red probe on the wire going into V clamp (fig. B.7). The voltmeter should read the supply voltage that was selected earlier on the Megadac card. This ensures that the sensor is receiving power. Now remove the wires from the + and R clamps (fig. B.7), wrap the bare end of the R wire around the black probe, and wrap the + wire around the red probe. Now induce a change in the sensor being calibrated and be sure the mV on the voltmeter changes. The sensor can now be calibrated. Once calibration is complete, plot measured unit vs. mV, draw a best fit line, and calculate the slope. Once this is completed for all sensors, sensor setup in TCS software can begin.

B.3.4   TCS for DOS

B.3.4.1   Directory Creation in DOS and Starting TCS

Turn on computer and start DOS (this was a selection at startup on the laptop used in this project). Next, create a directory (folder) where test information can be stored, so it can be easily found later. At the C:\ prompt, type:

 "md_Nameoffolder" (_ denotes a space) (md = make directory)

This creates the directory "Nameoffolder". Now each time DOS is started and the C:\ appears, type:

"cd_Nameoffolder" (_ denotes a space) (cd = change directory)

This will open the directory "Nameoffolder". Once the directory is open, i.e. "C:\Nameoffolder\" appears, type "tcs". The command line should look like this:

C:\Nameoffolder\tcs

Press enter and the TCS program will start.

NOTE: TCS must be started from the directory created above in order to access data that is saved in that directory.

B.3.4.2   Sensor Setup in TCS

At the opening screen for TCS press enter.

The "TCS Program Selections" screen will appear (fig. B.8).

NOTE: Use the arrow keys to scroll to selection. ESC can be pressed at any time to return to the previous screen.

```
                    TCS PROGRAM SELECTIONS

TESTING WITH TCS
     TCS (Define, Check, Run or Review Tests)  ————————

TCS SOFTWARE UTILITIES
     Utility Programs (Backup, Merge, Printouts, Etc)
     Examples of Keyboard Usage and Screen Interaction

     Example of Defining and Running a Sample Test

MEGADAC HARDWARE UTILITIES
     MAP (Add or Change MEGADAC Input/Output Cards)
     MEGADAC  Configuration  and  Version
     Directory of Tests On MEGADAC  Media
     Formatting the MEGADAC Media

OTHER UTILITIES
     Host Computer Communication Selections
     Communication Checkouts & Diagnostics
     Trouble Shooting & Reporting Problems
```

Figure B.8: TCS for DOS Program Selections Screen (Optim 1996).

Highlight "Testing with TCS"; press enter.

"TCS Main Menu for Test Name" screen will appear (fig. B.9).

```
TCS MAIN MENU FOR TEST NAME = YourTest

   Define Test Requirements
   Check Test Validity
   Record Calibration Data
   Record Test Data
   Review Test Data
```
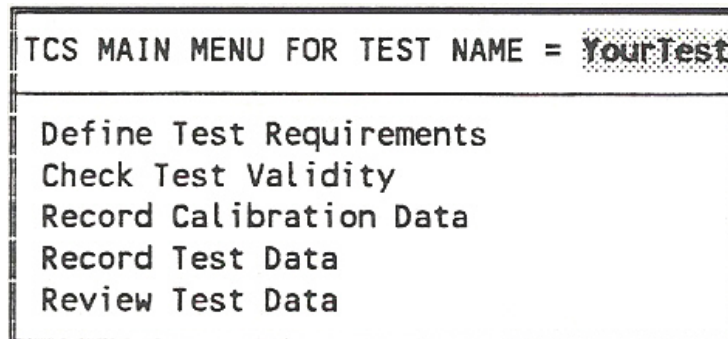
Figure B.9: TCS for DOS Main Menu for Test Name Screen (Optim 1996).

139

Enter a test name where "YourTest" is located Figure B.9. A name must

be entered before continuing.

Highlight "Define Test Requirements" (fig. B.9); press enter.

The "Define Test Requirements" screen will appear (fig. B.10).
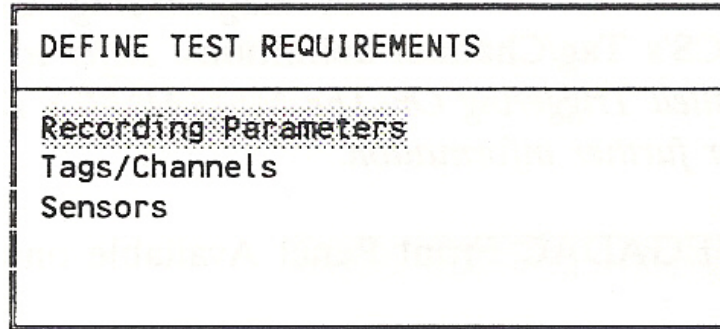
Figure B.10: TCS for DOS Define Test Requirements Screen (Optim 1996).

Highlight "Recording Parameters" (fig. B.10); press enter.

The "Recording Parameters" screen will appear (fig. B.11).

Figure B.11: TCS for DOS Recording Parameters Screen (Optim 1996).

140

On the "Recording Parameters" screen the user can choose the number of scans per second, how to stop and start testing, and where to record the test log. For triaxial testing, 5 – 10 scans per second should be used. Recording start and stop should be set to "CPU Function Key" which allows the user to press a key on the computer keyboard to begin and end recording, and test logs should be recorded to the "Megadac Memory".

Along the bottom of the "Recording Parameters" screen should be a list of functions for the Function (F) keys.

Find the F key corresponding to "PgRt" and press.

"Extended Features" screen will (fig. B.12).

```
MYTEST | Sample Test                              EXTENDED  FEATURES

        ┌─────────────────┐ ┌─────────────────────┐ ┌─────────────────────┐
        │    RECORDING    │ │     MONITORING      │ │       ALARMS        │
        │                 │ │                     │ │                     │
        │Interval Mode.......N│ │Digital Monitors.....Y│ │MEGADAC Alarms....N│
        │SubMultiplexing.....N│ │Plots................Y│ │TCS Alarms........N│
        │Automatic Transfers N│ │Peak Detection.......Y│ │                   │
        │Auto Restart....... N│ │DAC Outputs/Playback.N│ │                   │
        └─────────────────┘ └─────────────────────┘ └─────────────────────┘

        ┌─────────────────┐ ┌─────────────────────┐ ┌─────────────────────┐
        │BALANCE/CALIBRATION│ │      MEGADAC        │ │        TCS          │
        │                 │ │                     │ │                     │
        │Data Set Size..... 1s│ │External Clock.......N│ │Transform/Pseudos.N│
        │Bal Tolerance.....45%│ │Sample and Hold......Y│ │Display Card Gain Y│
        │Cal Tolerance..... 2%│ │MEGADAC COMM Address 1│ │Event Markers.....N│
        │Automatically Bal. N │ │Addressing is Standard│ │NoteBook..........N│
        │                 │ │ADC Module is  ADC5616│ │Snapshots=N  Size=1│
        └─────────────────┘ └─────────────────────┘ └─────────────────────┘
```

Figure B.12: TCS for DOS Extended Features Screen (Optim 1996).

Change the "Transforms/Pseudos" option in the bottom right box to "Y".
This allows access to the "Transforms/Pseudos" screen, which will be used later
and explained in Section B.3.4.3.

Press ESC to return to the "Define Test Requirements" screen. The screen
should now contain another option called "Transforms" (fig. B.13).


```
DEFINE TEST REQUIREMENTS

Recording Parameters
Tags/Channels
Sensors
Transforms
```
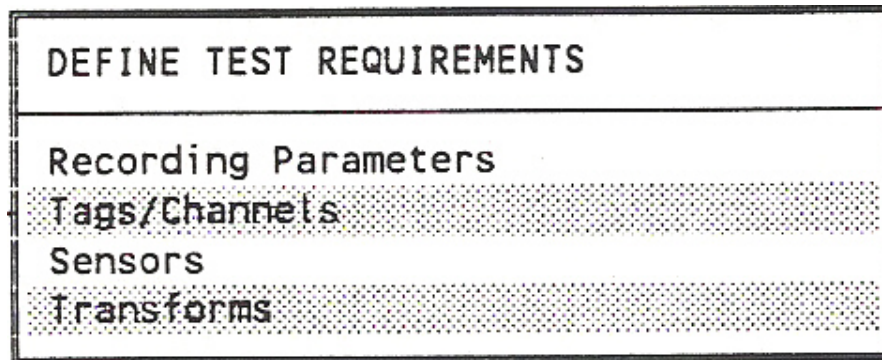
**Figure B.13: TCS for DOS Define Test Requirements Screen with Transforms option
added (Optim 1996).**

Once at the "Define Test Requirements" screen, highlight "Sensors"; press
enter.

The sensor library appears where the Megadac is told what type of sensors
will be used for testing. When "Sensors" is selected, a screen will pop up asking
what the sensor will be measuring, i.e. pressure, displacement, etc. Select the
appropriate measurement, and the "Sensor Information Screen" (fig. B.14) will
appear.

Scroll to "Sensor Name", and enter a name for the sensor such as
"loadcell".

Scroll to "Engineering Units", and enter the units the sensor will measure, such as "lbs".

Scroll to "Analog Input Card", press F7, and a screen will appear listing different types of Megadac cards. Choose the card type that is written on the front of the Megadac card being used. For this project the card was AD-1 808FB-1.

Scroll to "Description", and enter a description of the senor.

Scroll to "Sensor Number", and enter the serial number of the sensor.

Scroll to "Excitation Source". This should be the same as the "Analog Input Card" entered above.

Scroll to "Excitation Voltage", press F7, and a screen will appear listing 10, 5, and 2 volts. Choose the appropriate voltage for the sensor being used. This must match the voltage set on the Megadac Card in Section B.3.1.2.

Scroll to "Sensitivity", and enter the slope, in mV/unit, that was calculated during sensor calibration in Section B.3.3. Enter 1 as the last number under V.

Leave "Filter Frequency" as "Sys Filte Frq".

This process must be repeated for each sensor to be used with the Megadac. Once all sensors have been setup in the sensor library, return to "Define Test Requirements" (fig. B.10) by pressing ESC.

```
┌──────────────────────────────────────────────┐
│ YourTest │ Sample of a Sensor Screen          │
├──────────┴───────────────────────────────────┤
│                                               │
│  Sensor Name............ LOAD123              │
│  Engineering Units...... lbs                  │
│                                               │
│  Analog Input Card...... 684SH1               │
│                                               │
│  Description............ Load Cell            │
│  Sensor Number.......... Serial # 123         │
│                                               │
│  Excitation Source...... 684SH1               │
│  Excitation Voltage..... 10   Volts           │
│                                               │
│                   mV per lbs per Volts        │
│  Sensitivity..  -3.49 / 1.00  / 10            │
│                                               │
│  Filter Frequency....... Sys Filte Frq        │
│                                               │
└───────────────────────────────────────────────┘
```

Figure B.14: TCS for DOS Sensor Information Screen (Optim 1996).

Highlight "Tags/Channels"; press enter.

Here the Megadac is told what sensors are on what channels. "TagID" gives the channel a name chosen by the user. It is helpful to choose a name that describes the senor connected to the channel. The channel number is entered under "Channel". The channel number that a sensor is connected to is defined by the Megadac card and Figure B.6. When the column under "Sensor" is highlighted, press F7. This will open the sensor library. Choose the appropriate sensor description for the channel from the list. "Unit" should fill in automatically when the sensor description is chosen; if not, enter the appropriate engineering unit. Once

144

each channel is setup to read its corresponding sensor, press ESC until the "TCS Main Menu for Test" (fig. B.9) is reached.

Highlight "Check Test Validity"; press enter.

This will open the "Check Test Validity" screen (fig. B.15).

```
CHECK TEST VALIDITY

Test Logic
Equipment Checkout
Channel Checkout
Bal Check
Cal Check
System Noise Checkout
System Voltages Checkout
Single Tag Checkout/Physical Cal
Recording Time
Sample Run
Review Sample Run Data
```
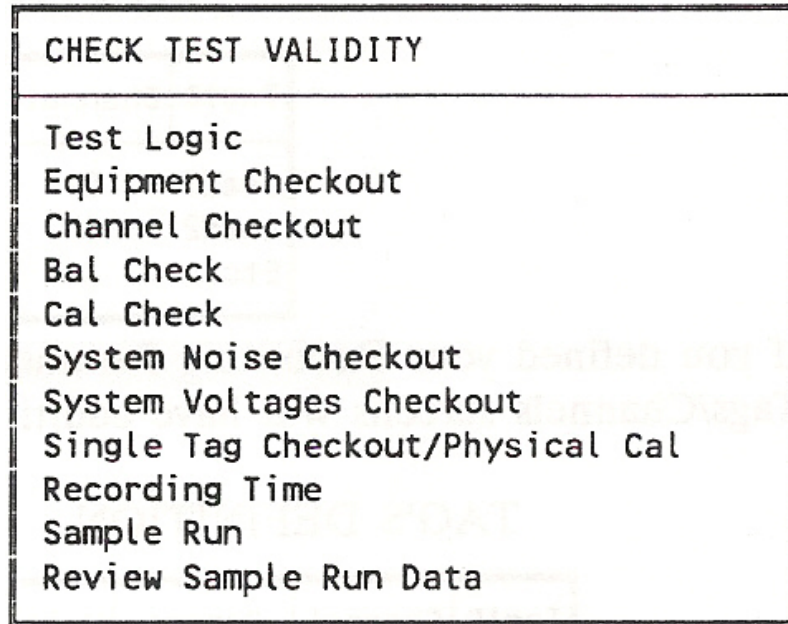
Figure B.15: TCS for DOS Check Test Validity Screen (Optim 1996).

Highlight "Bal Check"; press enter.

The Megadac will now match card settings and sensor inputs; this process is called "mapping". If the settings are correct a "Bal Check" screen will appear showing "TagID's" with current readings from corresponding sensors. If an error occurs check Megadac card and TCS inputs and consult the *Optim Technical Information: TCS* and *Optim Technical Information: Megadac 3415AC. NOTE: If there is a "Communications" error, make sure the Megadac is on*.

145

If no errors occur, be sure all sensors should read a value of zero, i.e. no displacement, pressure, or load is applied. The sensor readouts on the "Bal Check" screen will probably not be zeroed out, i.e. will not read 0. Record the zero reading (number that should be 0) for each sensor on a sheet of paper. If the sensor's zero reading is 0 then skip it. *NOTE: Numbers will jump around, but should consistently hover over a small range of values. Just record a number in the middle of this range.*

B.3.4.3 TCS Transforms

TCS Transforms perform a mathematical operation to the sensor reading. These operations include addition, subtraction, multiplication, and division and are used to zero the sensor readings. The "Transforms" screen is accessed through the "Define Test Requirements" menu (fig. B.13). Once at the "Transforms" screen, a "Transform I.D." and "Transforms Equation" must be entered (fig. B.16). "Transform I.D." is the name of the transform. A "Transform I.D." will be associated with each sensor and it's "TagID" name. It is helpful to name the transform after the sensor it will be attached to. Do not use the same name used for the sensor "TagID". "Transforms Equation" tells TCS what mathematical operation to perform to the sensor reading. The equation must be entered in this format: @_mathematical operation_number (_ denotes a space). For example, @ + 2, will add a value of two to the sensor reading. A list of all mathematical operations used in transforms is given in Figure B.16. Using the sensor readings recorded earlier,

fill in "Transform I.D." and "Transforms Equation" on the "Transforms" screen that

will zero each sensor.

RESERVED SYMBOLS	DESCRIPTION	SAMPLE EQUATION	RESULT
+	Add	2 + 1	3.0000
-	Subtraction or a negative number	2 - 1 2 + -1	1.0000 1.0000
*	Multiply	6 * 2	12.0000
/	Divide	6 / 2	3.0000
^	Calculates a value raised to a power You must use LOG for fractions	12.3450^2 12.3450^2.3 EXP(2.3*LOG(12.3450))	152.3990 Invalid! 323.9138
%	Modulus	12.3450%10	2.3450
()	Overrides mathematical precedence.	2 * 3 + 1 (2 * 3) + 1 2 * (3 + 1)	7.0000 7.0000 8.0000
;	Include comments in equations.	2 * (3 + 1) ;My Comments	8.0000
ACOS	Calculates arc cosine	ACOS(0.1230)	1.4475
ASIN	Calculates arc sine	ASIN(0.1230)	0.1233
ATAN	Calculates arc tangent	ATAN(12.3450)	1.4900
CEIL	Gives maximum integer value	CEIL(12.3450)	13.0000
COS	Calculates cosine	COS(0.1230)	0.9924
COSH	Calculates hyperbolic cosine	COSH(0.1230)	1.0076
EXP	Calculates exponential function	EXP(0.1230)	1.1309
FABS	Finds absolute value	FABS(12.3450)	12.3450
FLOOR	Gives minimum integer value	FLOOR(12.3450)	12.0000
LOG	Calculates natural logarithm	LOG(12.3450)	2.5133
LOG10	Calculates base-10 logarithm	LOG10(12.3450)	1.0915
MOD	Modulus (%)	12.3450 MOD 10	2.3450
SIN	Calculates sine	SIN(0.1230)	0.1227
SINH	Calculates hyperbolic sine	SINH(0.1230)	0.1233
SQRT	Finds square root	SQRT(12.3450)	3.5135
TAN	Calculates tangent	TAN(12.3450)	-0.2251
TANH	Calculates hyperbolic tangent	TANH(12.3450)	1.0000

Figure B.16: TCS for DOS Transform Mathematical Operations List (Optim 1996).

147

Return to "Define Test Requirements" screen by pressing ESC, and enter the "Tags/Channels" screen. Press "PgRt" until "Transform Information" page appears. Under "Transform I.D." (fig. B.17) fill in the name of the transform to use with each sensor. Also enter the "Transformed EngrUnit" (fig. B.17) (usually the same as "EngrUnit" already entered) which defines the unit the sensor reading will be transformed to. The now during testing all sensor readings will be transformed before being recorded. Now data recording can start. *NOTE: Using transforms is not a necessary operation. Data recording can begin after channel tag information is entered, and Megadac mapping is passed. Zeroing of values can be done during data analysis.*

```
          DEFINE TEST REQUIREMENTS

          Recording Parameters
          Tags/Channels
          Sensors
          Transforms
```

Tag I.D.	Chan Nmbr	Sensor Name	Engr Unit	FullScale PlotValue	Transform I.D.	Transformd EngrUnit	Start Pseudo@		Transform I.D.	: =	Transforms Equation	
GAGE1	1	VOLTS	V	10	add_1	V_1			add_1	:	a + 1	

```
The Transform this Tag is to perform ──┘            └─ The Transforms Name.
The Tag's Transformed Engineering Unit ────────────┘     Transforms Equation. ─┘
```

Figure B.17: TCS for DOS fields applicable to "Transforms" (Optim 1996).

B.4 Checking the Sensor Readings

Once all information has been entered for each sensor the sensor readings should be checked to see if they are reading correctly. Highlight "Bal Check" (fig. B.15) on the "Check Test Validity" (fig. B.15) screen. The Megadac will "map", and the "Bal Check" screen will appear. Using the same methods that were used to calibrate each sensor, such as in a triaxial cell full of water, cell pressure = pore pressure, check the sensor readings. However, do not use a voltmeter to measure the output mV; just take the readings from the TCS "Bal Check" screen. Check to see if the readings correspond to known values of pressure, load, displacement, etc. placed on the sensors. If the readings are correct, proceed to testing, if not, review all inputted data and/or refer to Optim Technical Manuals.

B.5 Recording Test Data

NOTE: Once a test is recorded, data entered into TCS is locked in and cannot be changed. A new test must be created if information needs to be changed. A new test can be created based on the existing information, eliminating the need to reenter data. To do this, highlight the test name, select the F key corresponding to "ADD" on the "TCS Main Menu for Test" (fig. B.9), and follow the instructions. To record a test, choose "Record Test Data" from "TCS Main Menu for Test" (fig. B.9). Press the F key labeled "Start", and the Megadac will begin recording. Once testing is finished press the F key again to "Stop" recording. Press ESC to return to the main menu.

B.6   Transferring Test Data to Other Computers

Upon returning to the main menu, highlight and select "Review Test Data". This will bring up the "Review Main Menu" (fig. B.18). Highlight and select "Export Data to Ascii, DIF, Etc." Here, choose where to export the data, such as "C:\Nameoffolder" and what format it will be in. Choose the ACSII format and label the file extension 000, e.g. test.000. Export the data.

Once the data has been exported, restart the computer with Windows. Open Windows Explorer and find the test file in C:\Nameoffolder. Copy the file to a ZIP disk. Now the file can be transferred to other computers.

```
REVIEW MAIN MENU FOR TEST NAME YourTest

  Change Review From/To
  Review Data With View Graphics
  Review Data With Digital Monitors
  Review Data With Plots
  Review Data With Peak Detect
  Export Data To Ascii, DIF, Etc.
  Transfer Data To Other Media
```
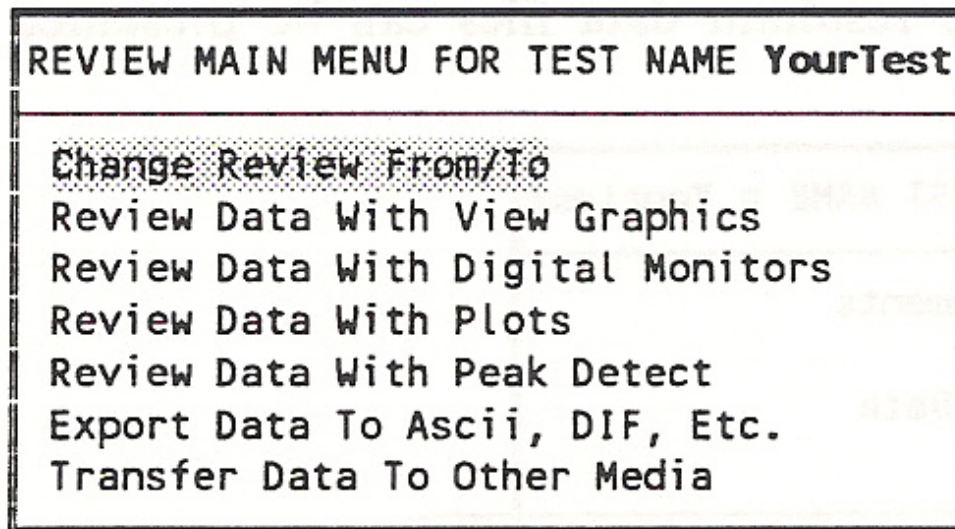
Figure B.18: TCS for DOS Review Main Menu.

APPENDIX C: DETAILED LABORATORY PROCEDURES

C.1 Procedure for Preparing Hydrogel

Note: Wearing a dust mask is recommended when handling powdered hydrogel.

1. Grind hydrogel from its granular form to a powder using a blender. When putting hydrogel into the blender, only put in about a cup. Since the blade of the blender is small, it is most effective to blend small amounts of hydrogel at a time. Blend granules for about 5 minutes.

2. Stack a No. 200 sieve on top of a sieve pan.

3. Empty the powdered hydrogel from the blender into the No. 200 sieve.

4. Place a sieve lid on top of the No. 200 sieve and firmly secure it by pressing it down. Together, the sieve pan, No. 200 sieve, and sieve lid are called the "sieve stack" (fig. 2.1 and 2.2).

5. Shake the "stack" either by hand or in a sieve shaking machine.

6. Use only the hydrogel that goes through the sieve into the pan. Left over hydrogel can be re-ground in the blender, if desired.

Figure C.1: (clockwise from top) A No. 200 sieve, sieve pan, and sieve lid.

Figure C.2: (from top) A lid, No. 200 sieve, and a sieve pan arranged in a "sieve stack".

C.2 Preparing the Sand / Hydrogel Mixture

1. Place 300 grams of Ottawa sand into five 1000 mL beakers.

2. Calculate the desired amount of hydrogel per beaker: [(% hydrogel / 100) x (1500 grams of sand)] / 5.

    Note: 1500 grams of sand is enough to over-fill a 6" long, 2.8" diameter mold.

3. Place the proper amount of hydrogel into each beaker.

4. Tilt the beaker approximately 45 degrees and rotate until you can no longer see hydrogel powder.

5. Combine the contents of the five beakers into one beaker and rotate (as in step 4) 3-4 times.

    Note: It is important to not over-mix the samples, or segregation will occur. Rotate only until hydrogel powder is no longer visible.

C.3 Preparing the Molds

1. Coat the inside of the mold with silicon spray, wipe off excess.

2. Cut a latex membrane (either used sample membranes or latex gloves) roughly twice the size of the mold opening.

3. Lay the latex over the mold opening and secure with a rubber band (fig. 2.3) (it is important that this seal is tight, so the rubber band may have to be double looped).

Figure C.3: Latex membrane secured over the mold with rubber bands during mold preparation. Notice there are no wrinkles under the rubber band.

4. Stretch the latex by pulling down on the sides until there are no wrinkles under or above the rubber band.

5. Flip the mold over so that the latex now serves as the bottom of the mold.

6. Place the mold in the freezer at -35°F.

C.4 Adding Sand/Hydrogel Mixture to the Mold

1. Place mold in freezer.

2. Place the sand/hydrogel mixture into the funnel/tube device by placing the sand in the funnel and pinching the tube approximately 6" from the free end so that the mixture will not flow out.

3. Place the tube in the mold no more than ¼" from the bottom, and let the mixture flow out by releasing grip on the tube.

4. Maintain the ¼" spacing while evenly distributing the mixture into the sample.

5. Fill until the mold is slightly over full.

6. Strike off the top of the mold with a straight edge (a piece of cardboard with a straight edge works well for this) being careful to not cause vibration.

C.5   Wetting the Sample

1. Fill syringe with deaired water.

   Note: Deaired water is water with the dissolved air removed from it either by boiling or vacuum. This project used the Nold Deaerator whose operation is described in "The Nold Deaerator" owner's manual."

2. Attach needle and inject water into the sample at various locations.

   Note: Water should be injected no faster than 1 mL per 5 seconds and at least five injection points evenly distributed around the sample should be used.

3. While injecting water, slowly raise the needle from bottom to top.

4. When water is observed at the top of the sample it is saturated.

   Note: The needle may become clogged from time to time. Clear the clog by taking the needle out of the sample and off the syringe. Then use a solid needle that fits inside the needle to push out the clog.

5. Allow at least three hours at -35°F for the sample to freeze.

C.6 Extracting the Sample

1. Remove sample from freezer (be sure to use insulating gloves as frostbite of the skin is possible).

2. Remove latex membrane and rubber band.

3. Place sample in Shelby tube extractor flush with the butt plate.

4. Turn the Shelby tube extractor on, the lever now allows for movement of the piston forward and backward.

5. Be sure the piston is lined up with mold by moving the piston very close to the sample. If the sample is not properly in line with the piston, the sample may break or the mold can be deformed.

6. Apply pressure to the sample – a loud pop may be heard when the sample breaks from the mold, but this is normal.

7. As the sample is extracted support it with your free, gloved hand.

8. Once the sample is removed, isolate from air by wrapping it completely in plastic wrap (or foil), secure wrap with rubber bands, and place back into freezer until testing.

   Note: If a sample is left in the freezer for a long period of time without being wrapped, sublimation will occur, leaving the sample unsaturated.

C.7 Confined Molds

C.7.1 Preparing the Molds

1. Once the mold is prepared as before, place the mold in the confining frame and place the top plate on top.

156

2. Adjust horizontal bar so that the thumb-screw will secure the top plate when tightened.

3. Remove the top plate and place the mold in the freezer at -35°F.

4. Swing the bar out of the way to allow soil placement as before.

C.7.2 Adding Sand / Hydrogel Mixture to Mold

1. After striking off the mold, place top plate on top being very careful not to cause vibration.

2. Swing the bar over and tighten screw, again being careful not to cause vibration.

C.7.3 Wetting the Sample

1. Insert the needle into a hole in the top plate and begin to inject water, slowly raising the needle as you do so.
   Note: Inject water no faster than 1 mL per 5 seconds.

2. Do this for as many holes as possible (10 or more) in an even distribution (i.e. do not inject water into only one area of sample).

3. When water is observed coming out of all the holes on the top plate the specimen should be saturated. Confirm this by injecting water into various locations and depths to see if water comes out of all top cap holes at all locations of injection.

4. Freeze sample for 4 hours.

C.7.3   Extracting the Sample after Freezing

1. Remove the mold from the freezer.

2. Use a wrench to loosen the screw.

3. Strike the top plate with the wrench to remove it from the mold.

4. Due to water expansion during freezing, the top of the sample may need to be squared off. This is done with a steel rasp. It is important that the top be as square as possible so that the load put upon it during testing is perpendicular.

5. Extract as before.

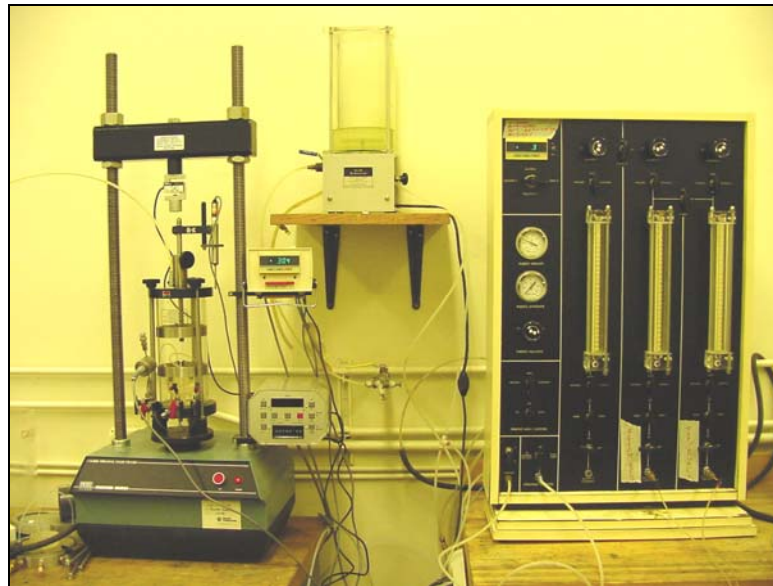### C.8   Consolidated Undrained Triaxial Testing

Figure C.4: (left to right): The Triaxial Test Cell and Load Frame, the Nold Deaerator, and the Panel Board that controls both the Triaxial Test Cell and the Nold Deaerator. All are used during triaxial testing.

C.8.1 Overview

Tests were run using a Brainard-Kilman S-600 triaxial load frame and triaxial cell. Pressures were regulated on a Brainard-Kilman S-500 triaxial/permeability panel board with an E-114 pressure transducer. Measurements were taken with the following sensors:

Brainard-Kilman E-124 pore pressure transducer, serial number 332

Brainard-Kilman E-214 load cell, serial number 138

Boart Longyear E-312 linear displacement transducer (LDT), serial number 134

Sensor readings were taken electronically with an Optim Electronics Megadac and Total Control Software (TCS) for DOS. The Megadac was set to take five readings per second, and the strain rate on the load frame was set to 0.01in/sec. With the readings from the sensors, pore pressure and load could be plotted against deformation from each test. These plots showed the effect of hydrogel on pore pressure and strength under triaxial loading.

C.8.2 Triaxial Testing Accessories

Accessories for triaxial testing including membranes and o-rings were obtained from:

Durham Geo (formerly Brainard-Kilman)

2175 West Park Court

Stone Mountain, Georgia 30087

(800) 837- 0864

Membranes are thin rubber tubes that fit around the sample and seal it from chamber conditions; therefore, it must not have any holes. A new membrane was used for every test. O-rings seal the ends of the membrane tube and connect it to the caps in the triaxial cell. O-rings were re-used for tests.
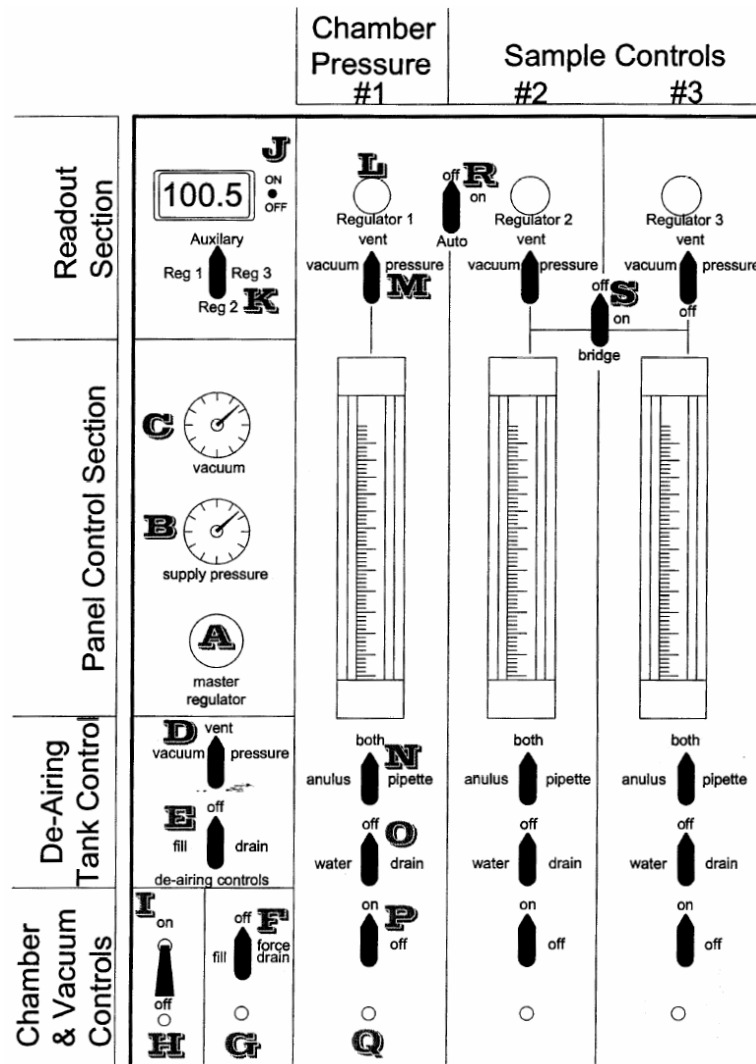
C.8.3   The Panel Board

Figure C.5: Schematic of the panel board with annotations of controls. The long tubes are referred to as reservoirs.

C.8.3.1 Organization of the Panel Board

The panel board is organized into three separate channels that occupy the right ¾ of the board. The channels are completely separate from each other, and the controls for each are separated visually by a long, vertical white line. The channels are numbered 1, 2, and 3 from left to right. Referring to the diagram (fig. 2.10) with the symbols given here in parentheses, each channel has its own pressure regulator (L), pressure/vent selector (M), annulus and pipette, annulus/pipette selector (N), water/drain selector (O), channel on/off valve (P), and quick connect fitting (Q). Channel 1 is used to control the chamber of the test cell that the specimen sits in and supplies chamber pressure. Channel 2 is used to control the influent water from the bottom and supplies back pressure. Channel 3 is used to control the effluent water, which exits from the top of the specimen and also supplies back pressure. The part that each channel controls depends on where the tubes leaving the channels (from Q) are attached on the test cell. It is important to make sure the proper channels on the panel board are connected to the proper ports on the test cell.

C.8.3.2 Panel Board Controls and Their Function

Master Regulator (A): The master regulator is connected to the house pressure supply and controls the maximum amount of pressure that is available in every channel. For example, if the master regulator reads 90 psi, the maximum amount of pressure you can apply to channel 1 is 90 psi. As with all of the regulators, turning it clockwise increases pressure, turning it counterclockwise decreases pressure.

Supply Pressure Gage (B): The supply pressure gage simply displays the maximum available pressure as regulated by the master regulator.

Digital Pressure Gage On/Off Switch (J): Turns the digital pressure gage readout on and off. Leave it on.

Digital Pressure Gage Channel Selector (K): The digital pressure gage channel selector allows you to choose which regulator pressure to view. For example, when switched to regulator 3, the pressure that the channel 3 L valve is set to will be displayed. To view pressures that regulators on the Auxiliary Panel are set to, switch to "Auxiliary", and then flip the switch above the desired channel regulator to "on".

Pressure/Vent/Vacuum Selector (M): The pressure/vent selector lets you choose between applying the pressure (to the annulus/pipette) that the channel pressure regulator (L valve) is set to, or venting the channel annulus/pipette to atmospheric pressure. The vacuum was not needed during testing.

Annulus/Pipette Selector (N): The annulus/pipette selector lets you choose between letting water flow into or out of the just the annulus (the larger cylinder that contains the pipette), just the pipette (the small cylinder with mL increments labeled on it), or both at the same time. **Note:** The term "reservoir" will be used to refer to both annulus/pipette for a channel (fig 2.10) (e.g. reservoir 1, 2, or 3). If just the annulus

or pipette is used, then "annulus" or "pipette" will be referred to for a channel (e.g. pipette 1 or annulus 3).

Water/Drain Selector (O): The water/drain selector lets you choose between adding or draining water from the annulus/pipette. "Water" connects the deaired water tank to the annulus/pipette. "Drain" lets water out of the annulus/pipette.

Channel On/Off Valve (P): The channel on/off valve serves as the barrier between the panel board and the tube (connected to the Panel Board at Q) leading to the test cell. When the valve is on, the conditions applied to the channel are connected to the tube leading to the test cell.

Quick Connect Port (Q): The quick connect port connects a particular panel board channel to a test cell port.

Autoload ®: The autoload feature allows the use of one regulator (L2) to control the pressure regulation for both channels 1 and 2, by only adjusting the pressure regulator on channel 2 (L2). When the valve is turned on, any adjustment to the channel 2 pressure regulator (L2) will cause a simultaneous, proportional change to the applied pressure in channel 1. For example, if you have the Autoload on and you increase the pressure regulation in channel 2 by 5 psi (by turning L2), you have also increased the pressure regulation pressure in channel 1 by 5 psi. In a sense, L2 becomes L1 and L2

when the autoload is on. This feature insures that the pressure in channel 1 always

remains above the pressure in channel 2.

Bridge (S): The bridge function is similar to the autoload. When the bridge is turned

on (and M3 is turned to "off"), L2 and M2 become the controls for channel 3 as well

as channel 2, making the pressure conditions in channel 2 and 3 identical. For

example, when channel 2 is vented, channel 3 is also vented – when channel 2 is at 50

psi, channel 3 is also at 50 psi.
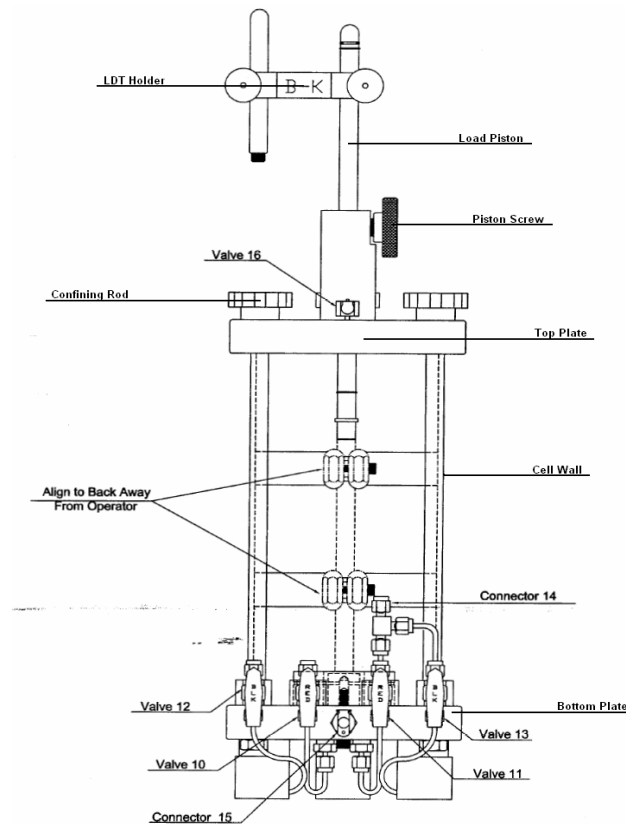

C.8.4   The Triaxial Test Cell

Figure C.6: Schematic of Triaxial Test Cell with labels of parts and controls.

164

C.8.4.1 Triaxial Test Cell Controls and Their Functions

LDT Holder: Holds the Linear Displacement Transducer that measures displacement during triaxial testing.

Load Piston: Transfers load to the sample during testing.

Piston Screw: Can be screwed or unscrewed to either inhibit or allow travel of the piston.

Top Plate: Holds the piston and creates the top of the test cell.

Cell Wall: Plexiglass tube that surrounds the sample.

Bottom Plate: Holds the bottom cap (fig. 2.12) and creates the bottom of the test cell.

Connector 14: Connects the Pore Pressure Transducer to the test cell.

Connector 15: Chamber connection. A tube connects between this connection and Q1 on the panel board. Allows for chamber pressure control.

Valve 10: Red valve that connects Q2 on the panel board to the bottom of the sample.

Valve 11: Red valve that connects the bottom of the sample to the Pore Pressure Transducer.

Valve 12: Black valve that connects Q3 on the panel board to the top of the sample.

Valve 13: Black valve that connects the top of the sample to the Pore Pressure Transducer.

Valve 16: Vent for the cell. An open tube is attached to it.

Confining Rod (3): Tighten to hold the test cell together while it is under pressure.

C.8.5   Procedure for Consolidated Undrained Triaxial Testing

C.8.5.1   Preparing Frozen Sample for Triaxial Cell

1. Remove the specimen from freezer and unwrap.

2. Weigh the sample and record as "sample wet".

3. Measure the height and diameter of the sample with calipers (measure the height and diameter each at five different locations on the sample; these values will then be used to calculate an average height and an average diameter for the sample). Record these values as "height" and "diameter".

4. Attach the latex membrane to the membrane stretcher and apply a vacuum with the house vacuum so that the membrane is pulled flush to stretcher.

5. Place the sample inside the membrane stretcher.

6. Turn the vacuum off and remove the membrane from the stretcher; now the membrane should be wrapped snuggly around the sample.

   Note: The membrane will extend beyond the sample ends on the top and bottom. This excess length will be used to attach the membrane to the top and bottom caps of the triaxial cell.

7. Fold the excess length back onto the sample so that the membrane does not extend past the ends.

8. The sample is now ready to be placed in the triaxial cell (the sample can be placed back in the freezer until the lines of the cell are flushed).

C.8.5.2 Flushing Air from the Triaxial Lines with Deaired Water

1. Be sure there is a full tank of deaired water in the Nold Deaerator. It is recommended that a fresh tank be made before each test and that the tank is filled and deaired while the sample is thawing.

2. Be sure valve D is turned to vent.

3. Refer to figures 2.10 and 2.11.

4. Connect the pore pressure transducer to the triaxial cell using "connector 14". This will occupy two of the four valves on the triaxial cell, one from the top cap and one from the bottom cap (fig. 2.12), and the average pore pressure from the two will be output (it is recommended the transducer be placed on the opposite side of the cell from the panel board).
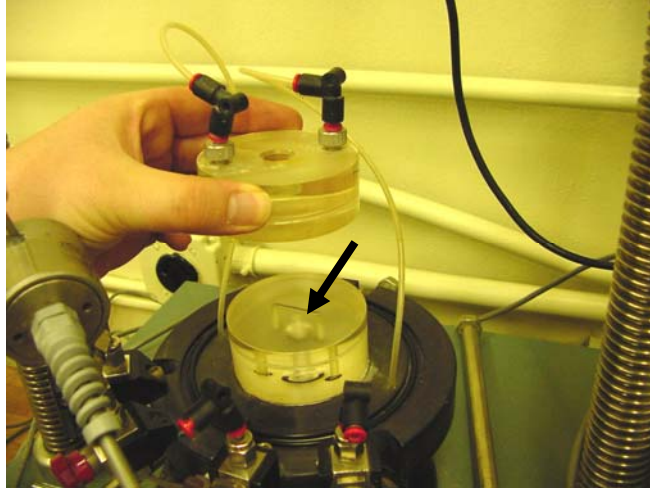
Figure C.7: Top and bottom caps on triaxial cell. Arrow points to the trench between holes on the bottom cap. The same can be seen on the under-side of the top cap.

5. Turn M1, M2, and M3 to "vent" and turn P1, P2, and P3 to "off" on the panel board.

6. Fill panel board reservoirs by turning N1, N2, and N3 to "both" and then O1, O2, and O3 to "water". When the reservoirs fill, turn O1, O2, and O3 to "off".

7. Connect tubes from panel board to triaxial cell. G to connector 15, Q2 to valve 10, and Q3 to valve 12.

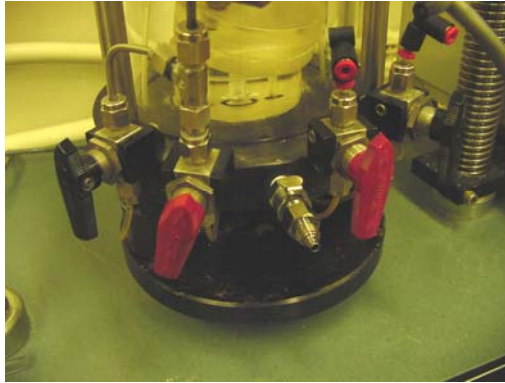8. Close valves 10, 11, 12, and 13 (fig. 2.13).

Figure C.8: Triaxial cell valves 10 – 13 and connector 15. Colors denote the top and bottom. In this case red is the bottom and black is the top.

9. Turn Q2 and Q3 to "on".

10. Remove the deairing valve on the pore pressure transducer (fig 2.14) and open valves 10 and 11.
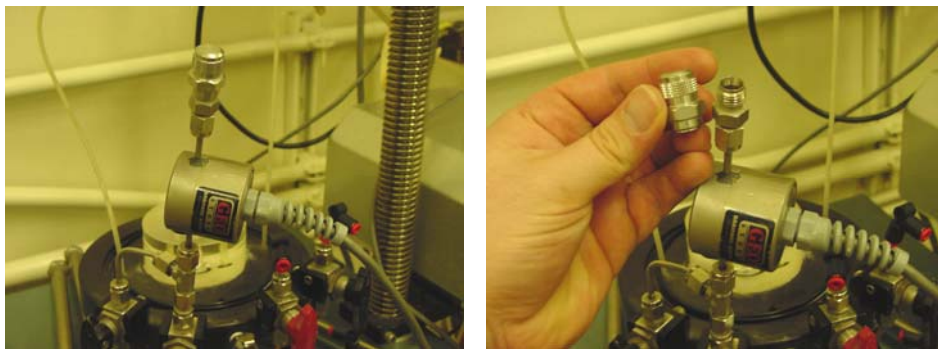

Figure C.9: Deairing valve on pore pressure transducer.

11. Water will now flow out of one hole of the bottom cap

12. When no air can be seen coming out of this hole, use a small piece of membrane and cover both holes on the bottom cap and apply pressure with

finger – this will force water through the trench (fig. 2.10) between the holes and out through the pore pressure transducer

13. Once no air is seen exiting the pore pressure transducer, close valves 10 and 11.

14. Use a one inch piece of 1/8" inside diameter flexible tubing to splice the tubes that lead to the top cap. To do this, slide the triaxial tubes inside of the 1/8" piece of tubing, making one tube out of two (fig. 2.15).

Figure C.10: 1/8" piece of tubing used in flushing water lines (left). Tubes spliced with 1/8" tube (right).

15. Open valves 12 and 13; water will now flow through the tube.

16. When no air is seen in the tubes or exiting the pore pressure transducer, close valves 12 and 13.

17. Replace deairing valve on the pore pressure transducer.

18. Lines are now flushed.

C.8.5.3 Placing the Sample in the Triaxial Cell and Cell Assembly

1. Clean the grooves and o-rings in the top and bottom plates of sand and debris (if it is not clean, a leak will develop when the cell is pressurized).

2. Remove sample from freezer (if needed).

3. Place deaired porous stone on top of the bottom cap.

   Note: Porous stones are deaired by placing them into a desiccator filled half way with deaired water. The desiccator is then placed under a vacuum of at least 20 in Hg. The stones are submerged in the deaired water and will be deaired after approximately 20 minutes under the vacuum.

4. Open valve 10 and press down on the stone. Water should seep out of the top of the stone. When it does close the valve to ensure stone saturation.

5. Dip a piece of filter paper in deaired water to saturate it.

6. Slowly lay the piece of filter paper over the stone starting at one edge and moving to the opposite in a "rocking chair" type motion (fig. 2.16). Laying the filter paper down all at once will trap air underneath it. Push trapped air bubbles out with fingers.

Figure C.11: Placing the filter paper on the porous stone in "rocking chair" motion.

7. Place the bottom end of the specimen over the filter paper and porous stone. The bottom of the sample is used because it will be smooth and perpendicular.

8. Pull the excess membrane down over the bottom cap.

9. Slide an o-ring down over the sample and into the groove in the bottom cap. Be sure there are no wrinkles underneath the o-ring and that it is secure in the cap groove.

10. Using a syringe (without the needle), from the hypodermic needle used before, squirt deaired water on top of the specimen (only enough to wet the top). This will allow for the filter paper to go on without producing trapped air bubbles.

11. Dip a piece of filter paper in deaired water to saturate it.

12. Slowly lay the piece of filter paper over the top of the sample starting at one edge and moving to the opposite in a "rocking chair" motion (fig. 2.16). Laying the filter paper down all at once will trap air underneath it.

13. Place a deaired porous stone on top of the filter paper, and squirt more water on top of the stone.

14. Place the top cap on top of the porous stone.

15. Pull excess membrane up over the top cap.

16. Place an o-ring in the groove of the top cap making sure there are no wrinkles underneath the o-ring and that it is secure in the groove

17. Pull the top cap tubes out of the one inch piece of 1/8" tube and connect them to the top cap.

18. Flush the trench between the top cap holes by removing the deairing valve on the pore pressure transducer and opening valves 12 and 13. This will allow water to flow from the top reservoir through the trench and out the pore pressure transducer.

19. When no air is exiting the pore pressure transducer, close the valves and replace the deairing cap on the pore pressure transducer.

20. Place the plexiglass cell wall over the sample and into the groove surrounding the sample on the base plate (be sure the o-ring is in the groove).

21. Loosen the piston screw on the top plate (i.e. the piston moves freely) if needed.

22. Place the bottom end of the piston in the cutout on the top cap mkaing sure it is all the way in.

23. Slide the top plate down the piston on top of the cell wall in the corresponding grooves (be sure the o-ring is in the groove).

24. When the top cap is in place, tighten the piston screw (i.e. the piston does not move freely).

25. Attach the three steel confining rods in the grooves around the cell and tighten by hand until they cannot be tightened anymore.

26. Place the LDT in its support attached to the piston. The LDT will rest on top of the top plate. Displace the LDT as little as possible, so the full travel of the LDT can be used.

27. Lower load cell on to the top of the piston using the bolts that control the height of the horizontal bar to which the load cell is attached to.

28. When the load cell is just touching the piston (i.e. one or two pounds is read on the load cell readout) tighten the bolts so that the horizontal bar cannot move.

29. Vent the cell by connecting an open tube to valve 16.

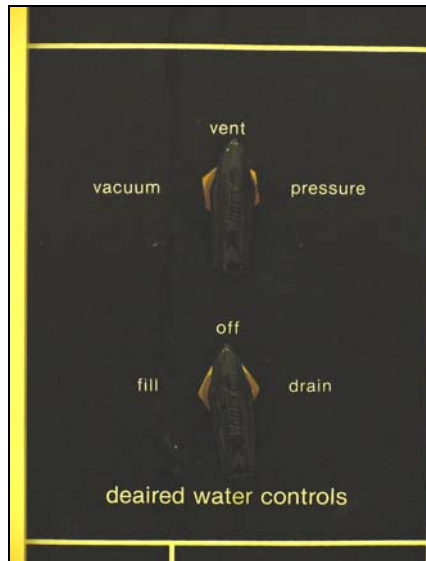30. Turn F to "fill", and the cell should begin filling with water.

Figure C.12: Deaired water controls

on panel board.

31. When the cell is filled, turn F to "off", and remove the vent tube.

32. Be sure all reservoirs are filled. If filling is required turn the corresponding

    N valve to "both" and O valve to fill.

33. Disconnect the tube from G.

34. Connect this tube to Q1.

35. Be sure valves 10 and 12 are closed.

36. Turn "autoload" switch to "on".

    Note: "autoload" operation is explained in Brainard-Kilman (Durham-Geo)

    S-500 Triaxial/Permeability Panel Board owner's manual.

37. Turn K to "regulator 1".

38. Turn L1 counter-clockwise until the digital readout reads zero.

39. Turn K to "regulator 2".

40. Turn L2 clockwise until pressure reads 43psi ("regulator 1" pressure should also be 43psi).

41. Turn K to "regulator 1".

42. Turn L1 clockwise until pressure reads 45psi.

43. Turn M1 and M2 to "pressure".

44. Turn P1 and P3 to "on".

45. Open valves 12 and 10.

46. The sample is now under pressure – let the sample thaw for three hours.

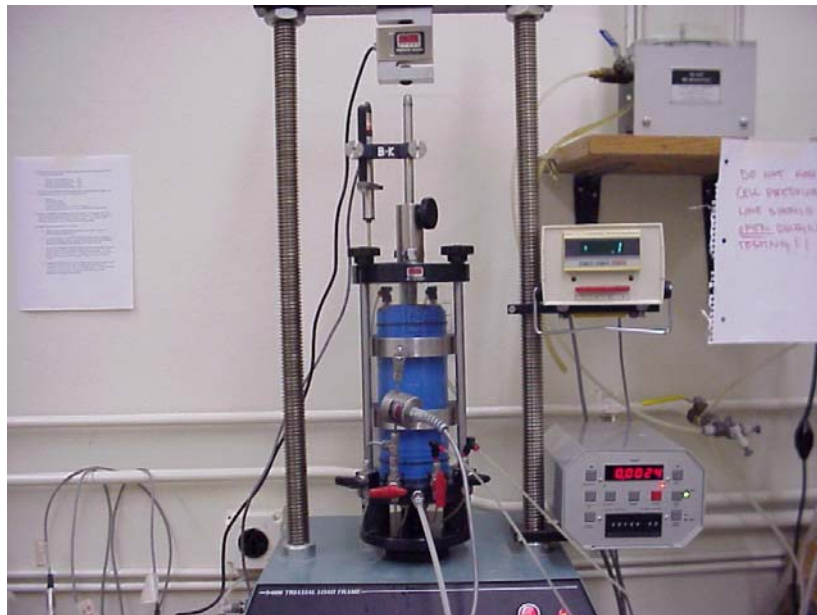47. Triaxial setup is now complete (fig. 2.18).

Figure C.13: Triaxial testing setup.

C.8.5.4 Post Test Procedure

1. Fill a squirt bottle with tap water.

2. Obtain a pan for use in oven drying, the bigger the better, as long as it will fit in the oven.

3. Weigh the pan, and record as "pan weight".

4. Turn P1, P2 and P3 to "off".

5. Turn M1, M2, and M3 to "vent". A hissing sound should be heard as the pressure is released.

6. Drain reservoir 3.

7. Turn P3 to "on".

8. Open valve 12.

9. Water from inside the sample will flow into reservoir 3 as pressure is released.

10. Disconnect the tube running between Q1 and connector 15.

11. Connect one end of this tube to G and the other to valve 16.

12. Connect a drain tube to connector 15. The drain tube is any long tube with one end open and the other end with a male quick connect fitting. Place the open end in the drainage bucket to the right and below the triaxial load frame before connecting the other end to connector 15.

13. Water from the cell should now be flowing into the drainage bucket.

14. Turn F to "force drain". This will pressurize the cell and force water out the drain tube. Hold on to the drain tube as it may be forced out of the bucket and squirt water.

15. When the cell is empty, turn F to "off", and remove tube from valve 16.

16. Tighten the Piston Screw.

17. Raise the horizontal bar that the load cell is on approximately 6" above the load piston.

18. Loosen and remove the Confining Rods.

19. Remove the top plate; set it aside. The piston will still be in the top cap and may need to be maneuvered to get it out.

20. Remove tubes from valves 10 and 12 and connector 15.

21. Remove pore pressure transducer from connector 14 and set aside.

22. Remove the base plate (with the sample and cell wall still resting on it), and set it on the table next to the load frame.

23. Remove cell wall; set it aside. The sample should still be standing on its own.

24. Remove the tubes going to the top cap.

    Note: From this point on do not lose any sand from the sample. All sand should go into the pan.

25. Remove the top o-ring and top cap. Rinse the bottom of the top cap off with the squirt bottle into the pan and set aside.

26. With fingers, get the porous stone and filter paper from the top of the sample. Rinse them off into the pan; set aside

27. Slowly turn the base plate on its side so that the sample is now laying flat in the pan.

28. Slowly remove the base plate and bottom cap from the sample. Rinse them into the pan; set aside.

29. Rinse and remove o-ring from the pan.

30. Remove and rinse porous stone and filter paper from the bottom cap into the pan; set aside.

31. Very carefully squeeze the sample sand out of the membrane into the pan.

32. Rinse the membrane into the pan; discard.

33. Rinse hands into the pan.

34. Place the pan into a 100°C oven overnight.

35. Once the sample is dry, weight the pan and sample together and record as "pan + sample".

36. Subtract "pan weight" from "pan + sample" and record as "sample dry" (ex. 2 lbs. – 0.2 lbs. = 1.8 lbs.).

37. Calculate the unit weight of the sample by dividing "sample dry" by the volume of the sample using the average height and diameter of the sample. (ex. (1.8 lbs / [(2.8"^2 *   / 4) * 6"])* (1728 in^3/1 ft^3) = 84.1 pcf)

38. Testing for sample is complete.

C.9   Flexible Wall Permeameter Testing

C.9.1   Sample Preparation and Extraction

Samples for permeability testing were made and extracted exactly the same way that triaxial sample were prepared. The only difference is the molds for permeability

samples are 2.8" tall and 2.8" diameter. Because of this, only 600 grams of sand is needed to overfill the mold.

C.9.2   Similarities in Triaxial and Permeability Testing

Test Cell Structure: The only difference between the triaxial cell and the flex-wall permeameter cell is that the permeameter does not measure load or displacement; therefore, the permeameter has no load piston or LDT holder.   The same model pore pressure transducer is used.

Test Cell Valves: The permeameter also has six connection ports and a top vent. The port corresponding to connector 15 is called "lateral". The ports corresponding to valves 12 and 10 are called "upper" and "lower" respectively. The other two ports are connected for use with a pore pressure transducer which has an equivalent connector 14 and will be called "transducer valve". The equivalent valve 16 on the permeameter will be called "vent valve".

Panel Board: The same model panel board from triaxial testing was used, so figure 2.10 applies to permeability testing. The deairing water controls were not connected to the panel board; therefore, the triaxial panel board had to be used to deair water.

Testing Procedures: Sample placement was performed in the same manner as triaxial testing. The only difference in sample preparation for the test cell is that the membrane may be cut to account for the shorter sample size (be sure to leave enough excess on the ends to fit over the top and bottom caps).

C.9.3 Flexible Wall Permeameter Testing Procedures

C.9.3.1 Filling the Chamber with Deaired Water

1. Place a male quick connect fitting in "vent valve".

2. Turn O1 to "water"; turn P1 to "on". P2 and P3 should be off.

3. The chamber should now fill with water. Fill until the water comes out of the quick connect fitting on the top steel plate. This will take a few minutes.

4. Turn the P1 valve to "off", and after letting the water level in reservoir 1 rise to about 1/2 full, turn the O1 valve to "off".

5. Remove the quick connect fitting from "vent valve" (fig 2.19).

Figure C.14: The Test Cell has been filled with water and the quick connect has been removed from the top steel plate. The Test Cell is ready to be pressurized.

6. Turn K to "regulator 1"; adjust L1 to 3 psi.

7. Turn M1 to "pressure".

8. Turn P1 to "on".

9. Let the sample thaw for three hours.

10. Deair another full tank of water while the sample is thawing.

C.9.3.2 Flushing Air from Lines with Deaired Water

1. Turn R to "on". This will adjust the channel 1 (Chamber) pressure automatically as you adjust the channel 2 (Lower) pressure. In this case, keep the chamber pressure constantly 3 psi above the lower pressure in the specimen.

2. Fill reservoir 2 by turning O2 to "water". Fill until nearly full, making sure not to overfill. Turn O2 to "off" when filling is complete.

3. Turn K to "regulator 2"; adjust the L2 valve to 5 psi.

4. Turn M2 to "pressure". There is now a pressure of 5 psi applied to the water in the reservoir 2.

5. Adjust the water level in the reservoir 3 to where it is nearly empty. Add water by turning O3 to "water"; remove water by turning O3 to "drain". Turn O3 to "off" when filling or draining is complete.

6. All valves on the test cell should be open. Open both P2 and P3 at the same time. Water will flow out of reservoir 2, through the specimen, and into reservoir 3. You will observe large air bubbles floating to the top of the water in reservoir 3.

Note: Do not let the water level in the reservoir 1 get too low or air will enter into the sample and de-saturate it.

8. While the water is flowing, close valves leading to "transducer valve" on the test cell for about 3 seconds and then re-open them. Do this a few times, leaving the valves open after the last time.

9. When the water in the reservoir 2 gets low, close P2 and P3.

10. Turn M2 to "vent" and fill the reservoir 2 with water as in step 2. After filling is complete, turn M2 to "pressure".

11. Drain water from the reservoir 3 as in step 5.

12. Repeat steps 5-11 until you do not observe any more air bubbles in the "Upper" annulus/pipette.

13. When no more air bubbles are observed, repeat steps 6-10 once more just to be safe (sometimes the air stubborn).

C.9.3.3 Attaching the Pore Pressure Transducer

1. Be sure P1 is "on", and P2 and P3 are "off".

2. Turn M2 to "vent".

3. Adjust the water levels in both reservoirs 2 and 3 so that they are filled halfway with water. Do this by turning O2 and O3 to "water".

4. The R valve should still be turned to "on".

5. Turn M3 to "off".

6. Turn S to "on".

7. Turn M2 to "pressure". The applied pressure should still be 5 psi.

8. Turn P2 and P3 to "on".

9. Close valves leading to "transducer valve" on the test cell. "Lower", "upper", and "lateral" should be open.

10. Loosen the deairing valve on the pore pressure transducer. This is **extremely important**. Failure to loosen this valve can result in breaking the transducer when applying it. The valve on the pore pressure transducer should be open whenever it is not attached to the Test Cell.

11. Attach the pore pressure transducer to "transducer valve".

12. Open valves leading to "transducer valve" on the test cell. Water will spray out of the top of the transducer, removing any air in the transducer. After about 5 seconds, close valves leading to "transducer valve". Keep an eye on the water levels in the reservoirs. Do not let them get too low.

13. Tighten the deairing valve on the pore pressure transducer. *Do not press down on the transducer*, or the tubes leading to it may break.

14. Open valves leading to "transducer valve" on the test cell.
    Note: Make sure there is no water seeping from valve on the transducer. Notice the pore pressure displayed on the "4 Channel Digital Readout". If the pore pressure begins to drop, the valve is not closed all the way.

16. Close P2 and P3.

17. Turn M2 to "vent", S to "off", and M3 to "vent".

18. Fill the reservoir 2 to nearly full by turning O2 to "water" and then to "off" when filling is complete.

19. Drain the reservoir 3 to nearly empty by turning O3 to "drain" and then to "off" when draining is complete.

20. Turn M2 to "pressure".

21. P2 and P3 to "on" at the same time. Water will flow though the sample just like before.

22. Watch for air bubbles moving through the lines and floating up in reservoir 3.

23. When the water in the reservoir 2 gets low, turn P2 and P3 to "off".

24. Turn M2 to "vent"; fill the reservoir 2 with water as in step 18. After filling is complete, turn M2 to "pressure".

25. Drain water from the reservoir 3 as in step 19.

26. Repeat steps 21-25 until you do not observe any more air bubbles in the lines or rising in the reservoir 2.

C.9.3.4 Saturating the Sample

1. Be sure P1 is "on" and P2 and P3 are "off".

2. M2 should be turned to "vent".

3. Adjust the water levels in both reservoirs 2 and 3 so that they are filled halfway with water. Do this by simply turning the O2 and O3 valves as previously discussed.

4. R should still be turned to "on".

5. Turn M3 to "off".

6. Turn S to "on".

7. Turn M2 to "pressure". The applied pressure should still be 5 psi.

8. Turn P2 and P3 to "on".

   Note: All valves on the test cell should be open. P2 and P3 should be "on".

10. Turn K to "regulator 1" and, if necessary, adjust the L1 valve to exactly 3 psi above the pressure of L2. Even with the Autoload feature, the difference of the pressure between channels 1 and 2 can deviate slightly from the initial difference. It may be necessary to switch the K valve back and forth between "regulator 1" and "regulator 2", checking the pressure difference and adjusting the L1 valve accordingly.

11. Turn K to "regulator 2" and slowly turn the L2 regulator clockwise increasing the applied pressure to 30 psi. Turning this single valve clockwise is increasing the applied pressure in all three channels: The autoload (R) is on, so the applied pressure in channel 1 (chamber) changes proportionally with channel 2. The bridge is on and channel 3 is turned off, so channels 2 (lower) and 3 (upper) are "bridged". This means that the pressure applied to channel 2 and 3 is the same, and changing the channel 2 pressure also changes the pressure in channel 3. Basically, the pressure applied to the lower and upper part of the specimen remains equally proportional, and the chamber pressure remains 3 psi above the lower/upper pressure (so the specimen does not explode). This process is called "back pressuring". The lower/upper pressure is called the "back pressure".

12. Keep the applied pressure at 30 psi for 15 minutes.

13. After the 15 minutes has passed, close "upper" and "lower" on the test cell.

14. The pore pressure displayed on the "4 Channel Digital Readout" located on the Triaxial Load Frame. The correct channel is channel 4. Record this as the "initial pore pressure" on the data sheet.

15. Switch the K valve to "regulator 1" which gives the Chamber pressure.

16. Record this as the "initial confining pressure" on the data sheet (fig. 2.20).

17. Slowly increase the chamber pressure by turning the L2 valve clockwise (since the valves to the lower and upper ports are closed on the test cell, you are only increasing the applied Chamber pressure) increasing the pressure by 5 psi. Record the final the pressure as the "final confining pressure" on the data sheet.

18. There will be a new pore pressure displayed on the readout. Record this pressure as the "final pore pressure" on the data sheet.

19. Divide the change in pore pressure by the change in chamber (confining) pressure. This value is known as the "B-value".

20. If the B-value is 0.98 or greater, open valves 4 and 5; proceed with the permeability test. If the B-valve is less than 0.98, open "upper" and "lower"; wait 15 minutes.

21. Repeat steps 13-20 until the B-valve is 0.98 or greater.

Permeability Test Data Sheet

Sample ID _____   Date _____

% hydrogel _____ (by weight)   Temperature (^{O}C) _____

Sample Dimensions

height (cm)	diameter (cm)
1) _____	1) _____
2) _____	2) _____
3) _____	3) _____
4) _____	4) _____
5) _____	5) _____

frozen mass (g): _____

Saturation Process

Confining Pressure (psi)			Pore Pressure (psi)			B-Value (Δpore/Δcell)
initial	final	change	initial	final	change	

Permeabiltiy (K) Test

Lower Pressure (psi): _____   Confining Pressure (psi): _____

Upper Pressure (psi): _____

Run	lower volume 1 (ml)	upper volume 1 (ml)	lower volume 2 (ml)	upper volume 2 (ml)	Time (s)
1					
2					
3					
4					
5					

Post Test

Drying in pan (ID): _____   Dry Mass (g): _____

Figure C.15: Data sheet for permeability testing.

C.9.3.5 Final Adjustments before the Permeability Test

1. Record the date and the room temperature on the data sheet.

2. Turn P2 and P3 to "off".

3. Turn S to "off".

188

4. Turn M2 and M3 to "vent".

5. Turn N2 and N3 to "annulus".

6. Drain the water out of the annulus for both channels 2 and 3 (by turning O2 and O3 to "drain"), leaving the annulus water level at approximately the "25" mark on the pipette.

7. Turn N2 and N3 to "pipette".

8. Adjust the water level in the pipettes 2 to the "5" mark and pipette 3 to the "20" mark. Record these levels on the data sheet as "lower and upper volume 1".

9. Turn M2 and M3 to "pressure".

10. Turn K to "regulator 2" and record the pressure as the "Lower Pressure" on the data sheet.

11. Turn K to "regulator 3".

12. Adjust the pressure in channel 3 by turning L3. Adjust to the appropriate pressure to produce the desired pressure gradient. For example, if you want a pressure gradient of 1 psi and the channel 2 (lower) pressure is 45 psi, adjust the channel 3 (upper) pressure to 44 psi. Record the pressure that L3 is adjusted to as the "Upper Pressure" on the data sheet.

13. Turn K to "regulator 1". If necessary, adjust the L1 valve so that the pressure in channel 1 is exactly 3 psi above the pressure of channel 2. Record the channel 1 pressure as the "Confining Pressure" on the data sheet.

14. Close valves leading to "transducer valve" on the Test Cell. "Upper" and "lower" test cell should be open.

C.9.3.6   Procedure for Permeability Testing

1. Open P2 and P3 at the same time. At the instant you open the valves, start a timer. It is possible to do this if you hold a stopwatch in one of your hands (finger on the start button), and hit start immediately when you open the valves.

2. Water should be flowing out of the pipette 2 and into the pipette 3.

3. Let pipette 2 water level go down to the "20" mark, allowing 15 ml of water to flow through the specimen.

4. When the water level gets to the desired stopping point, close both the P2 and P3 valves at the same time, and stop the stopwatch in the same manner as in step 1.

5. Record the final water levels as "lower and upper volume 2" and the time (in seconds) it took for the particular volume of water to flow through the sample in the corresponding "Time" box on the data sheet.

6. Turn M2 and M3 to "vent"; repeat the procedure, starting at step 8 of Final Adjustments before the Permeability Test, until the criteria for acceptable permeability (k) valves are met. It is important that the pressures used in the first run are kept constant – that way you will not have to record new ones when you repeat steps 10, 12, and 13 of Final Adjustments (you may have to make slight adjustments to the pressures before each run).

   Conditions for Acceptable Permeability (k) valves:

   1. The ratio of the outflow to inflow is between 0.75 and 1.25.

2. At least 4 values of k fall within a range of the mean of the values:

Average Permeability (k) Value (cm/s)	Allowed Range
$k \geq 10^{-8}$	+ - 25%
$k < 10^{-8}$	+ - 50%

Once these conditions are met, the average of the 4 (or more, although it's not necessary) permeability (k) values is the final k valve for the test.

C.9.3.7 Post Test Procedure

1. After the final permeability value has been obtained, the sample can be removed from the test cell, dried overnight in an oven, and weighed.

2. Select a pan to dry the specimen in. The pan must have a distinguishing label on it. Record this label on the Data Sheet in the "drying in pan (ID)" space.

3. Weigh the pan and record the mass under the "dry mass" blank on the data sheet.

4. P2 and P3 should be closed.

5. Turn M3 to "off".

6. Turn S to "on".

7. Turn M2 to "pressure".

8. P1 should be open. Turn P2 and P3 to "on".

9. Open valves leading to "transducer valve" on the test cell. All test cell valves should be open.

10. Turn K to "regulator 1".

11. Slowly turn L2 counterclockwise which will lower the pore pressure and Chamber pressure at the same time. Go slow, and keep an eye on the pore pressure. It must always remain below the Chamber pressure.

12. Continue turning L2 until the pore pressure readout is zero (or basically zero – such as 0.1 or 0.2). The Chamber pressure should read about 3 psi.

13. Turn L1 to "vent".

14. Turn P1, P2, and P3 to "off".

15. Close "lateral" on the test cell.

16. Attach a male quick connect fitting to "vent valve".

17. Remove the tube from the instant tube fitting "lateral" on the test cell.

18. Attach a tube to "lateral" on the test cell that leads to a bucket on the floor.

19. Open "lateral" on the test cell – water will flow out of the test cell and into the bucket on the floor.

20. After all the water has drained out of the test cell, unscrew the rods, remove the top steel plate, and remove the acrylic cell.

21. Carefully remove the top acrylic cap leaving the porous stone in place to keep sand from falling out.

22. Carefully remove the specimen from the bottom acrylic cap using the bottom porous stone to keep sand from falling out.

23. Immediately place the specimen in the pan from steps 1 and 2.

24. Remove the porous stones and the o-rings.

26. Rinse all the sand out of the membrane keeping all the sand in the pan with a squirt bottle filled with tap water.

27. Place the pan in the oven which should be set at 100°C and let the specimen dry overnight.

28. Once the specimen is dry, weigh the pan and record the mass next to the pan mass.

29. Subtract the pan mass from the mass of the pan and the dried specimen, giving the mass of the dried specimen. Record the dry mass in the blank provided on the data sheet.

C.10 Uplift Pressure Test

C.10.1   Sample Preparation

1. Mix sample as before.

2. Prepare mold as before.

3. Place mold in confining frame with the horizontal cross bar removed.

4. Center the confining frame on the load frame platen (this sample will not be frozen).

5. Place sand/hydrogel mixture in the mold as before.

6. Strike off the top of the mold without causing vibration; place confining mold top plate on top.

7. Using a 6" steel bolt, connect the top cap to load cell (i.e. the swell pressure will be transferred from the plate, to the bolt, to the load cell). The bolt is

used so that the hypodermic needle can be maneuvered to inject water into the sample (fig. 2.21).

Figure C.16: Uplift pressure test setup. Notice the bolt, transferring load from the load cell to the top plate (arrow points to bolt).

C.10.2   Sample Testing

1. Inject water using the same method described before.

2. After water begins to come out of the holes in the top cap, stop and note the readout from the load cell.

3. Wait 15 minutes; repeat steps 1 and 2.

4. Continue this process until the load no longer increases (one hour or more).

5. Record the maximum load.

6. Swell pressure = max load/circular area of inside of the mold.

C.11 Cyclic Mobility Test

C.11.1 Overview

During the later stages of testing, the issue of cyclic mobility was raised. Cyclic mobility refers to the lateral spread of soil during liquefaction conditions. This phenomenon is outlined in Chapter 1, Section 1.1.4.3. Discussions on the topic of cyclic mobility lead to the formulation of a test to investigate whether hydrogel effected lateral spreading during dynamic loading. Because cyclic testing equipment normally used to induce dynamic loads in earthquake research, i.e. cyclic triaxial, cyclic simple shear, cyclic torsional, or shake table, were not available to this project, a test was improvised using a flow table described in ASTM C 230/C 230M: Standard Specification for Flow Table for Use in Tests of Hydraulic Cement. This table used a motor to drop a table repeatedly over a set distance a chosen number of times a minute. This table provided the dynamic load necessary to test the effects of hydrogel on cyclic mobility of Ottawa sand samples.

C.11.2 Procedure for Cyclic Mobility Test

C.11.2.1 Sample Preparation

1. Mix sample as before.

2. Place brass mold in the center of flow table (fig. 2.22).

3. **Note:** Mold dimensions are:

   Top opening – 2.8"

   Bottom opening – 4"

   Height – 2"

4. Funnel mixture into mold using method described before.

5. Strike off top of mold, and place confining mold top cap over mold.

6. Secure top cap with a large c-clamp (fig 2.23). This will confine the sample when the hydrogel expands.

7. Inject water into sample using the method described before.

Figure C.17: Flow table and mold used in cyclic mobility testing.

Figure C.18: Top plate secured with c-clamp during sample preparation for cyclic mobility testing.

C.11.2.2 Sample Testing

1. Remove top cap and c-clamp from mold.

2. Remove mold.

3. Take pictures of undisturbed sample in horizontal, transverse, and vertical perspectives.

4. Press the red button and the test will begin automatically.

5. When the test has finished 25 blows, it will stop.

6. Take pictures.

APPENDIX D: RAW DATA PLOTS

Bryan Shiver
7/17/03
B = 0.95

Pore Pressure vs. Strain
SAND1: Ottawa Sand, $\gamma_{d\ initial}$ = 102.9pcf, σ_{3c} = 80psi
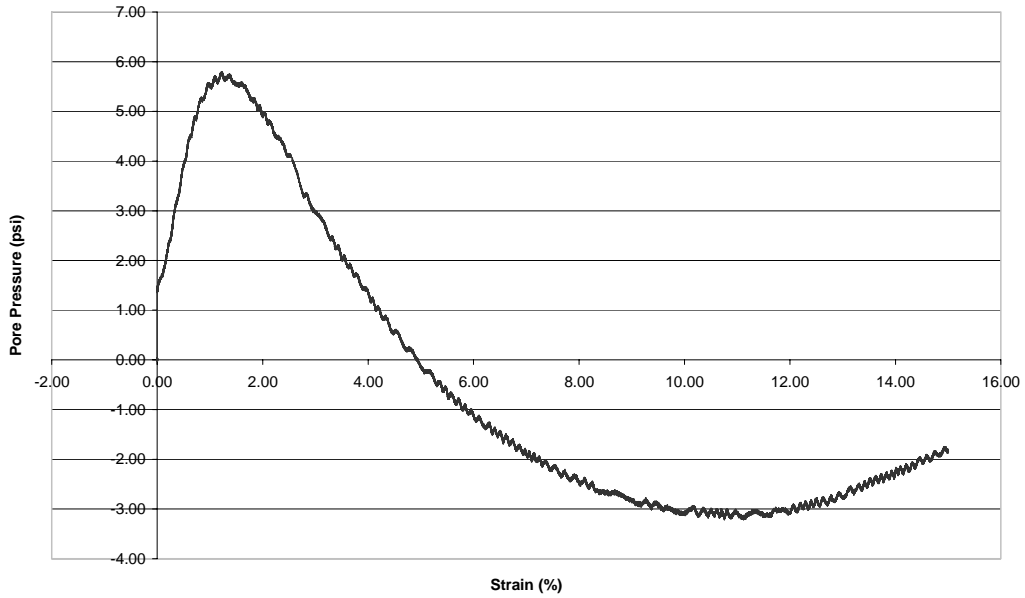
Figure D.1: Pore pressure vs. strain results from triaxial testing on SAND1.

Stress vs. Strain
SAND1: Ottawa Sand, $\gamma_{d\,initial}$ = 102.9pcf, σ_{3c} = 80 psi
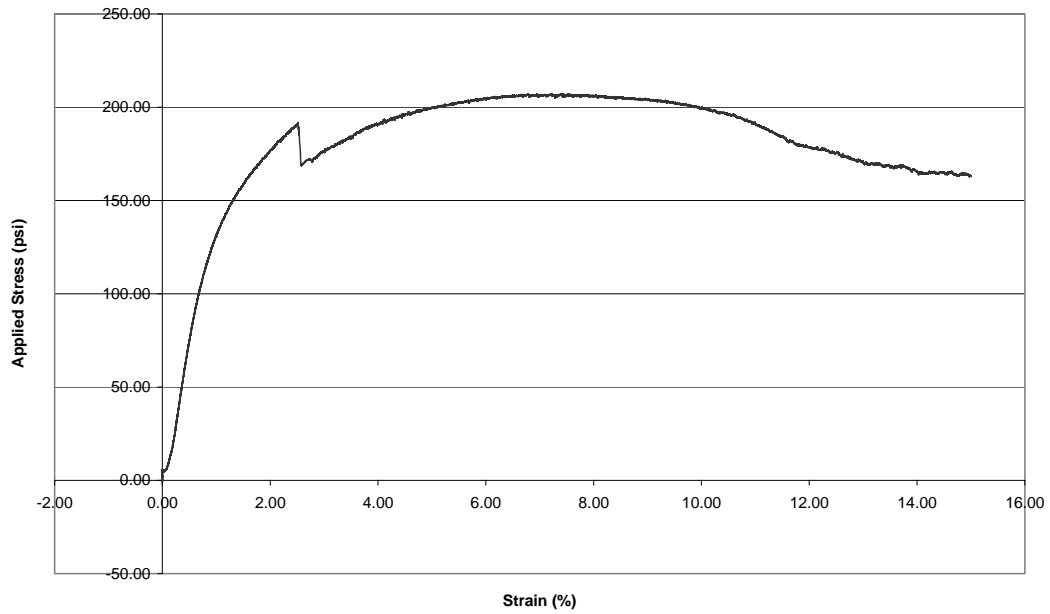
Figure D.2: Load vs. strain results from triaxial testing on SAND1.

Pore Pressure vs. Deformation
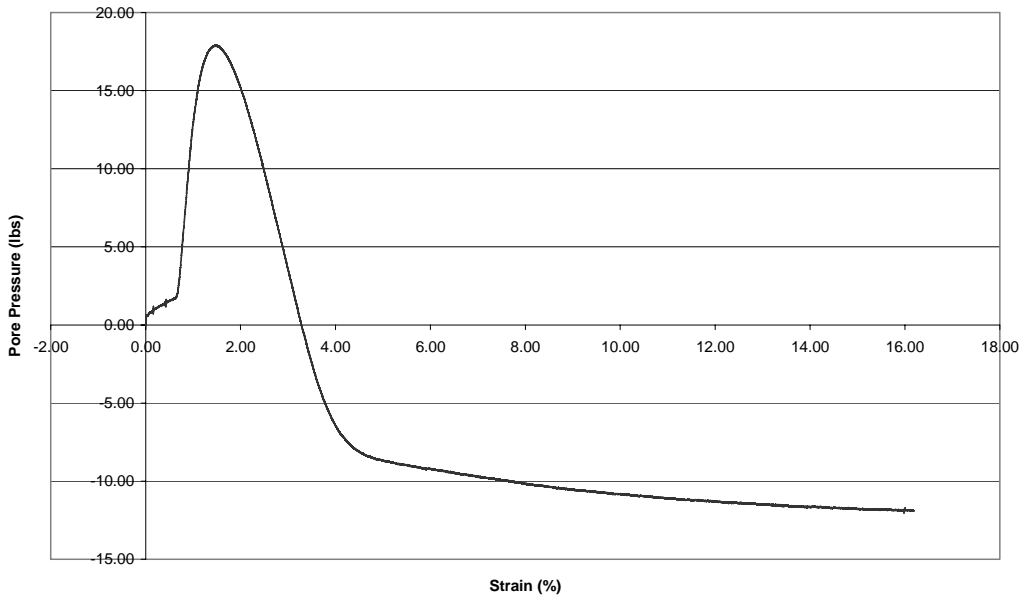**SAND5: Ottawa Sand, $\gamma_{d\,initial}$ = 103.0pcf, σ_{3c} = 45psi**
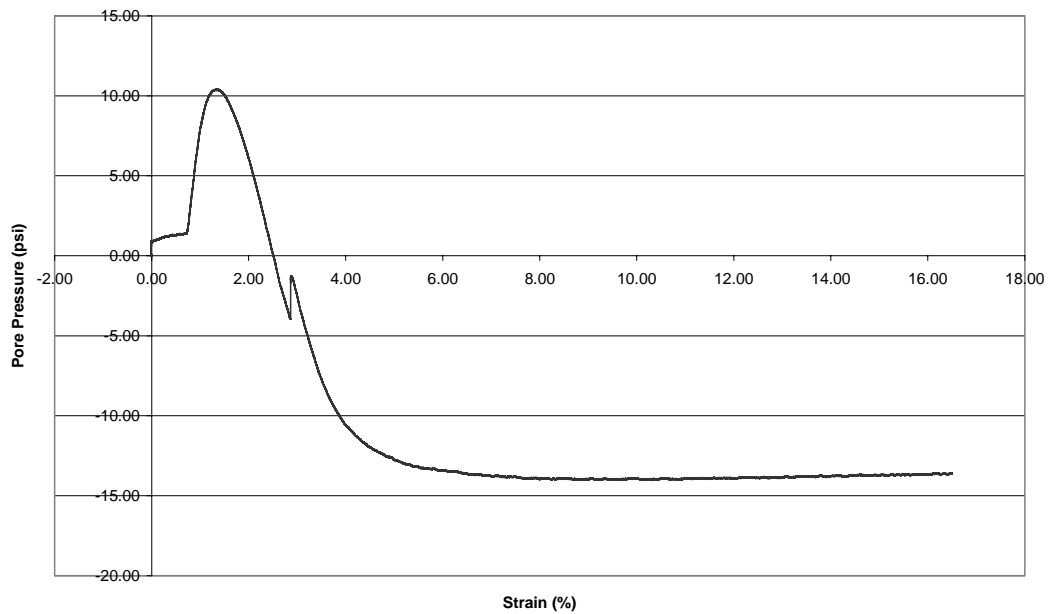
Figure D.3: Pore Pressure vs. strain results from triaxial testing on SAND5.

199

Bryan Shiver
9/1/03
B = 0.975

Stress vs. Strain
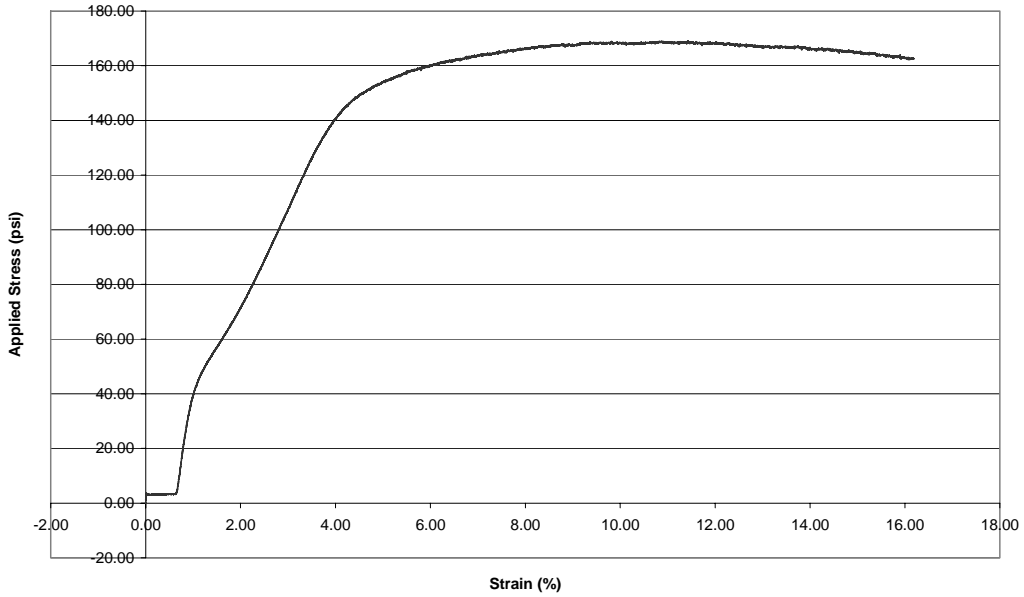**SAND5: Ottawa Sand, $\gamma_{d\ initial}$ = 103.0pcf, σ_{3c} = 45psi**
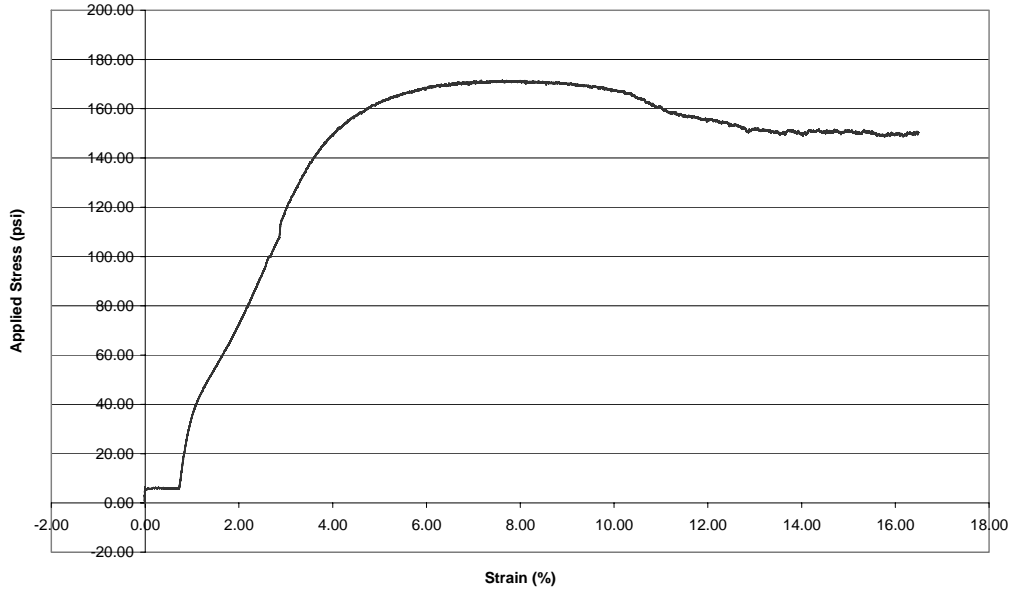
Figure D.4: Load vs. strain results from triaxial testing on SAND5.

Bryan Shiver
9/1/03
B = 0.975

Pore Pressure vs. Strain
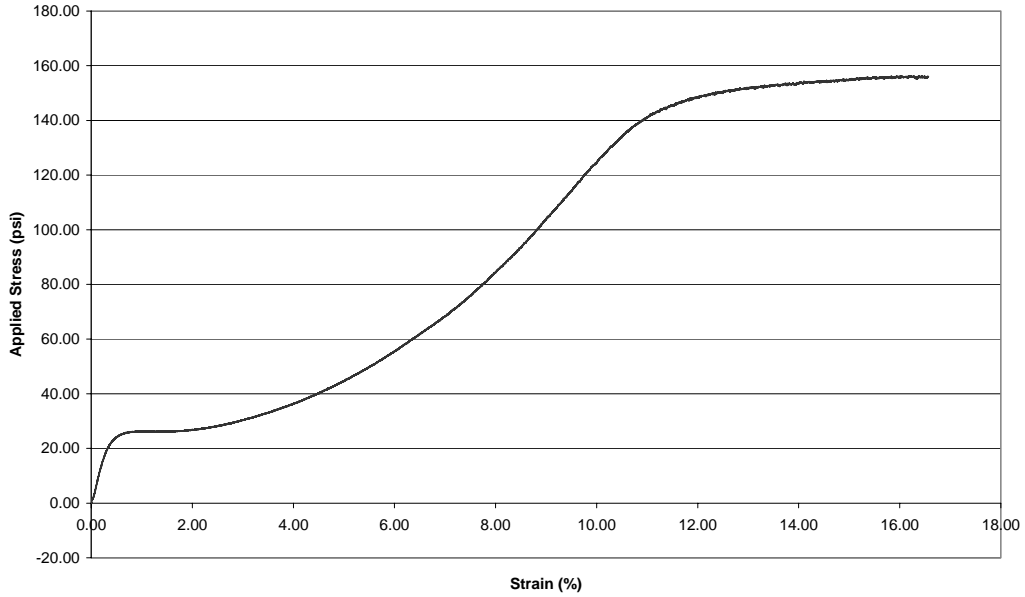**SAND6: Ottawa Sand, $\gamma_{d\ initial}$ = 103.8pcf, σ_{3c} = 45psi**
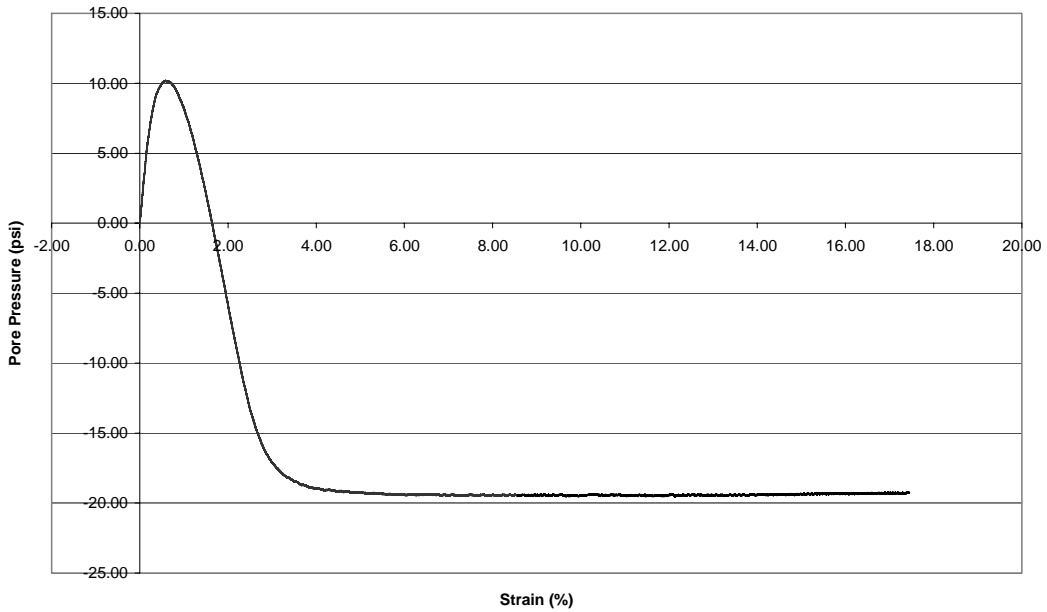
Figure D.5: Pore pressure vs. strain results from triaxial testing on SAND6.

Stress vs. Strain
SAND6: Ottawa Sand, $\gamma_{d\ initial}$ = 103.8pcf, σ_{3c} = 45psi
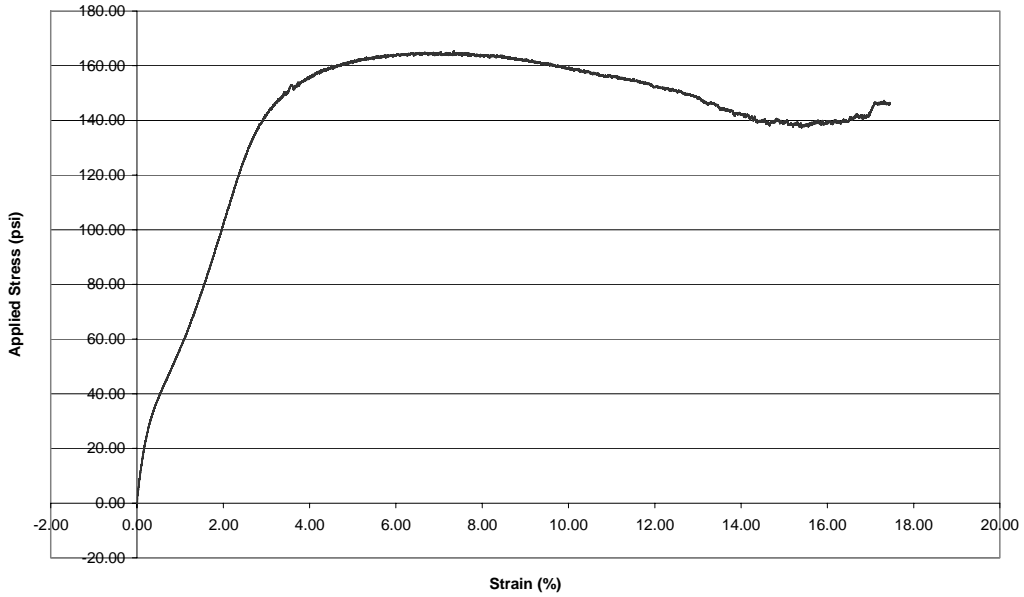
Figure D.6: Load vs. strain results from triaxial testing on SAND6.

Pore Pressure vs. Strain
SAND7: Ottawa Sand, γ_d = 102.9pcf; σ_3 = 45psi
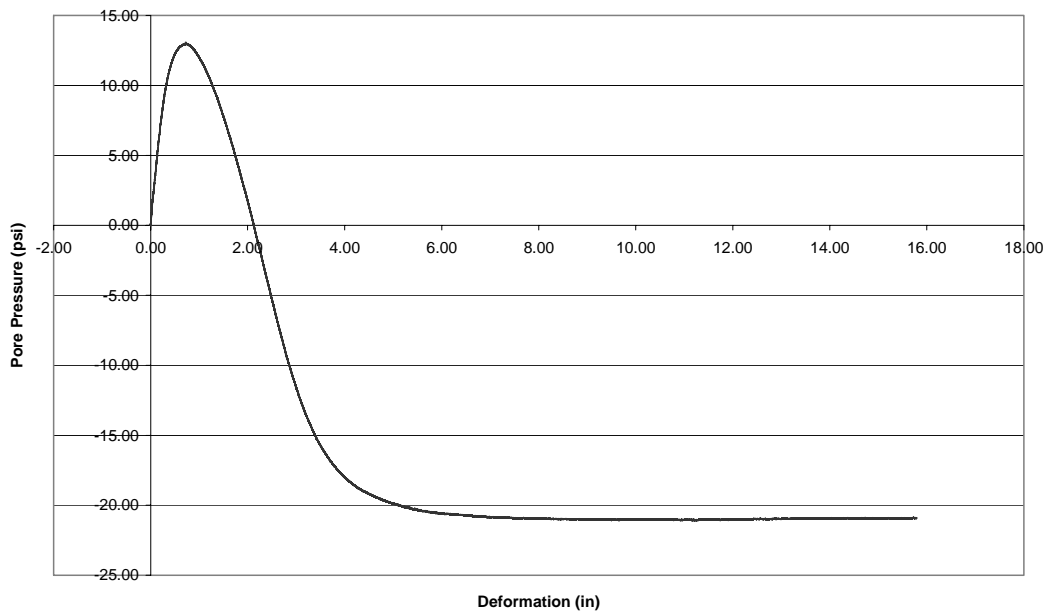
Figure D.7: Pore Pressure vs. strain results from triaxial testing on SAND7.
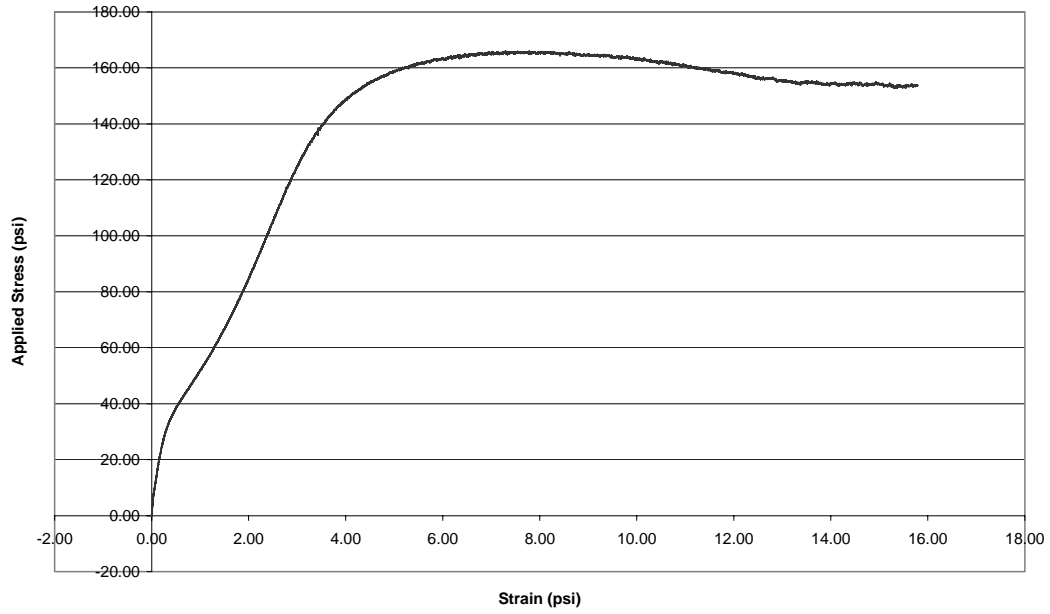
Figure D.8: Load vs. strain results from triaxial testing on SAND7.

Figure D.9: Pore pressure vs. strain results from triaxial testing on SAND8.

Stress vs. Strain
SAND8: Ottawa Sand, $\gamma_{d\ initial}$ = 101.9pcf; σ_{3c} = 45psi
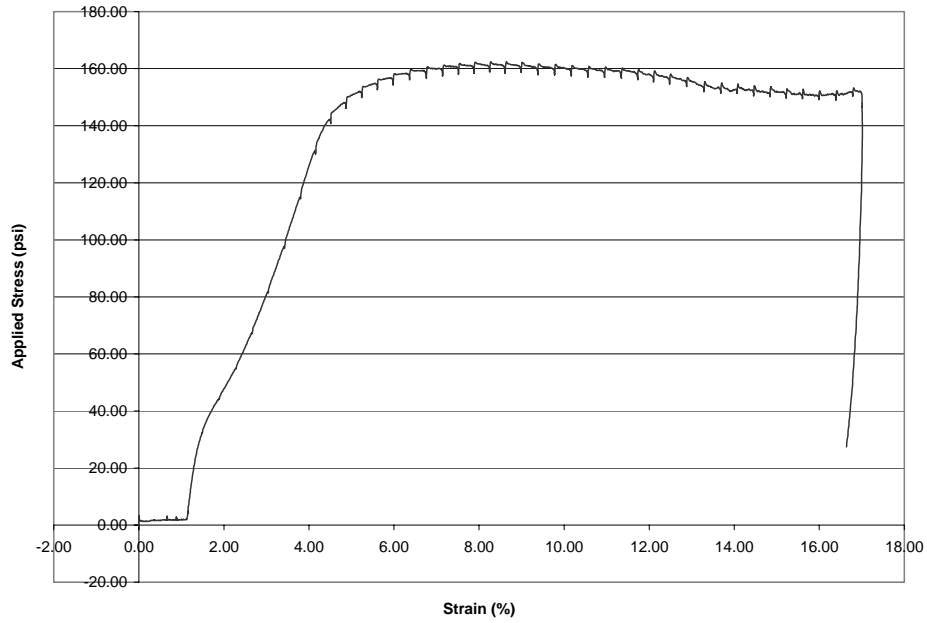
Figure D.10: Load vs. strain results from triaxial testing on SAND8.

Pore Pressure vs. Deformation
SAND9: Ottawa Sand, $\gamma_{d\ initial}$ = 98.6pcf; σ_{3c} = 45psi
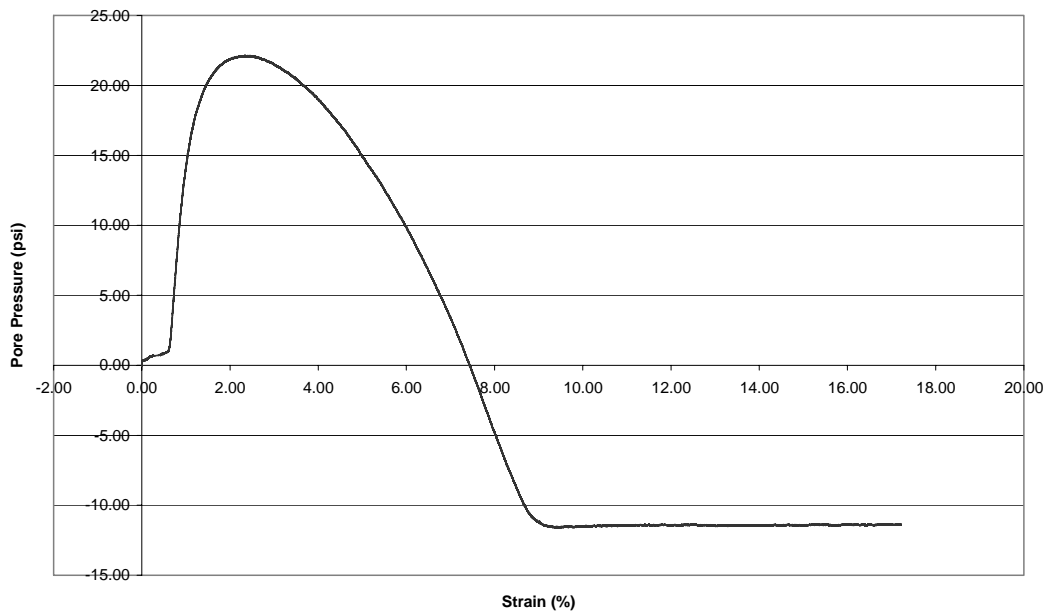
Figure D.11: Pore pressure vs. strain results from triaxial testing on SAND9.

203

Stress vs. Strain
SAND9: Ottawa Sand, $\gamma_{d\ initial}$ = 98.6pcf; σ_{3c} = 45psi
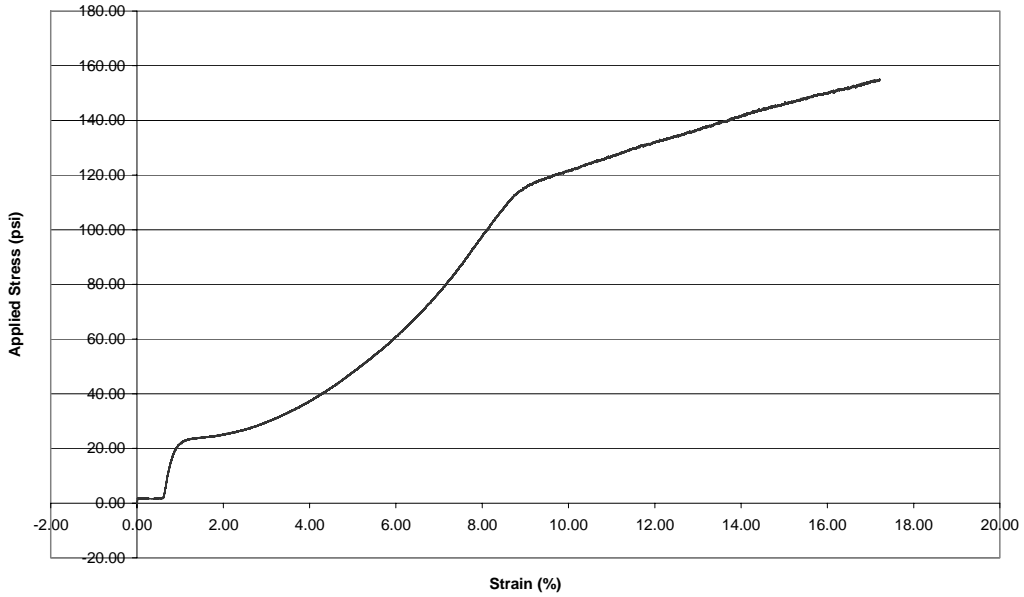
Figure D.12: Load vs. strain results from triaxial testing on SAND9.

Pore Pressure vs. Strain
SAND10: Ottawa Sand, $\gamma_{d\ initial}$ = 98.8pcf; σ_{3c} = 45psi
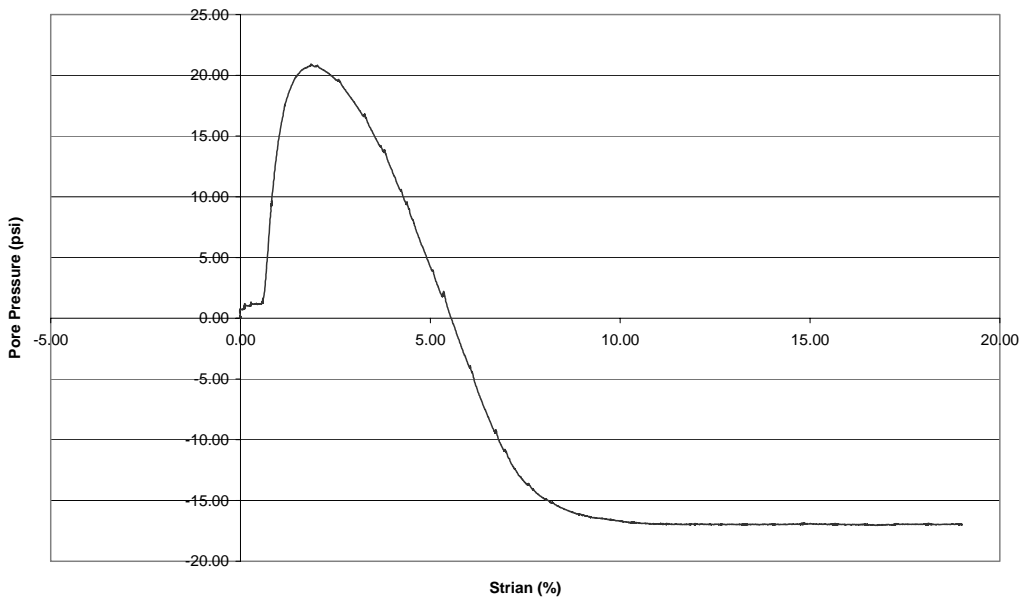
Figure D.13: Pore pressure vs. strain results from triaxial testing on SAND10.

Stress vs. Strain
SAND10: Ottawa Sand, $\gamma_{d\ initial}$ = 98.8pcf; σ_{3c} = 45psi
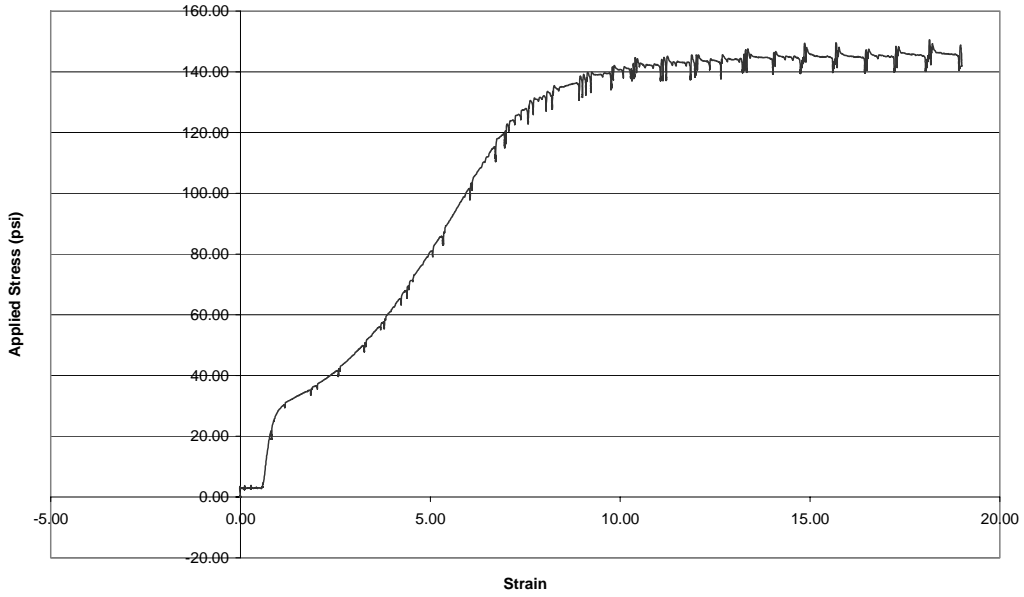
Figure D.14: Load vs. strain results from triaxial testing on SAND10.

Pore Pressure vs. Strain
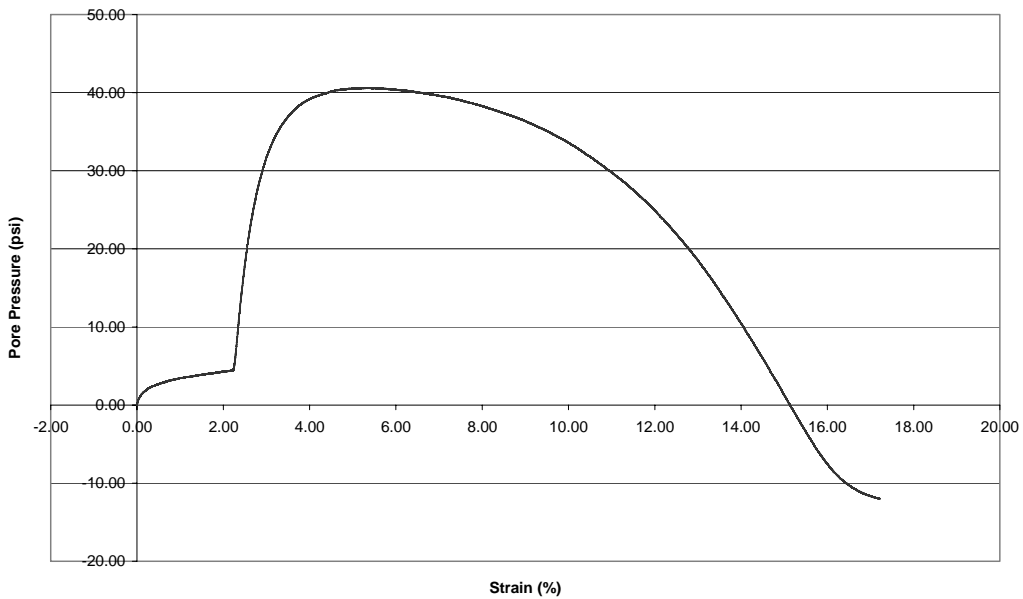**SAND11: Ottawa Sand, $\gamma_{d\ initial}$ = 102.5pcf; σ_{3c} = 49psi**

Figure D.15: Pore pressure vs. strain results from triaxial testing on SAND11.

Bryan Shiver
9/15/03
B = 0.992

Stress vs. Strain
**SAND11: Ottawa Sand, $\gamma_{d\ initial}$ = 102.5pcf; σ_{3c} = 49psi**

Figure D.16: Load vs. strain results from triaxial testing on SAND11.

Bryan Shiver
9/23/03
B = 0.998

Pore Pressure vs. Strain
SAND12: Ottawa Sand, $\gamma_{d\ initial}$ = 97.1pcf, σ_{3c} = 45psi
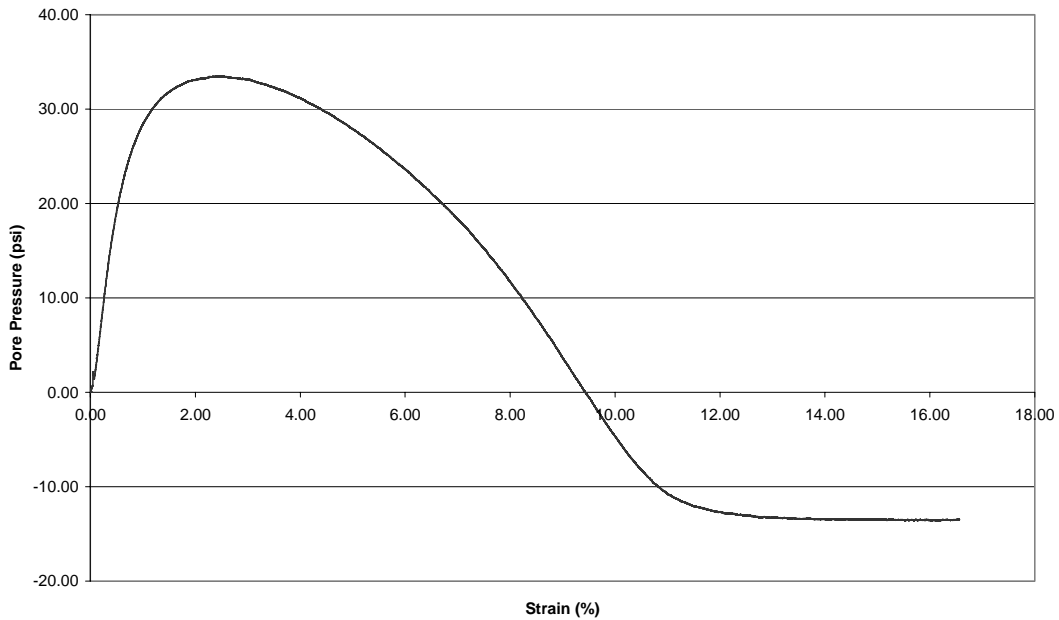
Figure D.17: Pore pressure vs. strain from triaxial testing on SAND12.

Stress vs. Strain
SAND12: Ottawa Sand, $\gamma_{d\,initial}$ = 97.1pcf, σ_{3c} = 45psi

Figure D.18: Load vs. strain results from triaxial testing on SAND12.

Pore Pressure vs. Strain
SANDHYDRO1: Ottawa Sand w/ 0.1% Hydrogel, $\gamma_{d\,initial}$ = 89.1pcf; σ'_{3c} = 45psi
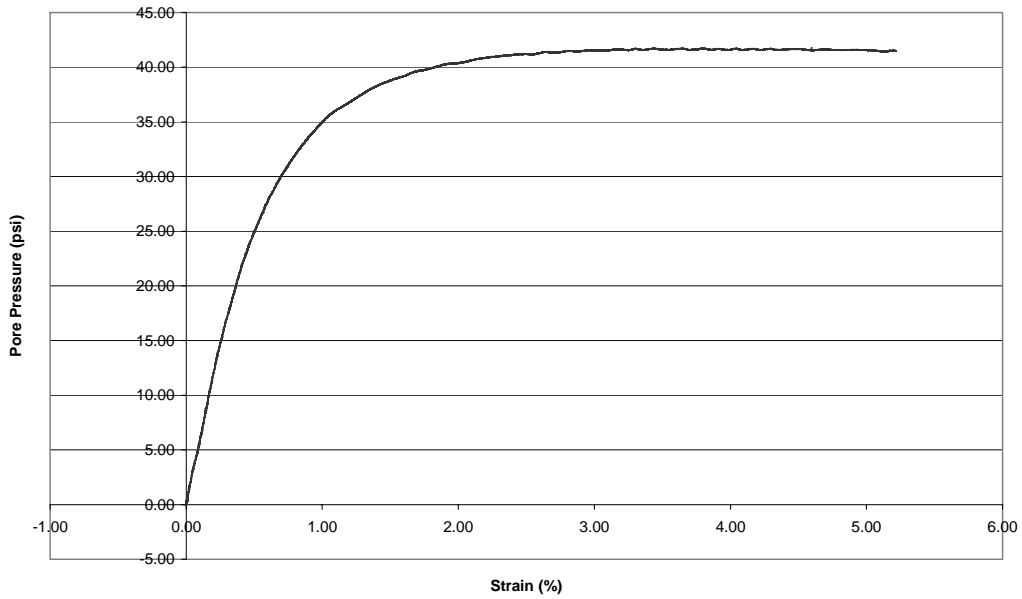
Figure D.19: Pore pressure vs. strain results from triaxial testing on SANDHYDRO1.

207

Bryan Shiver
9/11/03
B = 0.98

Stress vs. Strain
SANDHYDRO1: Ottawa Sand w/ 0.1% Hydrogel, $\gamma_{d\ initial}$ = 89.1pcf; σ'_{3c} = 45psi
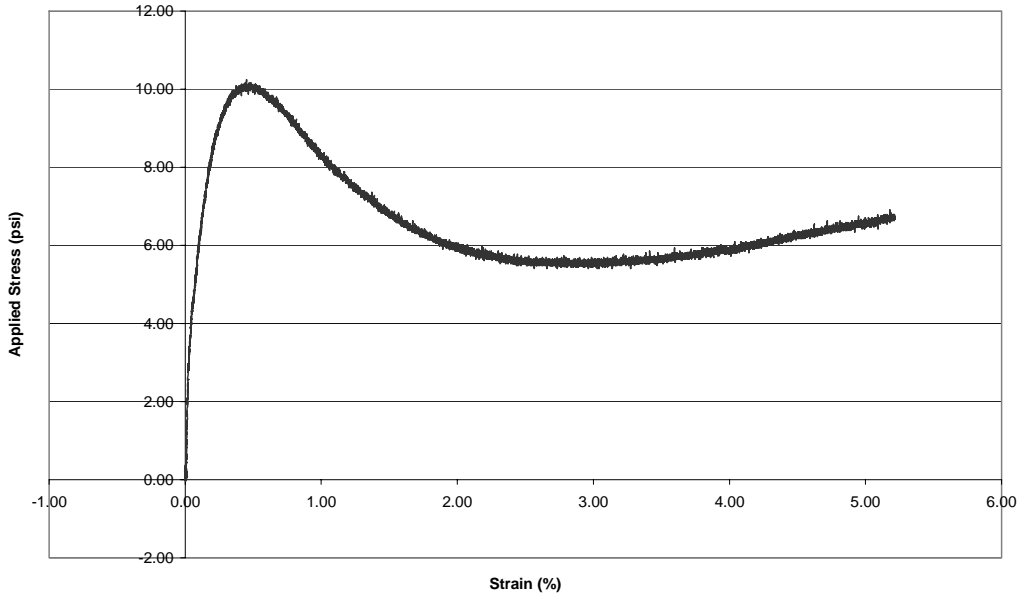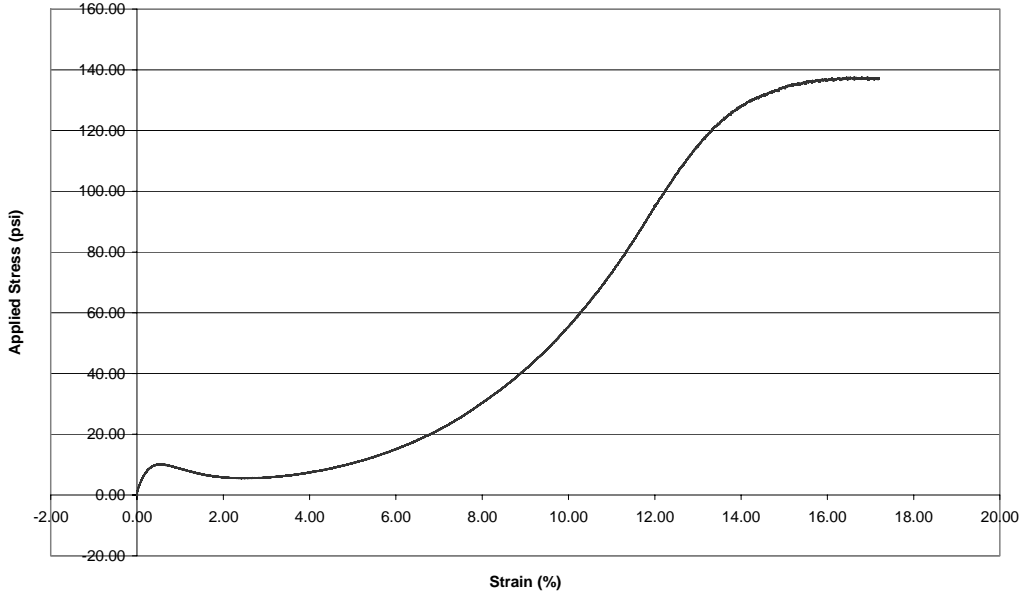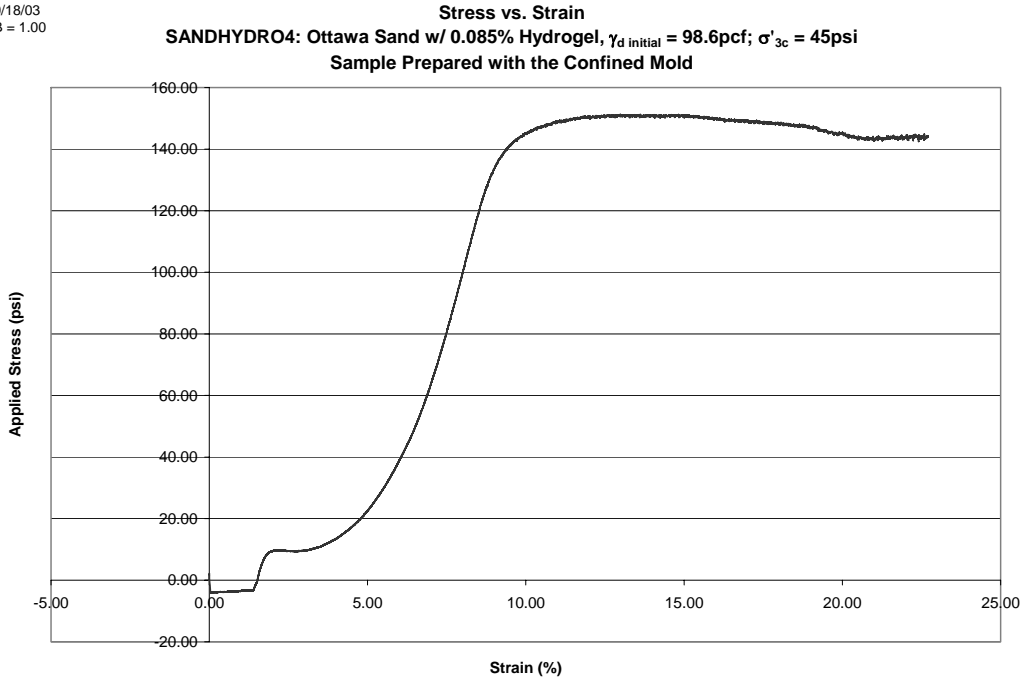

Figure D.20: Load vs. strain results from triaxial testing on SANDHYDRO1.

Bryan Shiver
9/13/03
B = 0.992

Pore Pressure vs. Strain
SANDHYDRO2: Ottawa Sand w/ 0.085% Hydrogel, $\gamma_{d\ initial}$ = 93.0pcf; σ'_{3c} = 45psi
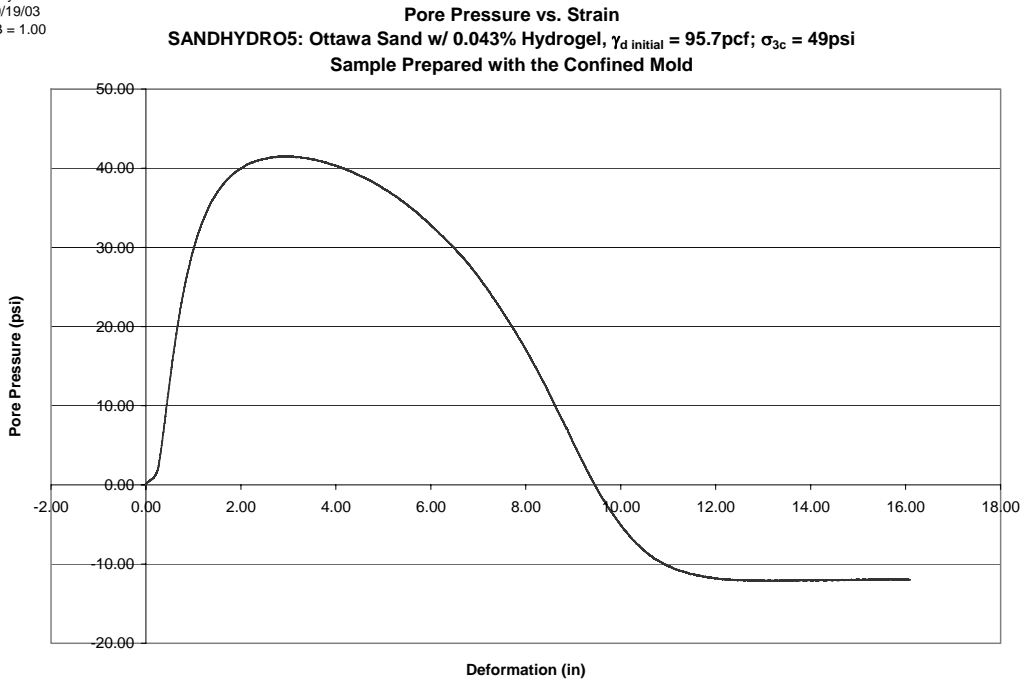

Figure D.21: Pore pressure vs. strain results from triaxial testing on SANDHYDRO2.

Bryan Shiver
9/13/03
B = 0.992

Stress vs. Strain
SANDHYDRO2: Ottawa Sand w/ 0.085% Hydrogel, $\gamma_{d\ initial}$ = 93.0pcf; σ'_{3c} = 45psi
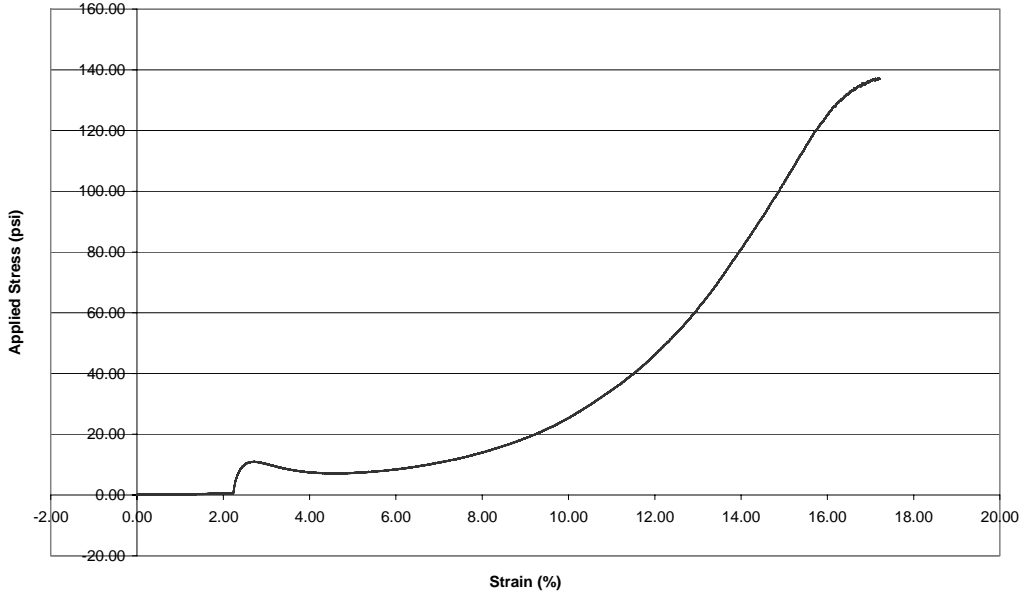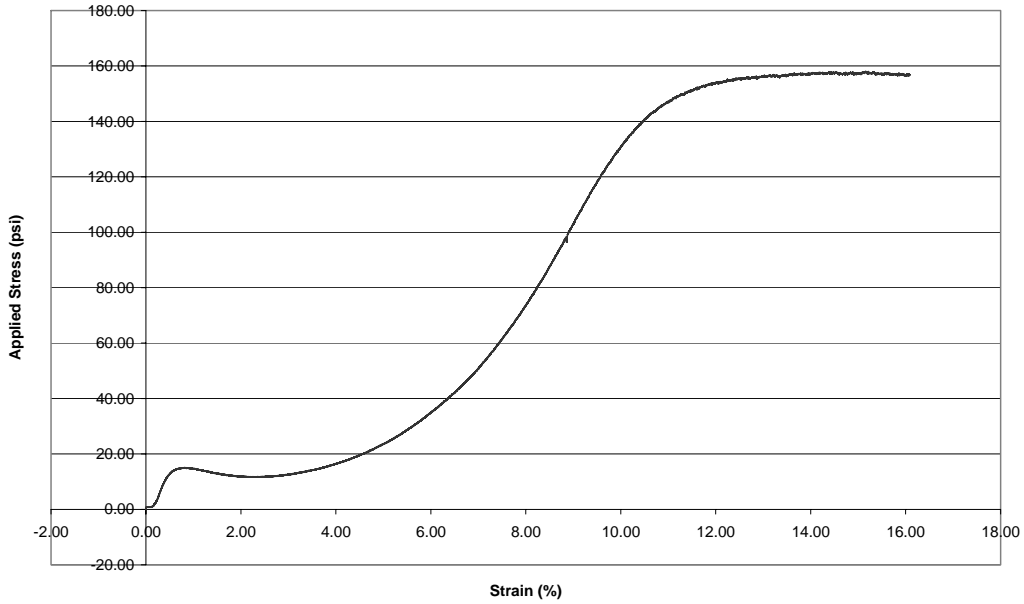

Figure D.22: Load vs. strain results from triaxial testing on SANDHYDRO2.

Bryan Shiver
9/14/03
B = 98%

Pore Pressure vs. Strain
SANDHYDRO3: Ottawa Sand w/ 0.085% Hydrogel, $\gamma_{d\ initial}$ = 93.6pcf; σ'_{3c} = 45psi
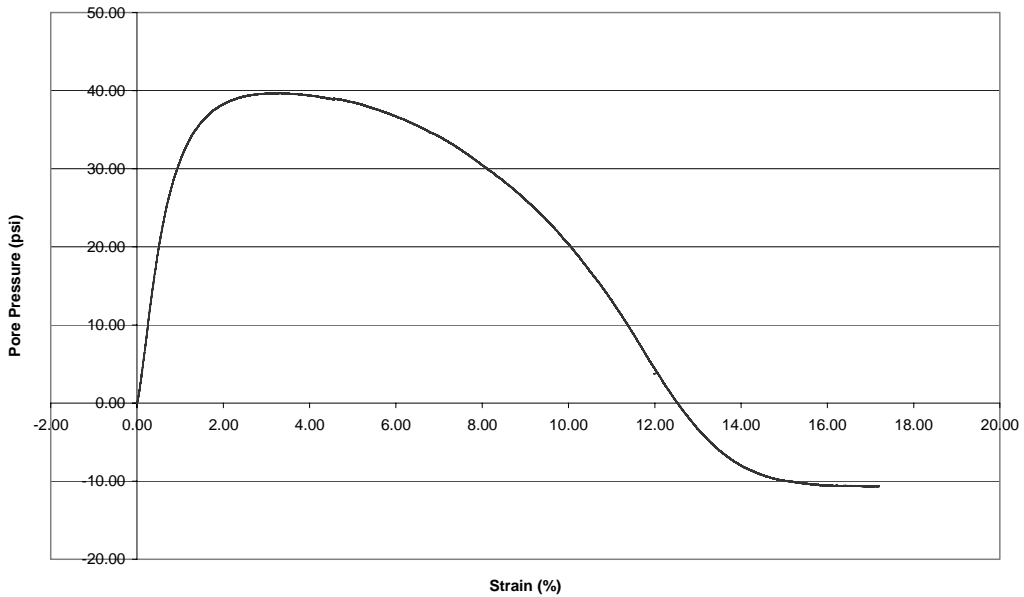
Figure D.23: Pore pressure vs. strain results from triaxial testing on SANDHYDRO3.

Stress vs. Strain
SANDHYDRO3: Ottawa Sand w/ 0.085% Hydrogel, $\gamma_{d\ initial}$ = 93.6pcf; σ'_{3c} = 45psi

Figure D.24: Load vs. strain results from triaxial testing on SANDHYDRO3.

Pore Pressure vs. Strain
SANDHYDRO4: Ottawa Sand w/ 0.085% Hydrogel, $\gamma_{d\ initial}$ = 98.6pcf; σ'_{3c} = 45psi
Sample Prepared with the Confined Mold
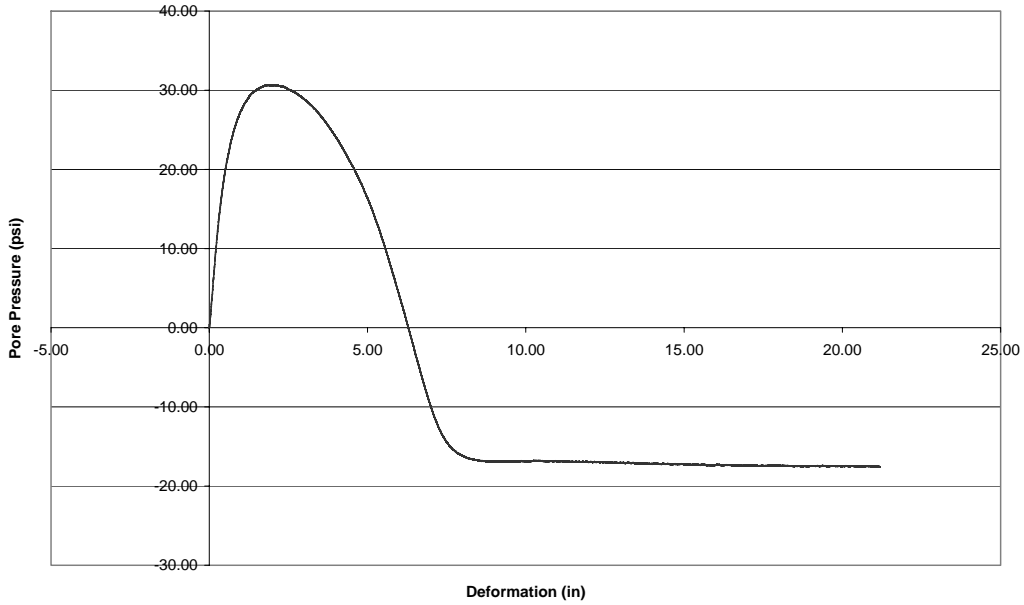
Figure D.25: Pore pressure vs. strain results from triaxial testing on SANDHYDRO4

210

Stress vs. Strain
SANDHYDRO4: Ottawa Sand w/ 0.085% Hydrogel, $\gamma_{d\ initial}$ = 98.6pcf; σ'_{3c} = 45psi
Sample Prepared with the Confined Mold

Figure D.26: Load vs. strain results from triaxial testing on SANDHYDRO4.

Pore Pressure vs. Strain
SANDHYDRO5: Ottawa Sand w/ 0.043% Hydrogel, $\gamma_{d\ initial}$ = 95.7pcf; σ_{3c} = 49psi
Sample Prepared with the Confined Mold

Figure D.27: Pore pressure vs. strain results from triaxial testing on SANDHYDRO5.

211

Figure D.28: Load vs. strain results from triaxial testing on SANDHYDRO5.

Figure D.29: Pore pressure vs. strain results from triaxial testing on SANDHYDRO6.

Stress vs. Strain
SANDHYDRO6: Ottawa Sand w/ 0.25% Hydrogel, gd initial = 95.7pcf; s3c = 47psi
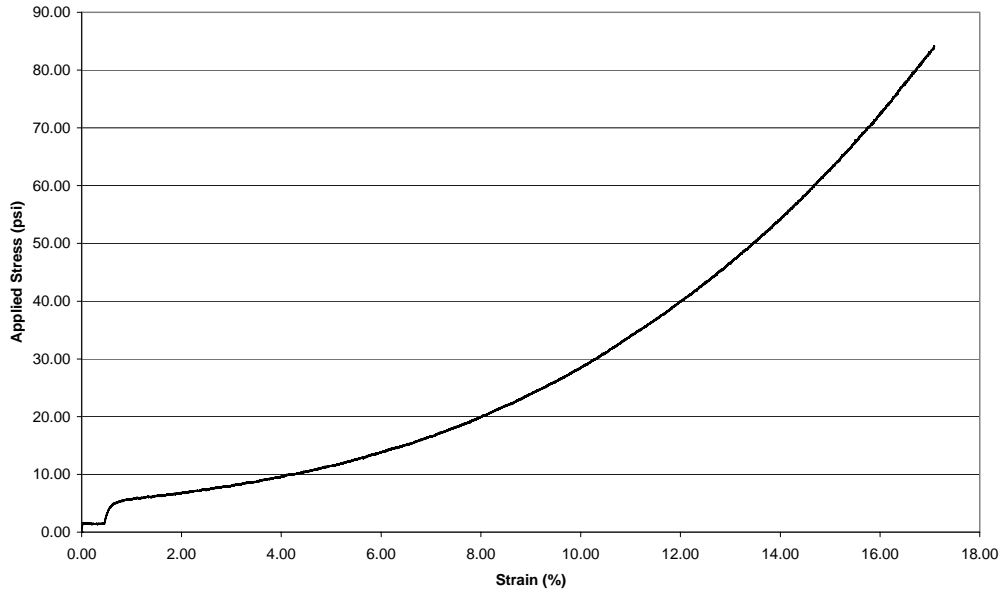**Sample Preapared with Confined Mold**

Figure D.30: Load vs. strain results from triaxial testing on SANDHYDRO6.

Pore Pressure vs. Strain
SANDHYDRO7: Ottawa Sand w/ 0.50% Hydrogel, $\gamma_{d\ initial}$ = 96.4pcf; σ_{3c} = 45psi
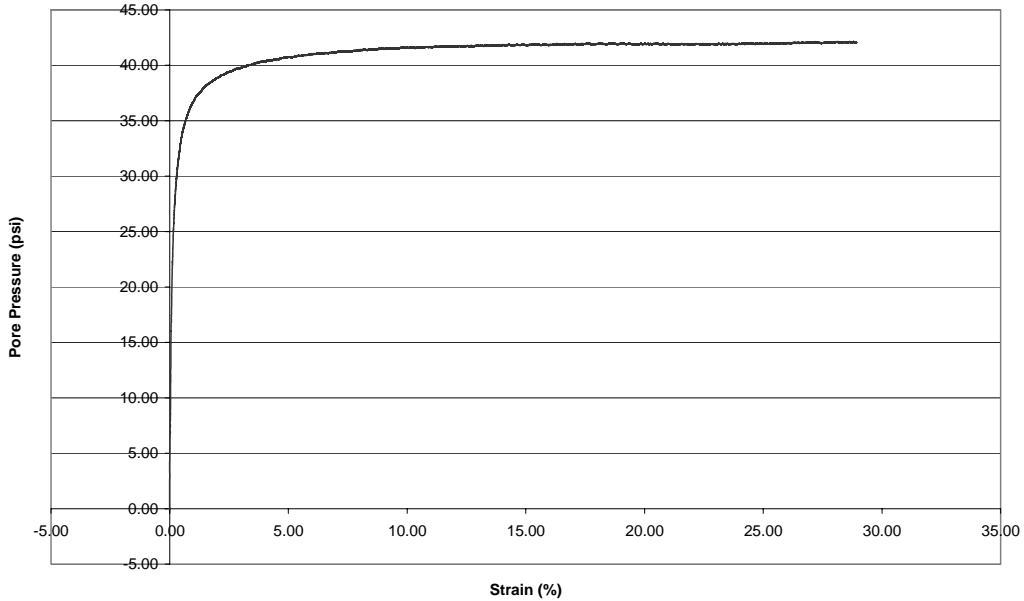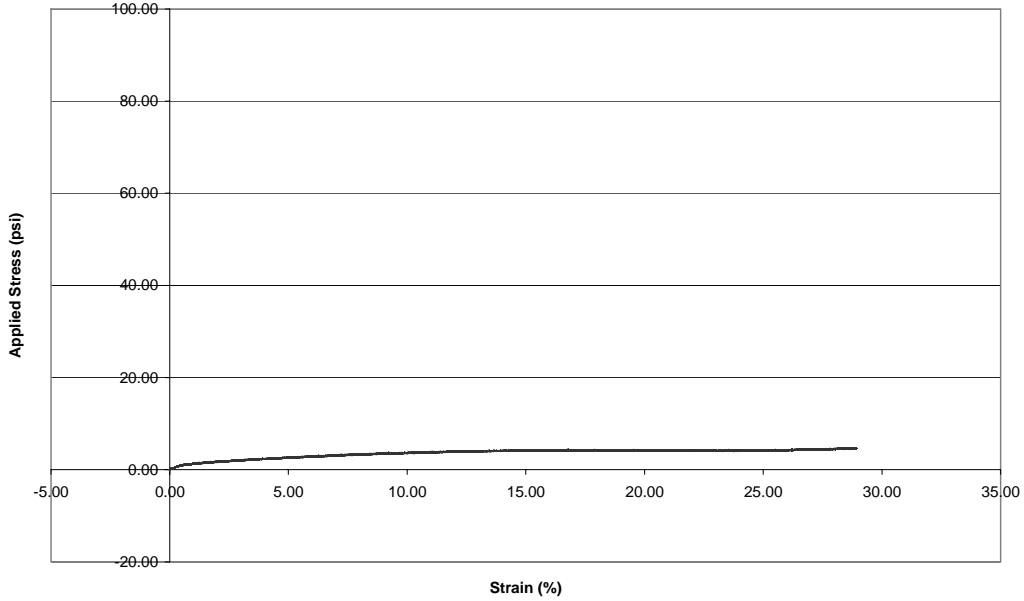**Sample Prepared with the Confined Mold**

Figure D.31: Pore pressure vs. strain results from triaxial testing on SANDHYDRO7.

Stress vs. Strain
SANDHYDRO7: Ottawa Sand w/ 0.50% Hydrogel, $\gamma_{d\ initial}$ = 96.4pcf; σ_{3c} = 45psi
Sample Prepared with the Confined Mold

Figure D.32: Load vs. strain results from triaxial testing on SANDHYDRO7.

Pore Pressure vs. Strain
HYDRO: 100% Hydrogel; σ_{3c} = 45psi
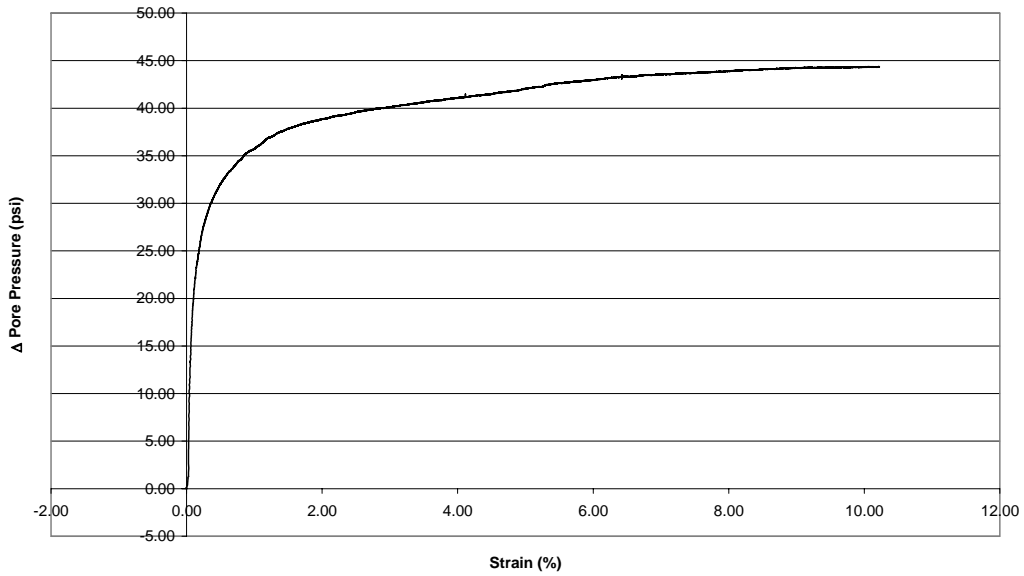**Sample Prepared with the Confined Mold**

Figure D.33: Pore pressure vs. strain results from triaxial testing on HYDRO.

214

Bryan Shiver
10/1/03
B = 0.996

Stress vs. Strain
HYDRO: 100% Hydrogel; σ'_{3c} = 45psi
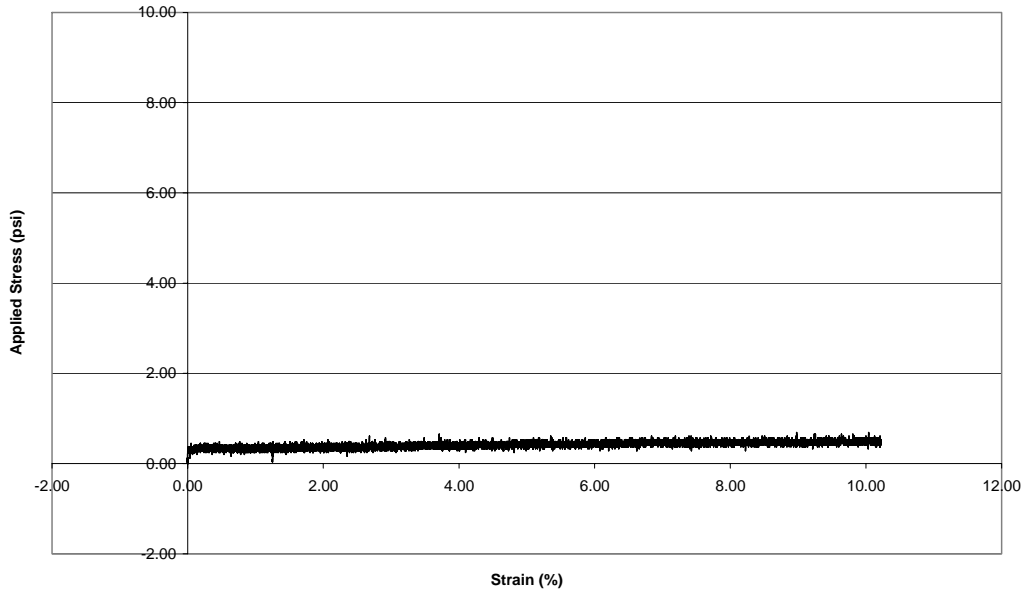**Sample Prepared with the Confined Mold**

Figure D.34: Load vs. strain results from triaxial testing on HYDRO.